CHARACTERIZATION OF CONDITIONS OF NATURAL GAS STORAGE RESERVOIRS AND DESIGN AND DEMONSTRATION OF REMEDIAL TECHNIQUES FOR DAMAGE MECHANISMS FOUND THEREIN

FINAL TECHNICAL REPORT

1 OCTOBER 2000 – 15 DECEMBER 2004

J. H. Frantz, Jr., Project Director, Schlumberger
K. G. Brown, Principle Investigator, Schlumberger
W. K. Sawyer, Principle Consultant, Schlumberger
P. A. Zyglowicz, Technician, Schlumberger
Dr. P. M. Halleck, The Pennsylvania State University
J. P. Spivey, Phoenix Engineering

December 2004

DE-FG26-99FT40703

Schlumberger
Data and Consulting Services
1310 Commerce Drive
Park Ridge 1
Pittsburgh, PA 15275-1011

DISCLAIMER

ABSTRACT

The underground gas storage (UGS) industry uses over 400 reservoirs and 17,000 wells to store and withdrawal gas. As such, it is a significant contributor to gas supply in the United States. It has been demonstrated that many UGS wells show a loss of deliverability each year due to numerous damage mechanisms.

Previous studies estimate that up to one hundred million dollars are spent each year to recover or replace a deliverability loss of approximately 3.2 Bscf/D per year in the storage industry. Clearly, there is a great potential for developing technology to prevent, mitigate, or eliminate the damage causing deliverability losses in UGS wells.

Prior studies have also identified the presence of several potential damage mechanisms in storage wells, developed damage diagnostic procedures, and discussed, in general terms, the possible reactions that need to occur to create the damage. However, few studies address how to prevent or mitigate specific damage types, and/or how to eliminate the damage from occurring in the future.

This study seeks to increase our understanding of two specific damage mechanisms, inorganic precipitates (specifically siderite), and non-darcy damage, and thus serves to expand prior efforts as well as complement ongoing gas storage projects. Specifically, this study has resulted in

1) An effective lab protocol designed to assess the extent of damage due to inorganic precipitates
2) An increased understanding of how inorganic precipitates (specifically siderite) develop
3) Identification of potential sources of chemical components necessary for siderite formation
4) A remediation technique that has successfully restored deliverability to storage wells damaged by the inorganic precipitate siderite (one well had nearly a ten-fold increase in deliverability)
5) Identification of the types of treatments that have historically been successful at reducing the amount of non-darcy pressure drop in a well, and
6) Development of a tool that can be used by operators to guide treatment selection in wells with significant non-darcy damage component.

In addition, the effectiveness of the remediation treatment designed to reduce damage caused by the inorganic precipitate siderite was measured, and the benefits of this work are extrapolated to the entire U.S. storage industry. Similarly the potential benefits realized from more effective identification and treatment of wells with significant non-darcy damage component are also presented, and these benefits are also extrapolated to the entire U.S. storage industry.

TABLE OF CONTENTS

List of GRAPHICAL MATERIALS

A recent GRI/DOE Halliburton study[3] identified several primary mechanisms that may be responsible for loss of deliverability over time in gas storage wells. They defined testing procedures in storage wells and in the laboratory to identify potential damage mechanisms. This study identified eight major categories of potential damage mechanisms. The study also generally discussed the possible reactions that need to occur to create the damage, but did not address the specific cause of damage, the most likely period of damage development (i.e., during the injection or withdrawal cycle), how to mitigate the damage, and/or how to prevent the damage from occurring in the future.

One of the major categories of damage identified by the Halliburton Study was inorganic precipitate. Siderite, $Fe(CO_3)$, is one specific type of inorganic precipitate prevalent in several storage fields in the US. Due to its ubiquitous nature, and the fact that an industry partner expressed interest in performing additional work on this specific inorganic precipitate, siderite was chosen for additional study in this project.

Another damage mechanism identified in the Halliburton report was non-darcy damage. The widespread nature of this type of damage, particularly in gas storage wells, has been noticed by Schlumberger, as they have consulted within the storage sector of the natural gas industry over several decades. We believe the negative consequences of this type of damage is both underestimated and erroneously considered to be irresolvable. Therefore, part of this study was aimed at increasing our understanding of this damage mechanism, assessing successfulness of treatments historically used to reduce non-darcy damage, and developing new tools to guide storage engineers as they evaluate remediation options available for reduction of non-darcy damage.

For ease of reading, the remainder of this report is split into two major sections. The first section thoroughly covers the portion of the project related to inorganic precipitate siderite. The second section of this report covers the portion of the project related to non-darcy damage.

INORGANIC PRECIPITATE SIDERITE

The UGS Industry and Inorganic Precipitate Siderite

A recent GRI/DOE Halliburton study[3] identified inorganic precipitates as one of the primary mechanisms responsible for loss of deliverability over time in gas storage wells. Siderite, $Fe(CO_3)$, is one specific type of inorganic precipitate prevalent in several storage fields in the US. Due to its ubiquitous nature, and the fact that an industry partner expressed interest in performing additional work on this specific inorganic precipitate, siderite was chosen for additional study in this project.

Damage and Remediation History in Subject Field

The subject field is located in Erie County, PA, was discovered in 1946 and converted to storage in 1959. Gas is stored in a combination stratigraphic/structural trap in the Oriskany formation at a depth of approximately 2300 ft. Discovery pressure and maximum operating pressure for storage are both $\pm$ 800 psi. There are currently about 45 injection/withdrawal wells and 4 observation wells in the field. Virtually all of the wells in this field have open-hole completions. Due to concerns of water production from lower portions of the Oriskany, all of the wells are partially completed in the top portion of the reservoir.

The operator became concerned about deteriorating deliverability in the field over the years, as declining deliverability was documented in several wells across the field. The ubiquitous reporting of “black dust” being recovered from wellbores in the subject field has a long history dating to pre-storage days. It was presumed that this black dust was the primary culprit leading to deliverability deterioration in the wells. Initially, deliverability was restored by periodically blowing/venting wells to the atmosphere. Although this procedure successfully increased the well’s deliverability, the procedure resulted in the expulsion of abundant amounts of “black dust” and natural gas into the air, which was an environmental concern. Consequently, this method of deliverability improvement was eventually abandoned.

The operator’s efforts to develop an alternate method of deliverability improvement started with attempts to identify the specific cause(s) of the damage. Through the 1980’s, work was done by the operator to determine the composition of the “black dust” prevalent in the wells. In 1989, rotary sidewall cores were retrieved from a well in the subject field and various lab analyses were performed on the samples. The major conclusions resulting from this work were as follows:

- The cause of damage is a variety of acid soluble and insoluble inorganic scale.
- Mackinawite (Fe_9S_8) and Marcasite (FeS_2) are the principle sulfide bearing scale species.
- Calcite, Siderite, and possibly dolomite occur as carbonate scale.
- Potential minor species include anhydrite and hematite.
- Iron bearing scale mineral phases were present in increasing abundance from the core matrix toward the wellbore face.
- Elemental abundance appears to increase toward the wellbore face, possibly due to increased pressure drop and therefore increase in precipitation tendency toward the wellbore.
- The majority of the scale is inorganic, mainly acid soluble and contains soluble sulfides.

- Mechanical removal and acid wash was the recommended remediation treatment.

Over the next several years, various treatments were attempted in an effort to remove damage and restore the wells' performance to their original deliverability levels. In 1990 five wells were blown to atmosphere and jetted with water to mechanically remove the near-wellbore damage and increase the size of the openhole. Test results were very impressive, showing rate increases of about 2 MMscf/D to 5 MMscf/D, which represented 90% to 2,600 % increase in deliverability.

In 1991, the same procedure was performed on 10 wells. However, additional testing was performed in some of the wells after blowing the well and before jetting the well, to determine the impact of individual treatment components. This testing revealed that most of the deliverability increase occurred after blowing the wells.

In early 1992, a down-hole camera run in a well that was jetted with water indicated that jetting with water caused very little increase in the openhole diameter. In the summer of 1992, seven wells were perforated in fluid and 5 wells were jetted using a larger OD jetting tool. The perforated wells showed either very little improvement or less deliverability after treatment. Some of these results may be explained by the fact that the hole was loaded with either acid or water before perforating, which could result in lower relative permeability to gas. Although the wells that were water jetted showed deliverability improvements ranging from 4% to 154%, all post-stimulation deliverabilities were still substantially lower than those originally reported when the wells were drilled.

During the 1990's, Halliburton conducted a major study aimed at the development and documentation of diagnostic techniques to identify the nature of wellbore damage in UGS wells. Additional work was performed by Halliburton on three wells in the subject field as part of this study. This work included running downhole videos and pressure transient tests, as well as retrieval and analyses of solid samples, liquid samples, and rotary sidewall core (RSWC) samples. The major conclusions drawn from this work were as follows:

- Damaged wells had significant scale deposition in the wellbore.
- The depth of damage is generally limited to less than 0.1 inches from the wellbore face
- Various damage mechanisms were identified through testing, including:
    i. Scale/Precipitation (NaCl, $MgCl_2$, siderite, calcite)
    ii. Bacteria and related iron and sulfur compounds
    iii. Particle plugging (silica/iron debris)
    iv. Organic compounds/residues

In 1998, Halliburton did work in the subject field as part of another GRI-sponsored study on the role of microbes in deliverability decline in natural gas storage wells. Halliburton concluded there is little evidence of microbial activity in the wells or separators, which suggests that microbes are not related to deliverability declines at Summit field.

Speculation on the root cause(s) of deliverability decline in the subject field is evident in various internal communications during the late 1990's. A summary of the key

observations, conclusions, hypotheses, and theories documented in the communications made available for review is included below:

- The storage sand doesn't appear to be sensitive to water from a clay standpoint.
- Siderite is ubiquitous in all areas of the field
- Analysis of downhole fluid samples suggest the environment is hypersaline, which would suggest that evaporite-types of minerals may play a role in the damage mechanism, and that buffering treatment fluids would be prudent to prevent adverse interactions between connate water and any spent sulfide acid.
- Difficulties encountered in a recent workover lead to analysis of flowback samples and additional speculation on the possible cause of damage, including organics and siderite.
- It would appear that by 1999, organics and microbes were pretty well ruled out and that the focus shifted to siderite as the primary causative agent of deliverability decline in the Summit field.

It is at this chronological juncture that the NETL-sponsored damage characterization and remediation study was initiated.

Goals & Objectives

In 2000, Schlumberger Data and Consulting Services was awarded this NETL-sponsored damage characterization project. This part of the project served to expand the efforts Halliburton started in the late 1980's and complimented recent GRI gas storage projects. Its purpose was to increase industry's understanding of inorganic precipitates, specifically siderite.

A primary objective of the inorganic precipitate portion of the project was to increase our understanding of the geochemical environment within which the inorganic precipitate siderite is formed. A necessary "tool" required to accomplish this objective was a lab protocol that can be used to identify inorganic precipitates using sidewall cores and solid, liquid, and gas samples from the well. In addition, we needed to identify the potential sources of the components necessary for siderite formation in the subject field.

We also sought to develop and field test a remediation treatment that could restore deliverability to a well damaged by siderite precipitate. Ideally, we would evaluate the proposed treatment in the lab before implementing it in the field.

Finally, we wanted to quantify the effectiveness of the proposed remediation treatment and extrapolate the results to the entire gas storage industry. This would be accomplished by comparing the results of pre-treatment multi-rate pressure transient test analyses with results of post-treatment multi-rate pressure transient test analyses

EXECUTIVE SUMMARY

Objectives

The primary objectives of the inorganic precipitate portion of the project can be summarized as follows:

1) Increase our understanding of the geochemical environment within which the inorganic precipitate siderite is formed, including:

    a) Development of a lab protocol that can be used to identify inorganic precipitates using sidewall cores and solid, liquid, and gas samples from the well.

    b) Identification of the potential sources of the components necessary for siderite formation in the subject field

2) Develop and field test a remediation treatment aimed are restoring deliverability to a well damaged by siderite precipitate.

3) Measure the effectiveness of the proposed remediation treatment designed to reduce damage caused by the inorganic precipitate siderite, and extrapolate the results to the entire gas storage industry.

Results

Multi-rate pressure transient testing was performed in nine wells to identify wells with damage. From these nine candidates, three were selected to test the proposed field remediation treatment. One of the candidate wells was subsequently replaced due to operational issues. However, no pre-treatment multi-rate pressure transient test was available from this well. The operator selected the well, based on "…evidence of deliverability deterioration…"

A lab protocol was developed to identify the inorganic precipitates present in rotary sidewall cores and evaluate the extent and location of permeability reduction caused by the damage. This protocol involved collection of four cores. The first core was to be used to characterize the damage in the core, and involved solvent extraction, gas chromatograph mass spectrometer (GCMS) analysis on organics to determine compounds present, preparation of thin sections, scanning electron microscope / energy dispersive x-ray (SEM/EDX) to map texture and identify inorganic scale elements, and examination with petrographic microscope for mineralogy and texture. In addition half of the core was to be sliced crosswise in 1/4-in increments and used to measure the permeability of each slice, allowing for the mapping of permeability with location. Solvent extraction was also planned for each 1/4-in increments as well as cation/anion analysis. GCMS measurements on liquid from each increment was also anticipated.

Cores 2 and 3 were to be used to evaluate conventional remediation treatments in the lab. Core 4 was to be used to evaluate unconventional treatments, in the event one was proposed. This involved measuring the gas permeability on entire core in both directions, treating the core with selected remedial method, and re-measuring the gas permeability

The protocol also involved testing any liquids or solids collected from the well, or any scrapings collected on logging tools coring tools, or other tools run in the wellbore (e..g., bailers, sinker bars, etc.). Tests planned for scrapings included hydrocarbon extraction, GCMS to determine hydrocarbons present, X-ray diffraction (XRD) on inorganic material,

and cation/anion analysis. Tests planned for wellbore/formation liquids included cation/anion analysis, total ion concentration, and pH.

Rotary sidewall cores were obtained from two wells. The first well cored was one that had previously been stimulated and deepened. This allowed a comparison of the virgin formation with the formation as it exists in its post-treatment state, and was used to qualitatively evaluate the impact of prior treatments. Due to recovery problems, however, not all of the tests prescribed in the protocol developed were possible. Obviously, since the well had been treated, no tests could be performed on these cores to evaluate the proposed treatment. Also, due to the amount of breakage in the recovered cores, the permeability could not be mapped as a function of distance into the formation.

The second well selected for coring was a damaged well selected for treatment. This well was selected to allow lab testing of proposed treatments. However, core recovery was very poor in this well, severely limiting our ability to perform the prescribed tests. We initially tried to recover these cores in air, but due to problems cutting the cores, the hole had to be loaded to continue operations, further complicating lab analyses.

Based on knowledge accumulated as a result of all previous testing and the testing accomplished in this study, a remediation treatment was designed for the study wells. However, due to the coring problems, lab testing of the proposed treatment was not possible, apart from fluid compatibility tests. The proposed treatment involved pickling the tubing, pressure washing the formation face with a sand laden fluid, and performing a small alcohol-based matrix acid job. Due to operational problems, sand was not used in the treatments as originally planned.

Post treatment multi-rate pressure transient test analyses indicated that the treatment was successful in two wells. In one well the treatment appears to have been initially successful, but not long lived, as evidenced by a significant increase in Q100 the first year followed by a significant decrease in the Q100 the second year. Although the current Q100 is still higher that the pre-treatment Q100, test results suggest that damage may be recurring in this well. Although we cannot quantify the amount of improvement in the second successfully treated well, we know its post-treatment Q100 is similar to the other successfully treated well.

The third well treated did not show any improvement in Q100 after treatment. In fact, it would appear that the well's performance is deteriorating with time, as evidenced by a significant decrease in the Q100 from the first post treatment test to the second post-treatment test.

Conclusions

Based on testing done to date, it is clear that siderite has been a long-standing problem that pre-dates storage operations and is prevalent throughout the study field.

Blowing the wells to the atmosphere is the only remediation treatment that has consistently been successful at removing siderite damage form the wellbore. However, this treatment (as it was previously practiced) is no longer considered viable due to environmental concerns.

Prior work identified inorganic scale deposition as the major damage component in the field, and verified that it is ubiquitous. Damage due to organics, bacteria, and clay problems were ruled out.

A lab protocol was developed as part of this study. Although poor core recovery prevented all of the tests prescribed in the protocol from being carried out, the testing successfully verified that the specific inorganic scale found in the samples was siderite.

Lab analyses of the rotary sidewall cores, solid samples, and liquid samples obtained during this study revealed a number of key facts:

1. Prior acid treatments have been fairly successful at dissolving siderite located in the formation fractures
2. Some of the material dissolved during prior acid treatments may have migrated to lower portions of the reservoir
3. Some damage remains in the full 2 inches of core.
4. Prior notions that organic materials were not the cause of damage were confirmed.
5. Solvent extraction process alone is capable of removing organics, so analysis via pyrolysis-gas chromatograph/mass spectrometry is not necessary
6. The majority of damage is limited to the very near wellbore region.

We believe deposition of scale occurs primarily as a result of dehydration of water solutions. This could occurs when gas is withdrawn if the gas in the reservoir is not already saturated with water and the gas passes through water in the pore space or water collected in the wellbore. It can also occur when dry gas is injected through residual formation water in the pore spaces. Deposition of scale above the reservoir formation and in the casing occurs via entraining solution droplets in upward flow. We believe the source of the scaling elements is formation water from the Oriskany.

Backpressure multi-rate pressure transient tests run after treatment indicate that two wells were successfully treated, with one well exhibiting nearly a ten-fold increase in deliverability. In one of these wells, the success only lasted one year, and the damage seems to be recurring by the second year. Success in the second well is inferred based on post-treatment well performance, since no pre-treatment test was available. The treatment was apparently not successful in the third well, as no improvement was realized after the first year and an increase in the damage level occurs two years after treatment.

Overall, post-treatment testing suggests that the proposed treatment can potentially remove a significant amount of damage in wells with siderite scale deposition, but that the treatment does not prevent re-precipitation of siderite after treatment. In short, we have developed a treatment capable of treating the problem but not preventing it.

Although inhibition was proposed, the operator did not find an inhibition product that he felt comfortable with. The operator has concerns that the available inhibition products will themselves cause damage in the reservoir or other operational problems.

Recommendations

Given the prevalence of the inorganic precipitate siderite in UGS fields, future R&D work should include siderite-related projects. One specific area that warrants additional R&D is inhibition.

The lab protocol developed in this study should be used to identify the specific inorganic precipitate causing wellbore damage.

The remedial treatment developed in this study should be used to remove siderite scale where appropriate.

Given that the only consistently effective treatment of siderite damage in this field has been blowing the well to atmosphere, we recommend that additional work be done to determine an environmentally friendly method of accomplishing the sudden, severe underbalanced conditions caused by blowing a well.

Additional tests should be run in the study wells that did not respond to treatment and/or evidence recurrence of damage to verify that siderite is indeed reforming.

EXPERIMENTAL

Identification, Testing, and Selection of Study Wells

Multi-rate pressure transient test analyses constituted the primary tool for identification and quantification of the type and amount of damage in wells before and after stimulation.

The general analysis approach involved evaluation of the pressure transient test data collected during the flow and shut-in periods to determine the total skin damage (S_{Total}), and plotting the test rates versus the corresponding S_{Total} value. The y-intercept of this plot represents the mechanical component of the total damage (S_m), and the slope of this plot represents the non-darcy damage coefficient (D). An example of this type of analysis is shown in **Figure 1** below:

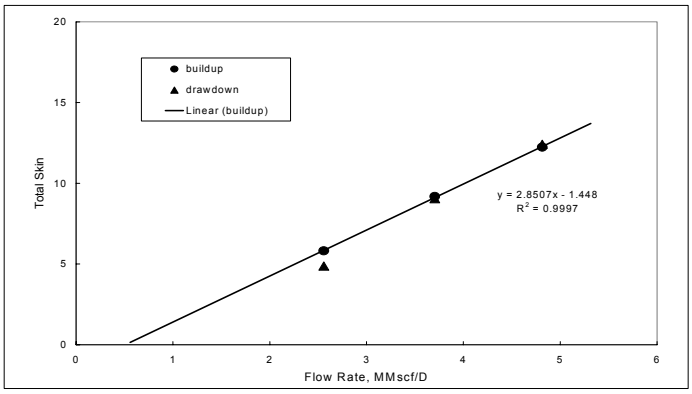

Figure 1: Example calculation of $S_{mechanical}$ and D from plot of rate vs total skin

Classical backpressure plots were also constructed using test data and used to compare Q_{100} values before and after stimulation.

The operator selected 9 wells to run multi-rate pressure transient tests in, based on their assessment of how the current deliverability potential compared with the original deliverability potential measured when the wells were first drilled. These tests were performed in March of 2002. A summary of the input parameters supplied by the operator and results of these tests is shown in **Table 1** below.

Table 1: Summary of pressure transient test analysis results

	Input Values					Output Values				
Well	h_{net}	phi	S_w	r_w	SG	AOF[1]	Kh	K	S_m	D
W1	1.5	14.0%	20.0%	0.255	0.58	1,265	1,575	1050	42.6	0.0335
W2	3.0	14.0%	20.0%	0.255	0.58	785	966	322	69	0.0097
W3	13.0	14.0%	20.0%	0.255	0.58	10,425	2,418	186	N/A[2]	N/A[2]
W4	5.0	14.0%	20.0%	0.255	0.58	20,442	5,085	1017	N/A[2]	N/A[2]
W5	6.0	14.0%	20.0%	0.255	0.58	4,757	1,800	300	2.5	0.0038
W6	2.0	14.0%	20.0%	0.255	0.58	7,992	1,632	816	N/A[2]	N/A[2]
W7	4.0	14.0%	20.0%	0.255	0.58	509	1,240	310	N/A[2]	N/A[2]
W8	2.0	14.0%	20.0%	0.255	0.58	6,252	885	442.5	-1.6	0.0009
W9	3.0	14.0%	20.0%	0.255	0.58	4,343	2,295	765	10.8	0.0051
W10	3.0	14.0%	20.0%	0.255	0.58	N/A[2]	N/A[2]	N/A[2]	N/A[2]	N/A[2]

1. AOF calculated at bottom hole conditions

2. N/A2 due to single rate test or poor Q vs S correlation

Based on this testing and other data, W1, W2, and W9 were identified as possible stimulation candidates, largely because they showed positive skin values. W1 was subsequently replaced with W10 due to operational issues. Although no pressure transient test was run in 1522, the operator selected this well as an alternate. This selection was based on the operator's belief that deliverability deterioration had occurred over time, as evidenced by excessive scale found in the wellbore during well maintenance operations.

W3 was drilled in 1956, completed in the Oriskany formation as an open hole well, and converted to storage in 1960. The well has 7" production casing set at 2277 feet and was originally drilled to a TD of 2285 feet. In 1992, a hydroblast treatment was performed. In August of 1999, a second hydroblast treatment was attempted in the well after testing indicated a mechanical skin factor of 26. Attempts to pump fluids into the reservoir failed, due to excessive injection pressures. However, acid was spotted across the reservoir. Post-treatment testing indicated that the mechanical skin was reduced to about 8. The operator subsequently decided to deepen Well 1527, and in August of 2000, the well was deepened to a TD of 2310 feet. During this workover, sidewall cores were recovered from both the old portion of the hole and the new portion of the hole, allowing a comparison of virgin formation with formation that had been used for 40 years.

W2 was drilled in 1956, completed in the Oriskany formation as an open hole well, has 7" production casing set at 2372 feet and was drilled to a TD of 2389 feet.

W9 1589 was drilled in 1955, completed in the Oriskany formation as an open hole well, has 7" production casing set at 2120 feet and was drilled to a TD of 2338 feet.

W10 was drilled in 1956, completed in the Oriskany formation as an open hole well, has 7" production casing and was drilled to a TD of 2390 feet.

Development of Lab Protocol for Damage Diagnosis

The protocol for lab analysis of rotary sidewall cores was developed by Dr. Phil Halleck, a Professor of Petroleum and Natural Gas Engineering at the Pennsylvania State University. He directed all laboratory investigations of the cores. The protocol, as well as the rationale for the various procedures is outlined below.

The sidewall coring program requires four sidewall cores from each well, plus samples of formation rock in its original condition. The objectives of testing performed on each core are summarized below, as well as the procedure employed to perform the stated testing

Core #1:

Objective - Damage Characterization

Slab the core lengthwise with a diamond saw, and perform the following analyses on the first half of core #1:

- Solvent Extract
- Gas Chromatograph Mass Spectrometer (GCMS) analysis on organics from this half to determine compounds present
- Prepare thin section
- Perform Scanning Electron Microscopy/Energy Dispersive X-Ray Analysis (SEM/EDAX) to map texture and identify inorganic scale elements

- Examine with petrographic microscope for mineralogy and texture

These tests are designed to identify the presence of various mineral scales and organic compounds in the pore structure and on the surface of the core. Solvent extraction using appropriate solvents in Soxlet apparati will dissolve any organic material and condense it into a separate container for analysis. The amount of organic material extracted from a given volume of rock allows us to determine how much of the pore space is occupied by the organic material. The GCMS, or gas chromatograph mass spectrometer, is used to separate the various components of the resulting mixture and determine their molecular weights and thus their composition. These data are useful in determining the source of the material as native organic liquids, compressor oil, production chemical, or reaction products of one of these with other chemical agents. If necessary, carbon isotope analysis is available to assist in determining the age of the organics.

The thin section will be used primarily for SEM (scanning electron microscope) and EDX (energy dispersive X-ray) analysis. These will provide a microscopic view of the pore structure of the rock as well as maps of the distribution of the specific elements composing any inorganic precipitates. The result is determination of the distribution of scale minerals in the pore structure, which will assist in determining the scale's affect on permeability. These data will be supplemented with bulk analysis of cation and anion composition as described below. Thin sections will also be used for standard petrographic examination of the rock's texture, mineralogy and pore structure.

Data from the sidewall core will be compared with a rock sample in its original condition. This is necessary both to evaluate the geochemical environment and to quantify how much of each mineral has been deposited by storage and production operations and how much may have been originally present.

Perform the following on the second half of core #1:

· Perform gas permeability measurement on the half core
· Slice second half crosswise in 1/4-in increments
· Retest permeability after taking each slice
· Solvent extract each 1/4-inch increment
· Perform X-Ray Diffraction (XRD) analysis on each increment
· Perform Inductively Coupled Plasma (ICP) and ion chromatographic analyses on each increment
· Perform Total Organic Carbon (TOC) measurement on liquids from each increment

These tests are designed to further identify the nature of any inorganic and organic materials on and in the formation rock, and to provide a course map of the severity of potential plugging. The gas permeability tests give the average permeability of the core as each slice of material is removed. The change in permeability after taking each slice allows determination of the permeability of the slice, thus obtaining a course map of permeability as a function of distance from the sand face. Analyzing each slice separately for the presence of organic and inorganic plugging materials allows the amounts of these compounds to be mapped as a function of distance from the sand face. XRD, or X-ray diffraction analysis, is used to identify the presence of specific minerals present in the rock. These are identified by their crystal structures as revealed by their diffraction patterns. Interpretation is assisted by knowledge of the cations and anions present. These data come from the EDX measurements described above and from ICP (Inductively Coupled Plasma) spectrophotometer analysis of cations. This test is performed by dissolving the mineral phases in appropriate acids to form a solution.

The solution is ionized in a plasma and the light emissions analyzed to determine the amounts of specific cations present. Ion chromatography is used to separate and quantify anions such as CO3-2, HCO3-, and SO4-2. TOC (or total organic carbon) measurements on each slice will determine how much organic material is present, again, as a function of distance from the sand face.

Core #2:

Objective - Relation of permeability damage to observed plugging mechanisms.

- Perform gas permeability on entire core in both directions
- Solvent extract entire core
- Retest permeability

Cores #3 and #4:

Objective – Evaluation of remediation techniques.

- Perform gas perm on entire core in both directions
- Treat core with selected remedial method
- Acidization
- Miscible solvent
- Heat/Pressure
- Mechanical removal of the sandface
- Re-measure gas permeability
- Several cycles of treatment may be possible
- If appropriate, evaluate post-treatment sample as for core #1

These tests are designed to determine the effectiveness of treatments that might be applied in the field. A special vessel will be fabricated to apply these treatments in a manner consistent with the downhole environment. Acids or miscible solvents will be injected into the sandface of the core. The core itself will be backed by additional formation rock so that spent acids and solvents are pushed through the core and into the backing rock. The spent treatment fluids will be recovered back though the test core to simulate actual down-hole processes. After completion of each treatment, gas permeability will be remeasured to determine the effects of the treatment. Due account will be taken of relative permeability effects.

Scrapings/Other non-core samples:

Objective: Evaluate lower-cost testing alternatives.

- Obtain samples from perforations and/or wellbore wall
- Extract hydrocarbons
- Perform GCMS to determine hydrocarbons present
- Perform XRD on inorganic material
- Perform cation/anion analysis on same material

These tests are designed to evaluate the effectiveness of lower-cost testing alternatives. The sidewall cores required for the above tests are quite expensive and simpler, more cost effective methods of determining the damage mechanisms are required. The intent of these tests is to evaluate whether cheaper, but less well-defined samples can be used to obtain the same information. The tests described have the same purpose as those run on sidewall core, except that permeability itself is not measured and distribution of

damage away from the sand face is not obtained. The results of these tests will be compared with those from the sidewall cores.

Wellbore Liquids and Formation Liquids Analysis:

Objective: Supplement mineralogical/chemical data obtained from formation mineralogy and pore fluid analyses

- Perform ICP and ion chromatographic analyses on well water
- Obtain total ion content and Ph to define environment

The intent of these tests is to supplement the mineralogical and chemical data obtained from formation mineralogy and pore fluid analyses. The combined data, plus historical records of production chemicals and previous remediation treatments used, form the basis for characterizing the geochemical environment. These data are needed to establish the precipitation reactions and phase behavior involved in depositing the observed scale. The intent is to go beyond remediation to develop operating procedures that prevent re-occurrence of permeability damage.

Dr. Halleck coordinated the design, construction, and calibration of the equipment required for the above testing. In addition, test runs were made on non-study cores to iron out operational, procedural, and/or technical problems prior to testing the study cores. It should be noted that, due to the condition of the cores taken from W2, most of the above analyses were not possible. Core recovery from W2 was very poor, and those cores that were recovered were broken to the point that very few prescribed tests were possible. Most of the above tests were performed on the cores from W3. However, it was not possible to map perm with distance due to the limited number of completely intact cores recovered from W3.

Development of Field Treatment Design

The results of testing and analyses strongly support the notion that the damage in the subject wells is very close to the wellbore and is primarily due to acid soluble inorganic precipitates. Therefore, a remediation treatment was designed with two primary objectives in mind: 1) mechanical removal of as much near-wellbore inorganic precipitate scale as possible, and 2) a small matrix acid treatment to dissolve any scale not removed via mechanical techniques.

We proposed performing a pressure wash treatment using *both* water and sand followed by a small matrix acid treatment. We believe this combination will maximize the probability of success at minimal incremental cost (i.e, the cost of the sand). Specifically, any increase in the wellbore radius will reduce the non-darcy flow in the near-wellbore region, thus increasing the deliverability to a level beyond that achievable using acid alone and/or hydroblasting without sand.

Although the magnitude of the anticipated benefit due to hole enlargement is difficult to predict directly with existing nodal analysis models, Ramey[1] has shown that the non-darcy skin factor (D) is inversely proportional to the wellbore radius. Using 6-1/4" open hole and an estimate of 2" of additional penetration from the hydroblast with sand treatment, the reduction in D would be about 25%, which was expected to result in a 10-15% increase in deliverability (due to hole enlargement alone).

We recommended performing the hydroblast with sand first, followed by a matrix acid job. This sequence was proposed in order to mechanically remove the majority of the scale prior to acidizing, thereby maximizing the formation area available for acid contact

and enhancing the effect of the acid. Prior to our proposed work, the operator had installed bridge plugs and dumped sand on top of the plug in order to replace top joints of casing in the wells. Therefore, it was necessary to wash sand and remove this plug before the proposed work could be performed.

The proposed well procedure is outlined below:

1. Move in & rig up coiled tubing unit with retrieving tool but no catcher assembly.
2. Run in hole and tag sand on top of bridge plug.
3. Circulate water and clean out sand on plug until bottoms up.
4. Start nitrogen and displace water out of hole.
5. Pull out of hole with coiled tubing unit.
6. Install retrieving tool on coiled tubing unit.
7. Run in hole to just above bridge plug.
8. Pressure wellbore with field gas to 800 psi.
9. Pressure wellbore to ±1,000 psi with nitrogen.
10. Set on bridge plug, equalize bridge plug, retrieve bridge plug. Pull out of hole.
11. Remove bridge plug and retrieving tool. Install jet blaster on coiled tubing unit.
12. Run in hole to bottom hole and perform pickle treatment using acid.
13. Perform jet blaster with sand over open hole interval.
14. Perform acid treatment through jet blaster by spotting acid across open hole interval, shutting in annulus, pulling coiled tubing up above acid, and pumping acid away. (Be prepared to open annulus immediately after pumping acid away).
15. Run in to bottom of hole.
16. Clean out acid with foam and nitrogen.
17. Circulate hole clean with nitrogen.
18. Pull out of hole.
19. Rig down and move off coiled tubing unit.

The pickle acid consisted of 15% HCl with 10% mutual solvent, 4 gal/1000 surfactant, 8 ppt reducing agent + 2 gal/1000 corrosion inhibitor. The jet wash fluid consisted of WF120 w/ 2% KCl, 5 gal/1000 slurry gel, 2 gal/1000 clay stabilizer, 2 gal/1000 surfactant + 200 scf/bbl N_2. The matrix acid was composed of 15% HCl w/ 30% methanol, 10 gal/1000 chelant, 5 ppt reducing agent, 2 gal/1000 clay stabilizer, 2 gal/1000 surfactant, 2 gal/1000 corrosion inhibitor + 200 scf/bbl N_2. **Table 2** below summarizes the fluid volumes proposed for each well.

Table 2: Proposed Treatment Fluid Volumes

Well	Gal Pickle	Bbl Jet	Gal Acid
W2	500	240	360
W9	500	260	390
W1	500	220	330
Totals	**1500**	**720**	**1080**

As noted above, the type of acid job proposed was a matrix acid job. Specifically, we proposed pumping the acid into the matrix and IMMEDIATELY flowing back the acid to prevent precipitation. Given the very short intervals being treated, diverters were not considered necessary. An alcohol-based fluid was proposed in order to minimize many of the flowback problems and promote faster cleanup.

Although this basic approach is similar to remediation approaches used in the recent past, there are several significant differences between the proposed treatment and prior treatments.

One primary difference is that we proposed to pickle the tubing. There are several reasons for this:

- To remove as much of the corrosion products as possible from the tubulars prior to the main treatment fluids.

- When wells are cycled between injection and production mode, corrosion products are inevitable, as some entrained air/ oxygen will be incorporated (particularly on reversion to injection mode).

- It is prudent to ensure that the concentration of iron oxide as Fe II and Fe III is minimized. This mitigates the risk of iron hydroxide precipitation in the formation. Fe III is the most problematic as it is soluble only below a pH of 2. Spent acid pH is around pH 5-6. Fe III can be formed in injector wells.

- Total Fe concentration removed from pickle treatment can exceed 10000 ppm and often much higher (30-100K ppm). This is difficult to control in a main acid treatment with iron control reagents so pickling is highly recommended.

- The amount of iron removed during these treatments can be assessed by an analysis of the pickle flow back.

The main acid treatment fluid proposed is also similar in many respects to that used previously (iron control and corrosion additives, clay control), with one very important difference. We proposed incorporating 20-30% methanol to provide an "Alcoholic acid" treatment for the following reasons:

- Incorporation of an alcohol in the acid formulation forms a more volatile liquid. Therefore the spent acid will be much more mobile at reservoir temperatures due to an increase in vapor pressure. This results in lower water saturation and improved productivity via reduction of relative permeability effects.

- The inclusion of alcohol significantly reduces the surface tension of spent acid in the pore throats of the formation. This reduces the effect of capillary forces and improves clean up. The benefit here is that the fluid will be unloaded or displaced by the gas from the well much more easily. It also ensures deeper penetration of live acid into the rock.

Jet Blasting *with sand* was also proposed, and was considered by us to be a substantial improvement to pressure washing with water alone, as it would likely result in some hole enlargement, and the physical removal of near wellbore damage. The combination of chemical dissolution and physical abrasion should ensure very efficient scale removal.

Notwithstanding the above comments, we acknowledged that it was possible the proposed treatment would not constitute a long-term solution, as the siderite scale could reform over time due to continued flow of gas associated with wellbore pressure drops and the resulting flow of under-saturated gas through formation water.

Therefore, we proposed working with an alliance chemical supplier to determine which scale inhibitor is fit for purpose (i.e, will inhibit iron carbonate scale build up). We recommended testing the compatibility of an inhibitor (a compound manufactured by NALCO called L66) with gas well fluids and proposed "trickling" L66 into the wellbore during the final period of gas injection. To date the operator has not performed any inhibitor testing and no inhibitor has been pumped into their wells.

Assessment of Treatment Success

As was the case for the selection of study wells, multi-rate pressure transient test analysis constituted the primary tool used to quantify the amount of damage in study after treatment. The general analysis approach involved evaluation of the pressure transient test data collected during the flow and shut-in periods to determine the total skin damage (S_{Total}) for each flow period. Using the results of these analyses, we estimated the mechanical component of the total damage (S_m) and the non-darcy damage coefficient (D), by plotting rate versus total skin and determining the slope (D), and y-intercept (S_m). Classical backpressure plots were also constructed using test data and used to determine Q_{100} values after stimulation.

RESULTS AND DISCUSSION

Results of Lab Analyses

W3 Lab Analysis Results

Rotary sidewall cores from W3 were obtained during deepening operations in August 2000, and eight sidewall core samples were delivered to Penn state for analysis The cores were photographed and, where possible, scanned by X-ray computed tomography (CT).

There are clear distinctions between the cores taken from the old and new sections of the well. The former are gray in color as opposed to the light tan coloration in cores from the new section. Most of the cores from the older, upper section show evidence of previous acid treatments as open fractures where carbonate material has apparently been dissolved away. These features are not present in cores from the newer section. On the other hand, X-ray CT shows higher concentrations of a high-density material in the cores from the newer section. This high-density material may be the carbonate material (calcite or siderite) that was dissolved from the upper section.

Three of the cores, two from the new section and one from the older section were damaged or crushed to the point that no permeability measurements were possible. In addition, all but one of the cores from the upper section contained large open fractures or vugs, apparently from acidization. This left only two cores for which permeability measurements were possible.

Two of the broken samples, one each from the new and old sections of the well, were subjected to pyrolysis, analyzing the evolved vapors using a gas chromatograph and mass spectrometer. These analyses reveal very low levels of organic material, dominantly paraffinic compounds, although others are also present. Elemental sulfur is also present in the core from the new section, confirming previous observations. Pyrolysis of material previously extracted using methylene chloride shows that the solvent extraction process alone should be capable of removing the organics in future tests.

The amounts of organic material and their nature suggest that these are not the causal mechanism of permeability reduction.

Core Descriptions and Qualitative CT analysis

Each of the cores was photographed and scanned in three dimensions using X-ray CT analysis. The results are summarized below. The positions of the cores are marked on the accompanying well log (**Fig. 2**).

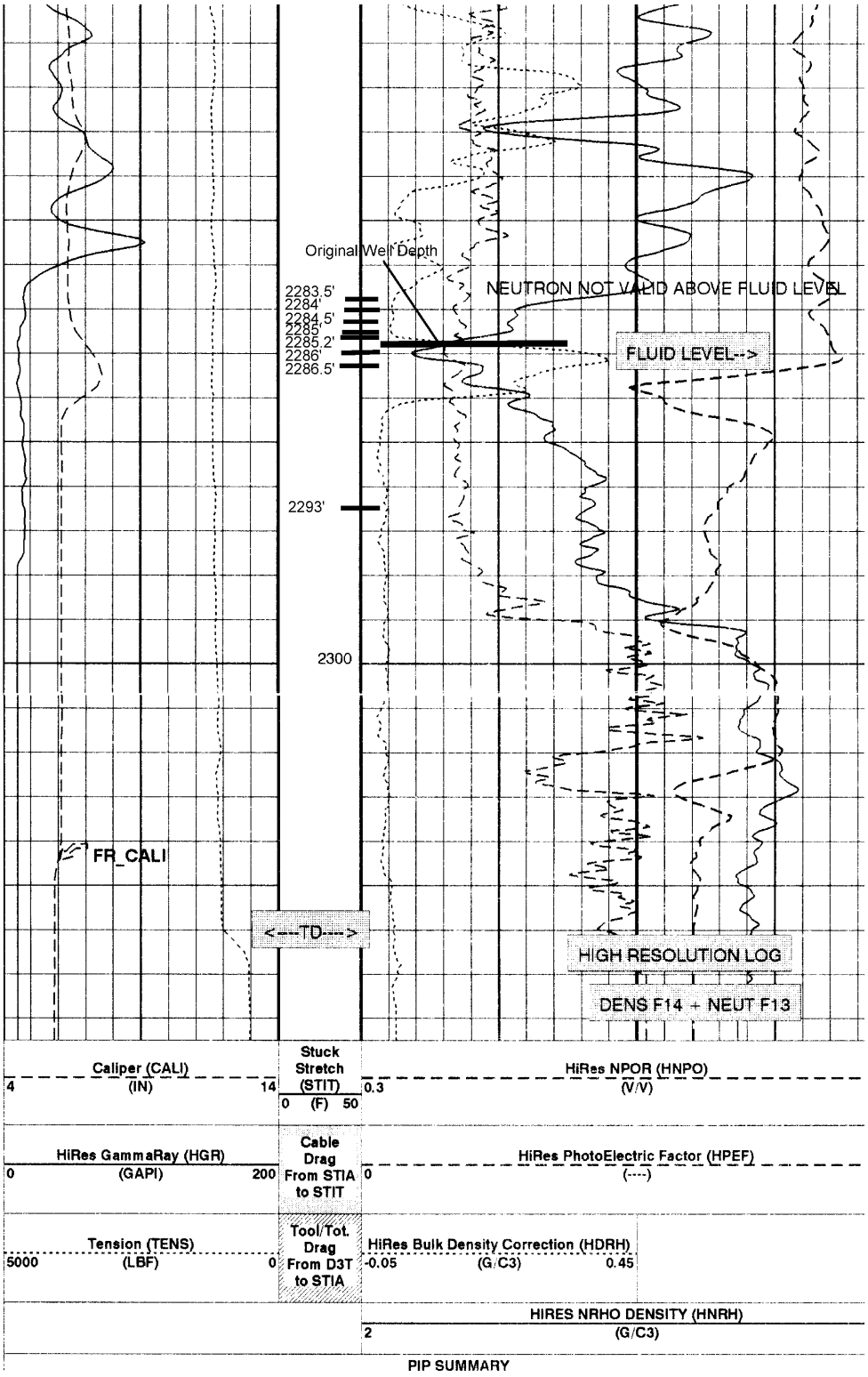

Figure 2: W3 Log Showing Sidewall Core Locations

Core #1 (**Fig. 3**) was taken at a depth of 2283.5 feet The core is a sandstone, dark gray in color, 23.3 mm in diameter and 42 mm long. One end is terminated by a smooth curved surface indicating the sand face of the well. The other end is a broken surface where the core was broken off. Large vugs are present with apparent remnants of calcite fracture filling. Previous acid treatments have apparently dissolved most of the calcite, leaving open spaces.

Figure 3: Photograph of Core #1

The X-ray ct images of Core #1 (**Fig. 4**) are at 2-mm spacing along the core, starting at the well's sand face from left to right. Red indicates high density or atomic number while blue/black represents low density or voids. There is a concentration of high-density material in the first 1.4 mm of rock. An empty fracture is clearly visible starting with the seventh image.

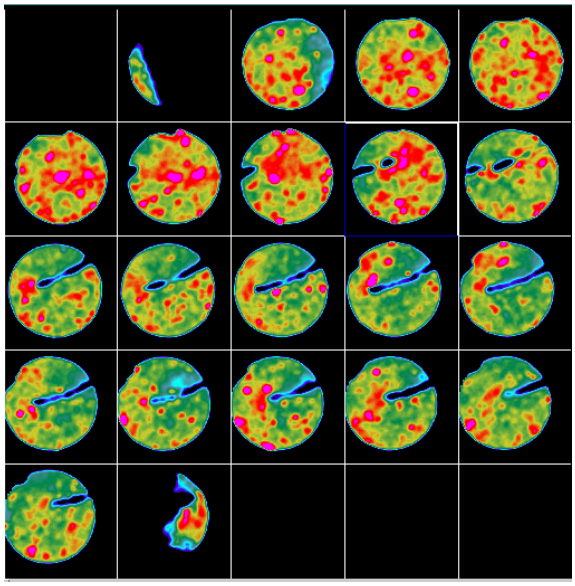

Figure 4: X-Ray CT Images of Core #1

Core #2 (**Fig. 5**) was taken at a depth of 2284 feet. The core is a sandstone, dark gray in color, 23.3 mm in diameter and 37 mm long. One end is terminated by a smooth curved surface indicating the sand face of the well. The other end is a broken surface where the core was broken off. The core appears uniform with no visible vugs or fractures.

Figure 5: Photograph of Core #2

The X-ray ct images of Core #2 (**Fig. 6**) are at 2-mm spacing along the core, starting at the well's sand face from left to right. The few red spots indicate high density or atomic number while blue/black represents low density or voids. The rock appears uniform with no evidence of fractures or dissolution features. Overall density appears lower than the core at 2283.5 feet.

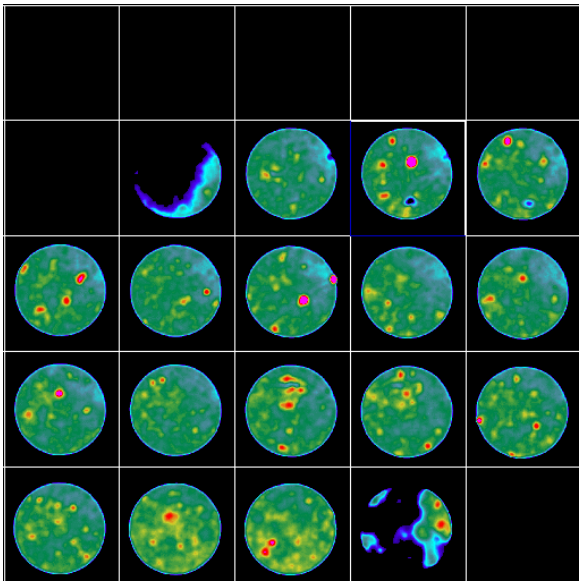

Figure 6: X-Ray CT Images of Core #2

Core #3 (**Fig. 7**) was taken at a depth 2284.5 feet. The core is a sandstone, dark gray to brown in color, 23.4 mm in diameter and 38 mm long. One end is terminated by a smooth curved surface indicating the sand face of the well. The other end is a broken surface where the core was broken off. A major dissolution feature is present on the side of the core along its entire length.

Figure 7:Photograph of Core #3

The X-ray ct images of Core #3 (**Fig. 8**) are at 2-mm spacing along the core, starting at the well's sand face from left to right. Red areas present in the first 12 slices indicate high density or atomic number while blue/black represents low density or voids. The red areas decrease in portion of the core furthest from the sand face. In addition to the dissolved volume visible in the photo, the scans reveal a second internal void of the same magnitude.

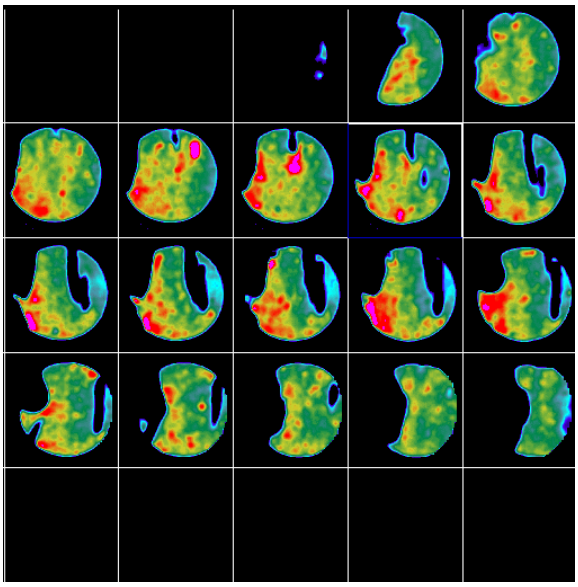

Figure 8: X-Ray CT Images of Core #3

Core #4 (**Fig. 9**) was taken at a depth 2285 feet. The core is a sandstone, dark gray in color, 23.5 mm in diameter and 41 mm long. One end is terminated by a smooth curved surface indicating the sand face of the well. The other end is a broken surface where the core was broken off.

Figure 9: Photograph of Core #4

The X-ray CT images (**Fig. 10**) of Core #4, again at 2-mm spacing along the core, reveal a hidden empty fracture in the interior starting about 8mm into the core. A high-density (red) feature in the forth and fifth images correspond with the plane of the fracture in subsequent images and may represent the material that was dissolved. In general there is less of the high-density material present in this core. It closely resembles core #2 except for the fracture.

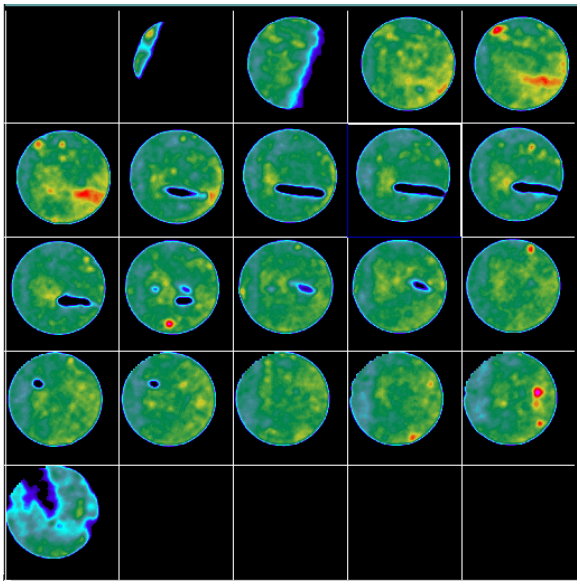

Figure 10: X-Ray CT Images of Core #4

Core #5 (**Fig. 11)** was taken at a depth of 2285.2 feet. The core is a sandstone, dark gray in color, 23.5 mm in diameter and ~22 mm long. One end is terminated by a smooth curved surface indicating the sand face of the well. The core is fractured and the fracture surfaces do not match. An additional piece is missing from the sand face. The material appears homogenous. No X-ray CT scans were taken

Figure 11: Photograph of Core #5

Core #6 (**Fig. 12**) was taken at a depth 2285.2 feet. The core is a sandstone, tan color, 22.5 mm in diameter and 23.5 mm long. Both ends are fracture surfaces and there is an additional axial fracture at one end. This is apparently the first sidewall core from the newly drilled section of the well and there is a distinct difference in color.

Figure 12: Photograph of Core #6

The X-ray CT images (**Fig. 13**) of Core #6 are at 2-mm spacing along the core, starting at the well's sand face from left to right There is significantly more high-density (red) material present than in many of the shallower cores. The fracture is clearly visible in the fourth through seventh images.

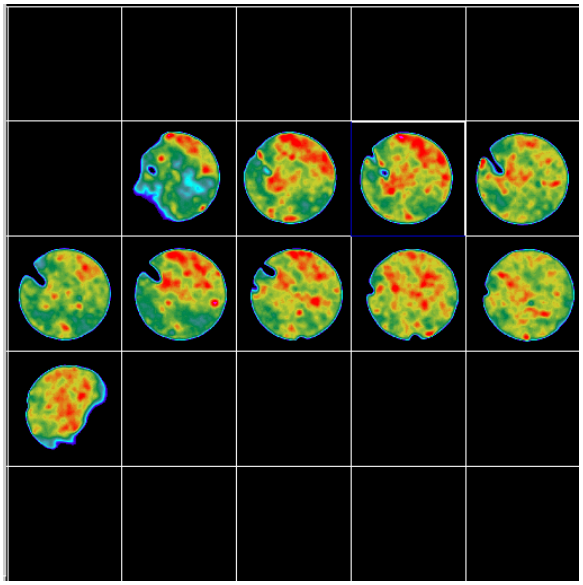

Figure 13: X-Ray CT Images of Core #6

Core #7 (**Fig. 14**) was taken at a depth 2286.5 feet. The core is a sandstone, tan color. The core is largely fragmented with only one small piece of full diameter. No X-ray CT images were taken.

Figure 14: Photograph of Core #7

Core #8 (**Fig. 15**) was taken at a depth of 2293 feet. The core is a sandstone, tan in color, 23.3 mm in diameter and 41 mm long. One end is terminated by a smooth curved surface indicating the sand face of the well. The other end is a broken surface where the core was broken off. The sample appears uniform, although mineralized veins are evident on one side.

Figure 15: Photograph of Core #8

The X-ray ct images (**Fig. 16**) are 2mm thick starting at the well's sand face from left to right. There is significantly more high-density (red) material present than in many of the shallower cores. There is no evidence of fractures or dissolution features.

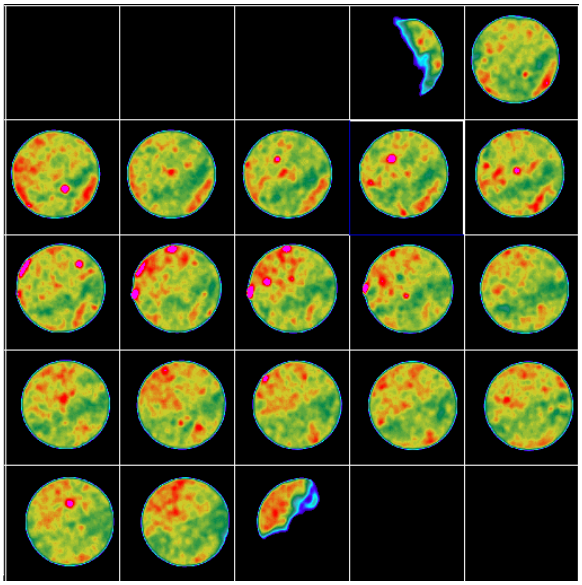

Figure 16: X-Ray CT Images of Core #8

Broadly speaking, these analyses clearly demonstrated the heterogeneous, fractured nature of the Oriskany formation, and highlighted the differences between the "old" and "virgin" portions of the formation. The old section of formation evidenced a fairly successful well treatment (dissolved materials in vugs and fractures), with some

remaining damage extending the full length of the cores. The “virgin portion of the formation evidenced much less damage.

Analysis of Organic Content

The extractable organic matter in cores 2285.2’ and 2286.5’ were analyzed employing two methods: (i) pyrolysis-gas chromatography/mass spectrometry (py-GC/MS) and (ii) extraction with organic solvent. Both methods yielded a paucity of compounds comprised primarily of relatively heavy aliphatic hydrocarbons.

For analysis by Py-GC/MS, approximately 50 mg of sample was loaded into a quartz pyrolysis boat then inserted into a Chemical Data Systems Pyroprobe 1000. The probe was then inserted directly in to the injection port (maintained at 280°C) of a Hewlett Packard 5890 gas chromatograph.

Once in the injection port, the pyroprobe was ramped to a temperature of 610°C at 5°C/ms. Volatile and cleaved organic compounds are swept into the gas chromatograph for separation and identification by the HP 5971 mass spectrometric detector (**Fig. 17**). Pyrolyzate abundances for both samples showed remarkably low total organic carbon content (~0.5-.05%). The major compounds observed were long chain alkanes ranging in carbon number from C20 to C45 with the bulk of the pyrolyzate represented by an unresolved complex mixture (UCM) also representative of aliphatic hydrocarbons. A less abundant suite of chlorinated alkanes was observed for both samples.

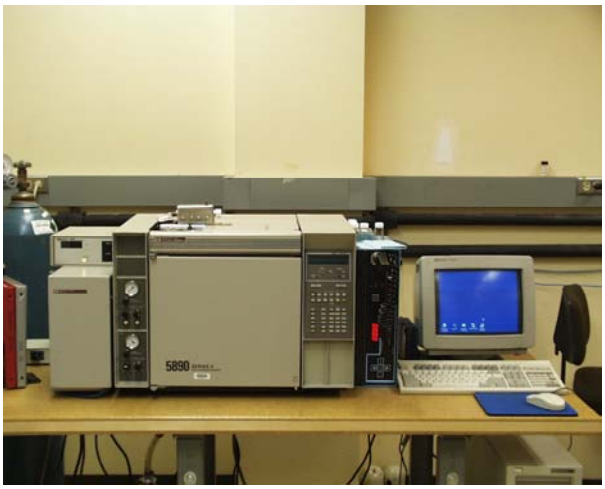

Figure 17: HP 5971 Mass Spectrometric Detector

Additional samples from each of the cores were Soxhlet extracted with methylene chloride for 48 hours to isolate volatile organic compounds. Extraction yields were 0.18% and 0.10% by weight for the upper and lower cores respectively.

The extracts were then further processed by passing samples through an aluminum oxide column to isolate GC-amenable compounds. Yields of this process as a fraction of total sample extracted (26.141 g and 25.231 g) were 0.05% and 0.04% for the upper and lower cores, respectively. The sample extracts were then subjected to analysis by GC/MS for separation and compound identification. The instrument used was a Shimadzu QP5000 (**Fig. 18**).

Figure 18: Shimadzu QP5000

The resulting chromatogram from the upper core is shown below (**Fig 19**), and indicates a homologous series of straight chain alkanes ranging between 20 and 45 carbons comparable to the results of py-GC/MS analyses. Again, the majority of compounds elute as an UCM comprised of aliphatic hydrocarbons. A notable difference was the presence of orthorhombic sulfur (S8) in the extract of the upper core sample.

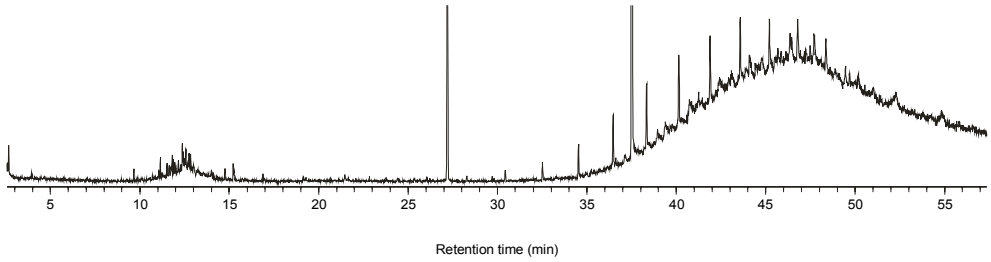

Figure 19: GC/MS trace for W3, core 2285.2'

Both samples were also subjected to analysis utilizing a simulated distillation column and high temperature GC, which allows for observation of relatively 'heavier' hydrocarbons. Chromatograms showed an extended homologous series of straight chain alkanes ranging between C20 and C60 with evidence of an asphaltene-like component eluting at relatively high temperature (450°C).

The solid residue following extraction with methylene chloride was analyzed py-GC/MS. No compounds were observed which means that solvent extraction was sufficient to the removal of organic material.

The core samples delivered to the operator were all from the new portion of the wellbore. The operator sent the cores to Omni Laboratories in Texas for conventional porosity and permeability measurements. Stressed (to 800 psi) porosities in these samples range from 10-16% and the Klinkenberg permeabilities range from 300-1000 md over the interval 2285.5 - 2297'. Details of these analyses are included in **Appendix I** of this report.

W2 Lab Analysis Results

Rotary sidewall cores were taken in W2 in August 2004. Comprehensive RSWC analysis of samples obtained from this well was not possible, due to the fact that virtually all of the cores recovered were extensively broken up. As much analysis as possible was performed on the sample pieces that were collected, as outlined below.

Well Sample Analysis

Black powder samples were recovered from bailed water from W2 from the last core run (cores 2384', 2383' and 2398.8'). The sample was filtered in a glove box containing only nitrogen gas and transferred to a sealed chamber for XRD analysis. Diffraction lines are fully explained by the presence of quartz, calcite and siderite. We exposed the sample to air for fifteen hours, after which the black powder turned brown on the surface. The diffraction pattern however did not change to any appreciable degree with the possible exception of slightly lower siderite peaks.

We collected a small sample from the sandface of core 2387.5. This was mostly quartz with only two other faint lines consistent with calcite and siderite. We then mounted the entire sand face of the core, which is covered with a fine red-brown material. The pattern from this procedure is not as good due to misalignment and roughness of the sample surface. Quartz lines are still prominent, but other unexplained lines do not appear consistent with calcite or siderite (we suspected hemetite or goetite).

Interpretation of Lab Analyses

Based on the analysis results, it appears that most of the damage occurs close to the wellbore, fractures are present in the reservoir, there is very little damage due to organic plugging materials, and the organic compounds that are present are mainly aliphatic hydrocarbons, long chain alkanes, and a very small amount of chlorinated alkanes.

A comparison of the cores from the old section of the wellbore with those from the newly drilled section of the wellbore suggests that prior stimulations were reasonably effective at removing iron-related damage. Nonetheless, some mechanical damage remains, and it appears to be iron-related damage. The color of the entire core differs, depending on whether it is from virgin formation or previously exposed formation. This *may* suggest that some damage occurs deeper in the formation. Notwithstanding this observation, the majority of the visible damage may occur within a few millimeters of the wellbore.

Based on the testing conducted to this point, we were able to state with some certainty the following facts:

1. The elements observed in the scale are and have been iron, calcium, magnesium, sodium, chlorine, sulfur, and oxygen (the presence of carbonate is chemically uncertain).
2. The wells have always produced “black dust” even before conversion to storage. Early examination of the black dust showed Fe0, FeS2, Fe9S8, Fe3O4, SO. More recent examination of wellbore surface scale have also shown FeCO3, FeO(OH), Fe3(O,OH,Cl), MgCl2, NaCl, and SO.
3. Headers contain water condensate and have been known to contain scale.
4. Original gas content contains “mercaptan” of unspecified composition
5. There is no record of H2S, but there is a record of Carbonyl Sulfide (COS) in water solution.

6. Based on camera runs, build up of scale on tubulars and openhole sections can be on the order of ¼ inch thick and extends well above producing formation and casing shoe. Although there is no direct evidence of pitting in the tubulars, this cannot be ruled out.

Hypotheses Based on Lab Analyses Results

Deposition of scale may occur primarily as a result of dehydration of water solutions. This can occur when dry gas is injected through residual pore water in the formation. This can also occur when gas in withdrawn if the reservoir gas is not already saturated with water.

Deposition of scale above the reservoir formation and in the casing occurs by entraining solution droplets in upward flow. The source of the elements in the scale is dominantly from the Oriskany, although some iron may come from tubulars and some sulfur may come from odorizers. The source of the water is the Oriskany. Although some water may come from formations between the casing shoe and the Oriskany or from the formation below the Oriskany, this is unlikely in W3 because of the short distance and the nature of these rocks. Natural fractures or faults could allow water to move between zones.

Discussion of Remediation Field Tests

Summary of Field Activities

The proposed field activities essentially went as planned with two exceptions. First, although the plugs in the wells were eventually pulled successfully, there were some problems washing over the plug latch in some of the wells. Second, sand was not used during the pressure washing phase due to operational problems. A summary of treatment pressures, rates, and activities are shown in **Figures 20-22** below. Summaries of daily stimulation activities are included in **Appendix II**.

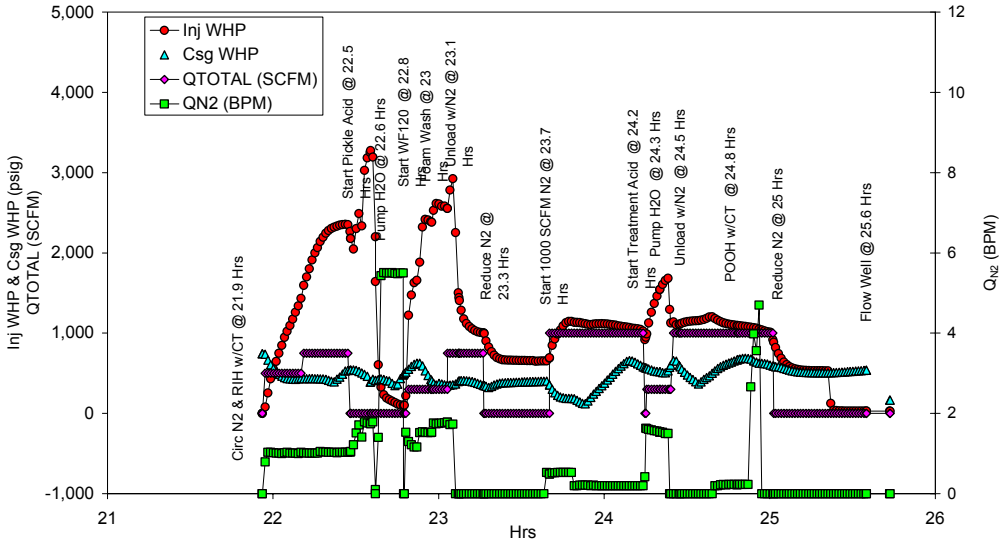

Figure 20: W10 Treatment Summary

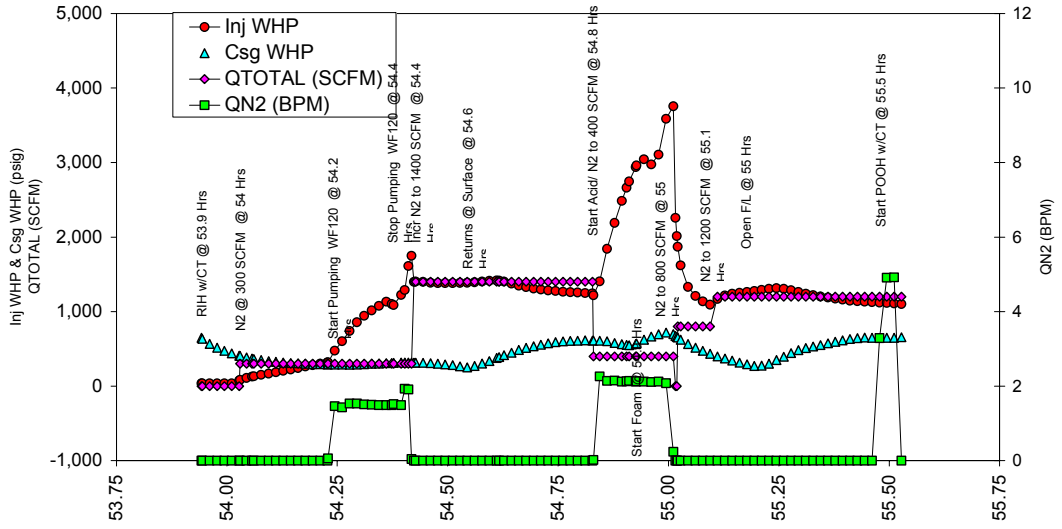

Figure 21: W2 Treatment Summary

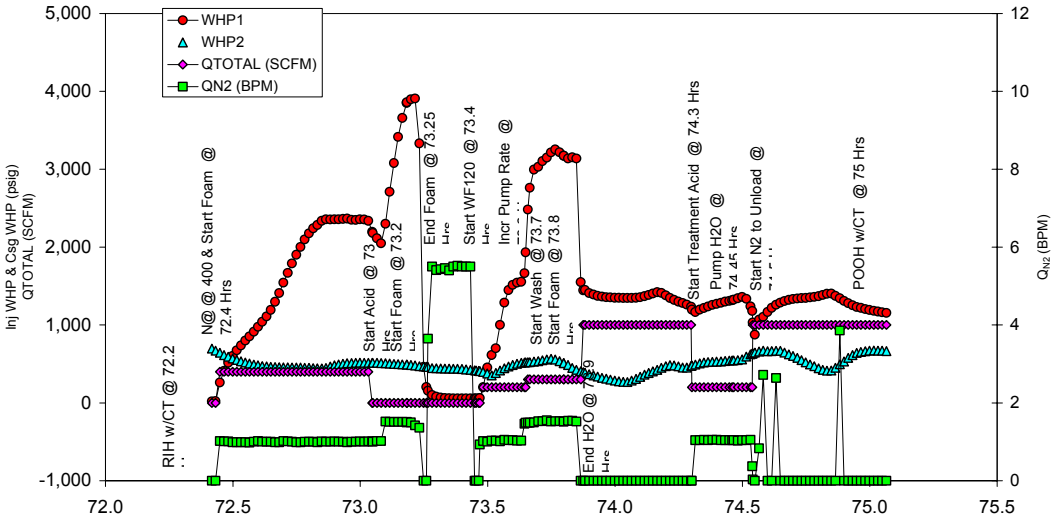

Figure 22: W9 Treatment Summary

Remediation Field Test Results

Overview

In 2002, pre-stimulation tests were run in W2 and W9. These tests consisted of multi-rate pressure transient test using bottom hole pressure recorders. No pre-stimulation test was available from W10.

In the beginning of the project, it was reported that W10 *could not* be flowed. Accordingly, we planned on assuming that any flow observed after stimulation was due entirely to the stimulation. However, in 2004, we learned that W10 was *capable* of flowing, but the well was shut-in due to safety concerns. Consequently, we cannot calculate the *change* in deliverability potential in W10, but only compare the post-stimulation performance of the well to the post-stimulation of other successfully treated wells in the subject field.

Post-stimulation pressure transient tests were not run in 2003, since the likelihood of incomplete cleanup was high the first year after stimulation. Instead, a single-rate backpressure test was performed in 2003 using surface pressure recorders. Comparison of the surface backpressure plots from 2002 and 2003 were used to provide a preliminary and qualitative estimation of the treatment success. Final post-stimulation testing was performed in 2004 and consisted of a multi-rate pressure transient test using bottom hole pressure recorders.

Two analyses techniques were used to assess treatment successfulness. First, the pre-stimulation and post-stimulation backpressure plots constructed using surface pressures were compared for each well. Surface pressure data was used to allow comparison of the 2002 and 2004 data with the 2003 data, since no bottom-hole pressure data was available for the 2003 tests. Second, estimates of mechanical skin and the non-darcy flow coefficient derived from pre-stimulation and post-stimulation plots of rate versus skin were compared for each well. Since the 2003 testing was only a single point test, mechanical and non-darcy skin could not be distinguished for these tests. In addition, as discussed above, no pre-stimulation test was performed in W10.

Results Summary

Table 3 below summarizes test results for the three study wells.

Table 3: Summary of Backpressure and Multi-Rate Pressure Transient Testing in Summit Field

Well	2002			2003			2004		
	Q100WH MMscf/D	Sm Dim'less	D-Factor 1 / MScf/D	$Q100_{WH}$ MMscf/D	Sm Dim'less	D-Factor 1 / MMScf/D	$Q100_{WH}$ MMscf/D	Sm Dim'less	D-Factor 1 / MMScf/D
W2	177	69	0.0096	1,141	N/A	N/A	518	12	0.0058
W9	1,233	11	0.0051	1,117	N/A	N/A	626	43	0.0082
W10	N/A	N/A	N/A	N/A	N/A	N/A	1,178	15	0.0036

Based on these results, W2 appears to have been successfully treated, as evidenced by a reduction in both mechanical skin and the non-darcy flow coefficient from 2002 to 2004. However, damage may be reoccurring, as evidenced by a decline in the Q_{100} value from 2003 to 2004.

Although we cannot assess the *change* in deliverability potential resulting from treatment of W10, we can say that the post-stimulation deliverability potential (i.e., Q_{100}) is similar

to the 2003 post-stimulation Q_{100} in the successfully treated well, W2. Based on 2004 testing, the kh in W10 is comparable to that of well W9.

It appears that the treatment in W9 was unsuccessful, as it resulted in higher mechanical skin and non-darcy flow coefficient (both of which appear to be worsening with time).

W10 Pressure Transient Test Analysis Details

A summary of post-stimulation backpressure test analyses results from W10 are summarized in **Figure 23**. Note that the test in 2003 was a single rate test.

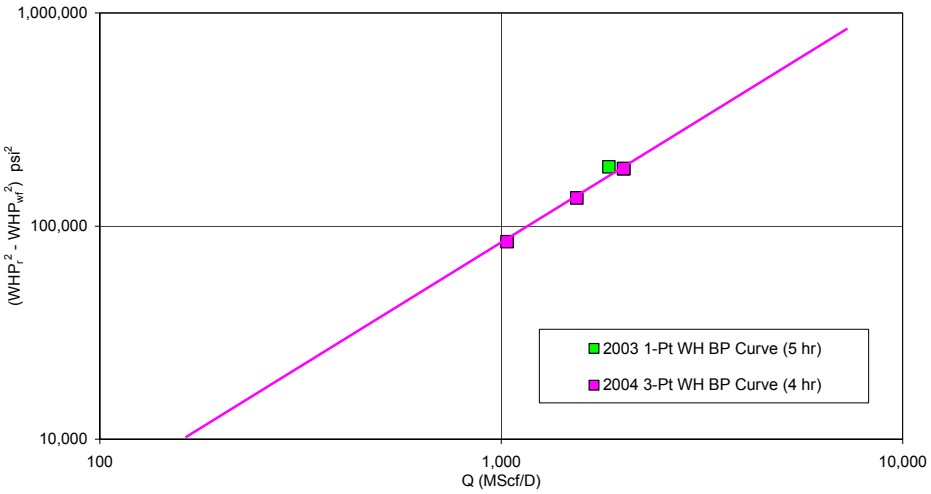

Figure 23: Comparison of Post-Stimulation Backpressure Test Results from W10

Using deliverability at a delta-pressure squared value of 100,000 psi^2, we see the post stimulation deliverability potential in W10 is similar to the 2003 post-stimulation deliverability potential in W2 (shown below in **Figure 25**), which appears to be a successful treatment. We cannot say anything about the *change* in deliverability potential in W10.

A summary of the post-stimulation, multi-rate, pressure transient test results from W10 are summarized in **Figure 24.** This plot indicates that the non-darcy flow coefficient is small and that the mechanical skin and non-darcy flow coefficient in 2004 are similar in magnitude to those from the W2 well's 2003 test.

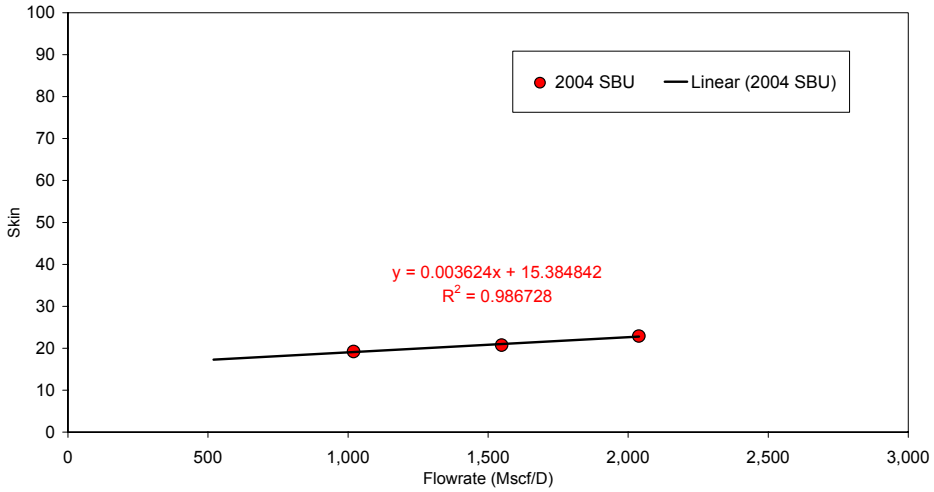

Figure 24: Summary of Post-Stimulation Multi-Rate Pressure Transient Test Results From W10

W2 Pressure Transient Test Analysis Details

A summary of pre- and post-stimulation backpressure test analyses results from W2 are summarized in **Figure 25** (Note: only stabilized points are shown on this plots for clarity).

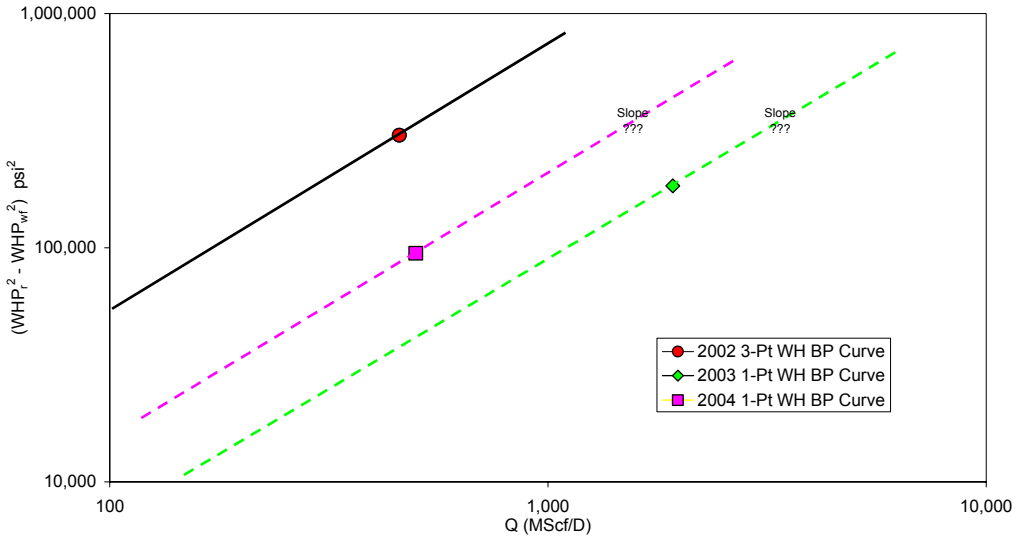

Figure 25: Comparison of post-stimulation skin values for W2

As seen in **Figure 25**, W2 initially (from 2002 to 2003) experienced a very significant increase in its deliverability. However, from 2003 to 2004, we see a significant decrease in deliverability, suggesting that the treatment may have been short-lived, and/or the original source of the damage was not effectively treated. Nonetheless, this well is still much better that before the treatment.

A summary of the post-stimulation, multi-rate, pressure transient test results from W2 are summarized in **Figure 26**, which indicates a significant reduction in the mechanical skin and non-darcy flow coefficient in 2003 and 2004. However, the (calculated) total skin in 2003 at the test rate used in 2004 indicates that total damage (at this rate) has increased slightly from 2003 to 2004.

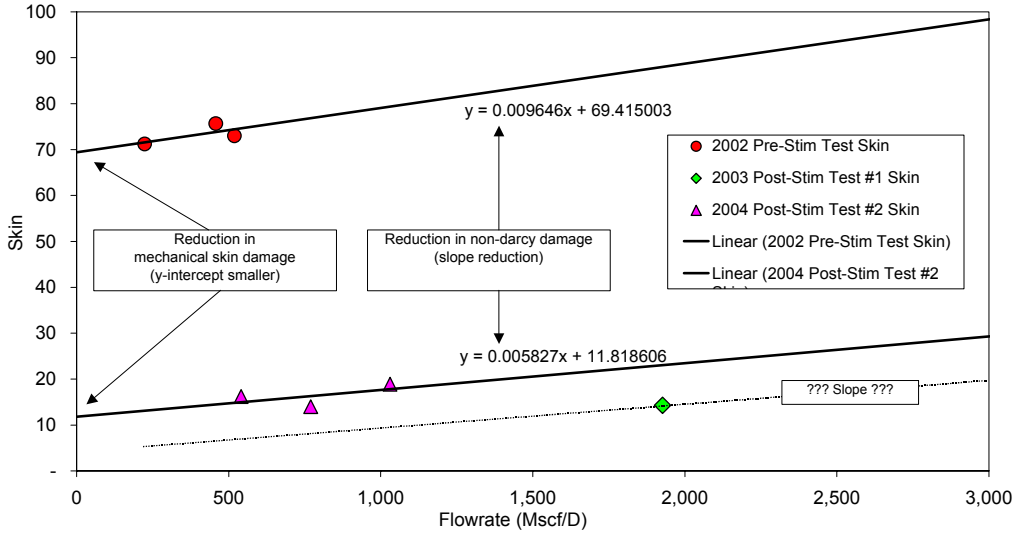

Figure 26: Summary of Multi-Rate Pressure Transient Test Results From W2

W9 Pressure Transient Test Analysis Details

As seen in **Figure 27**, the estimated Q_{100} for W9 has decreased in each of the post-stimulation tests. It would appear from this data that the well is getting progressively worse over time. (Note: only stabilized points are shown on this plots for clarity).

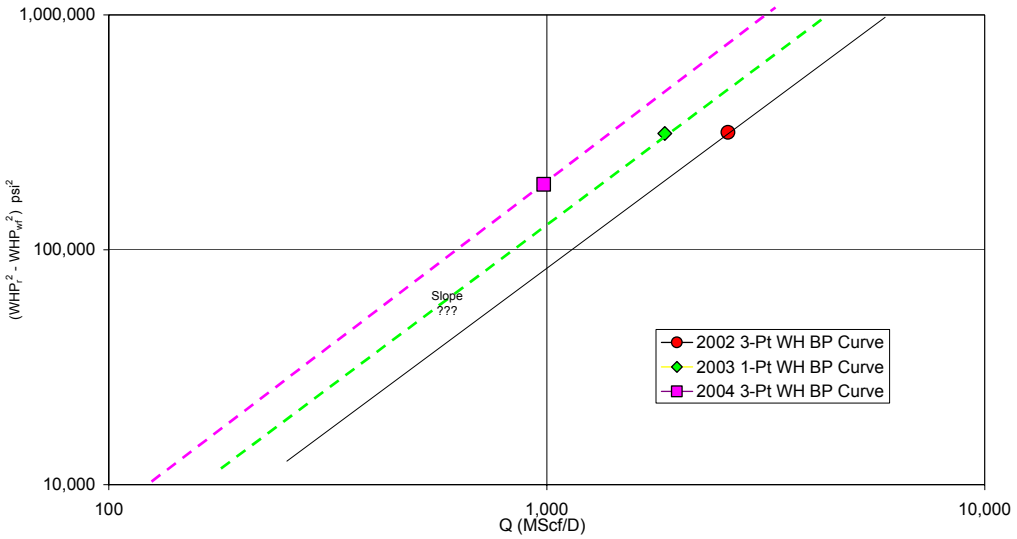

Figure 27: Comparison of Backpressure Test Results from W9

A summary of the post-stimulation, multi-rate, pressure transient test results from W9 are summarized in **Figure 28**, which indicates an increase in the estimated total skin and non-darcy flow coefficient from 2002 to 2004. This also suggests that the well is getting progressively worse over time.

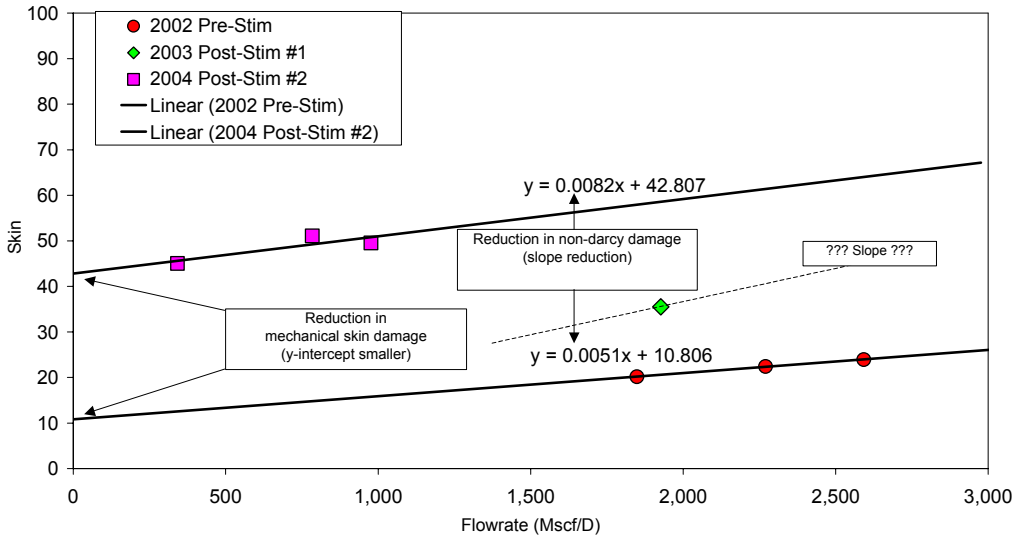

Figure 28: Comparison of skin values from pressure transient test analyses for W9

CONCLUSIONS

Based on testing done to date, it is clear that siderite has been a long-standing problem that pre-dates storage operations and is prevalent throughout the study field. This problem also occurs in many other storage fields.

Initially, the operator successfully restored deliverability in wells damaged by siderite by blowing the well to atmosphere. Several other types of treatments have been tried (e.g., blowing and jetting, perforating, etc.), but testing revealed that blowing the wells was the only consistently successful treatment. However, the operator stopped the practice of blowing wells when it became evident that there were adverse environmental side-effects associated with the practice of blowing wells. To date, no treatment attempted has been as successful as blowing the well. Considering this history, it may be prudent to find an environmentally friendly way to blow the well (from a remediation standpoint – not a prevention standpoint).

A significant amount of prior work aimed at characterization of damage has been done in the study field, which has resulted in several important observations. First, this work identified inorganic scale deposition as the major damage component in the field, and verified that it is ubiquitous in the field. Damage due to organics and bacteria were specifically ruled out. Testing also showed that there is not a significant amount of water sensitive clay in the formation. In addition, the downhole environment was found to be hypersaline, suggesting that evaporate-types of minerals were involved and that buffering treatment fluids would be prudent to prevent adverse reactions between connate water and spent sulfide acid.

A lab protocol was developed as part of this study to confirm that the inorganic precipitate siderite was the damage mechanism. This protocol involved testing of sidewall cores, liquid samples and solid samples. After obtaining rotary sidewall cores, wellbore liquid samples, and solid samples from the two cored wells, this protocol was used to guide testing and analyses of these samples. Although poor core recovery prevented all of the tests prescribed in the protocol from being carried out, the testing successfully verified that the specific inorganic scale found in the samples was siderite.

Multi-rate pressure transient testing successfully identified three damaged wells for use in the study. Rotary sidewall cores were collected in one of the damaged wells selected. The second well selected for rotary sidewall cores was one that had been previously treated and deepened, to allow a comparison of “virgin” formation and the older treated formation, and an evaluation of prior treatment effectiveness. No core was taken in the third well.

Lab analyses of the rotary sidewall cores, solid samples, and liquid samples obtained during this study revealed a number of key facts. Cores from the virgin portion of the formation were distinctly different. These differences suggest that prior acid treatments have been fairly successful at dissolving siderite in fractures, that some of the dissolved material may have migrated to the lower portions of the reservoir, and some damage remains in the full 2 inches of core. Prior notions that organic materials were not the cause of the damage were confirmed, as evidenced by the small amount of organic materials present in the cores. These analyses also suggest that the solvent extraction process alone is capable of removing organics, so analysis via pyrolysis-gas chromatograph/mass spectrometry is not necessary. Finally, analyses suggest that the majority of damage is limited to the very near wellbore region.

Based on all testing to date, we believe deposition of scale occurs primarily as a result of dehydration of Oriskany water, which can occur when dry gas is injected through

residual formation water in the pore spaces. This may also occur when gas is withdrawn if the gas in the reservoir is not already saturated with water. Deposition of scale above the reservoir formation and in the casing occurs via entraining solution droplets in upward flow. We believe the source of the scaling elements is formation water from the Oriskany.

A remedial treatment was proposed that was based on the information derived from all testing done to date. This treatment consisted of pickling the tubing, and pumping a small alcohol-based matrix acid job that was buffered and inhibited. The proposed treatments were executed in the field after running fluid compatibility tests in the lab.

Backpressure multi-rate pressure transient tests run after treatment indicate that two wells were successfully treated. In one well, testing performed one year after treatment indicated that the Q100 increased significantly (nearly a factor of ten). However, the Q100, mechanical skin, and non-darcy damage coefficient worsened at year two. Nonetheless, they were still better than pre-treatment levels. The second well did not have a pre-treatment test run in it, but post-treatment performance was similar to the other successfully treated well.

Testing suggests that the treatment had little or no effect on the third well, as evidenced by no improvement after the first year and an increase in the damage level two years after treatment. Apparently, the proposed treatment did not address the root cause of the damage and/or damage is recurring in this well.

Overall, post-treatment testing suggests that the proposed treatment can potentially remove a significant amount of damage in wells with siderite scale deposition, but that the treatment does not prevent re-precipitation of siderite after treatment. In short, we have developed a treatment capable of treating the problem but not preventing it.

Inhibition was proposed, but the operator did not find an inhibition product that he felt comfortable with. The operator's specific concerns/issues were not communicated to us. Apart from additional operator input we can only assume that there are concerns that the available inhibition products will themselves cause damage in the reservoir or other operational problems.

Recommendations For Future Work

It has been demonstrated that the inorganic precipitate siderite is a common problem in the study field. Experience with many other UGS operators suggests that this specific problem is not limited to the study field, but is prevalent in many UGS fields across the US. Therefore, we recommend future R&D work include siderite-related projects

This study demonstrated the value of the lab protocol developed and the proposed remediation treatment. Therefore, we recommend continued use of the lab protocol and implementation of the treatment where appropriate.

Nonetheless, failure to get good core recovery and the poor quality of recovered cores was a major problem during this study, and prevented full implementation of the lab protocol developed. Inconsistent core recovery and core quality have been problematic in harder rocks typical of some storage reservoirs for some time. Therefore, we recommend future work to develop a RSWC tool that can consistently achieve good core recovery and high quality core samples hard rock formations when coring in a gas environment. Although putting fluid across the formation can improve coring in such environments, this is not recommended, as it will affect the core and result in a sample that may not be representative of the in-situ conditions at the time of sampling.

Long term testing suggests that the damage is recurring after just 2 years in some of the treated wells. Inhibition was proposed to the operator but not pursued. Therefore we propose additional work be done in the area of inhibition. Specifically, we propose that

operators be surveyed to determine their specific concerns related to inhibition. If these concerns are valid, future work should focus on resolving these concerns. If the concerns voiced are not valid, work should focus on educating operators on proper use of inhibitors.

Historically, the only consistently effective treatment of siderite damage in this field has been blowing the well to atmosphere. Obviously, environmental concerns prevent implementation of this remediation method today. However, the fundamental mechanism involved in blowing a well (i.e., exposing the wellbore to instantaneous and severe under-balanced conditions) appears to be consistently successful. Therefore, we recommend that additional work be done to determine an environmentally friendly method of accomplishing the sudden, severe underbalanced conditions caused by blowing a well. One possible scenario might be to set some sort of “ventable” plug near the bottom of the well and evacuating the top portion of the casing, then rapidly blow down the small volume below the plug through the vented plug into the evacuated (top) casing volume. Perhaps this process could be enhanced if the evacuated volume was expanded to include a portion of the header system.

Given that the fundamental mechanism for siderite formation in the study wells involves dehydration of water solutions, the problem will probably never be resolved completely, since some level of water production is inevitable. Therefore, consideration should be given to the design of economical means of continuous removal of water from the wells in an effort to remove one of the components necessary for siderite formation. Such means may include siphon strings, pumps, or gas lift.

NON-DARCY DAMAGE

The Underground Gas Storage Industry and Non-Darcy Well Damage

Non-Darcy pressure drop occurs when gas velocities in the reservoir and/or completion exceed laminar flow. Since any pressure drop that does not result in additional flow in a well is generally considered as "damage," this phenomenon is also commonly referred to as non-darcy damage. In this report, we will use the terms non-darcy pressure drop and non-darcy damage interchangeably. In contrast, mechanical damage is considered to be any physical blockage to flow in the near-wellbore region, such as scales, emulsions, clay swelling, etc.

By their very nature, UGS wells are very prone to non-darcy pressure drops during normal operations. This is primarily due to the very high permeability and rates at which UGS wells operate compared to typical production wells. Typical production wells deplete reserves of similar magnitude over decades, while typical UGS wells deplete "reserves" of similar magnitude over a much shorter timeframe – usually on the order of a few months or less.

The authors have increasingly noticed the widespread occurance of non-darcy damage, particularly in gas storage wells, as they have consulted within the storage sector of the natural gas industry over several decades. We believe the negative consequences of this type of damage is both underestimated and erroneously considered to be irresolvable. Therefore, this portion of the study was aimed at increasing our understanding of this damage mechanism, assessing how successful historical treatments have been at reducing non-darcy damage, and developing new tools to guide storage engineers as they evaluate remediation options available for reduction of non-darcy damage.

Non-Darcy Damage Study Goals & Objectives

Broadly speaking, the non-darcy damage component of this study seeks to increase the UGS industry's awareness of the prevalence, significance, and treatment of non-darcy damage in UGS wells, as well as provide a tool to aid in treatment selection in wells having large non-darcy damage components.

Our first objective involved the collection and analysis of multi-rate backpressure test data from UGS wells that had been treated for damage. Our goal was to obtain at least one pre-treatment well test and one post-treatment well test.

After organizing this data and applying quality control measures, we then sought to evaluate the extent and magnitude of non-darcy damage in UGS wells. The f-factor was developed and used as the primary indicator of non-darcy damage. The f-factor represents the fraction of total dP^2 attributable to non-darcy flow, where $dP^2 = P_r^2 - P_{wf}^2$.

Using the f-factor, we then wanted to identify the types of treatments that were historically successful at reducing the amount of non-darcy damage in a well. Ranking from most successful to least successful by lithology was the end result we desired.

Our second objective involved the development of a spreadsheet tool that can be used by operators to guide treatment selection in wells with significant non-darcy damage component. We envisioned this tool to be one in which we could input known reservoir and completion properties for the damaged state and various treated states, and compare the resulting increase in well performance. Development of such a tool would allow operators to quickly and easily evaluate the various treatment options available. We believe this would prove to be a valuable screening tool for UGS operators.

It important to note, that our analyses focused solely on the non-darcy component of the damage issue. Consequently, our results should reveal which treatments best address the non-darcy component the total damage. However, our rankings may not be indicative of which treatments result in the best overall increase in deliverability. Nonetheless, given that in over 50% of the study wells the *majority* of total dP^2 was non-darcy in nature, we would expect the rankings to be similar.

EXECUTIVE SUMMARY

Objectives

This study had two primary objectives:

1. Increase the UGS industry's awareness and understanding of the prevalence, significance, and treatment of non-darcy damage in UGS wells.
2. Provide a tool to aid in treatment selection in wells having a large non-darcy damage component.

These objectives were accomplished by:

1. Collecting and analyzing multi-rate backpressure test data from UGS wells that have been treated for damage.
2. Evaluating the extent and magnitude of non-darcy damage in UGS wells.
3. Identifying the types of historical treatments that have been successful at reducing the amount of non-darcy damage in a well, and
4. Developing a tool that can be used by operators to guide treatment selection in wells with significant non-darcy damage component.

Results

A database was developed and used to study non-darcy damage in UGS wells. The database contains information on 103 treatments (64 in sandstones and 39 in carbonates). Data was available for 22 treatment types, which were grouped into 13 treatment categories for analysis.

Study data suggests that fewer treatments types have historically been used in carbonates reservoirs than in Sandstones reservoirs. In carbonates, only one treatment category (acidizing) was available for inclusion in the study database. It is not known whether these jobs were pumped at matrix or fracture rates.

Study data also suggests that the non-darcy component of total dP^2 is very significant in both sandstone and carbonate reservoirs. Overall, the non-darcy component of the total dP^2 exceeded 50% in nearly half of the wells tested.

In carbonates, the non-darcy damage component was much larger than in sandstones. The non-darcy component of the total dP^2 exceeded 50% in about 74% of wells in carbonate reservoirs, whereas in sandstones the non-darcy component of the total dP^2 exceeded 50% in about 18% of the wells. These results were similar both before and after stimulation, however, the post-treatment rates were considerably higher.

Benchmarks were established to rank the *technical* success of a treatment's ability to reduce the non-darcy fraction of total dP_2. The technical benchmark (the f-factor) was used to compare levels of non-darcy pressure drop before and after well treatment. This benchmark represents the fraction of total dP^2 that is non-darcy in nature. A reduction in the f-factor after treatment was inferred to be the result of reducing the non-darcy portion of the total dP^2 in the well. The economic benchmark (Mscf/D per $1,000 of treatment cost) was used to rank the economic success of the various treatments.

The importance of using a *normalized* pre-treatment f-factor to ensure valid comparison of pre- and post-treatment f-factors was presented. The potential for a 100% error in the estimation of non-darcy pressure drop using *non*-normalized pre-treatment f-factors was demonstrated.

Study data suggests that a treatments ability to reduce non-darcy dP^2 is influenced by the amount of non-darcy dP^2 in the well prior to stimulation:

1. Wells in which less than 25% of the pre-treatment dP^2 was non-darcy in nature virtually always resulted in wells with *higher* percentage of non-darcy dP^2 after treatment.
2. Wells in which 50% or more of the pre-treatment dP^2 was non-darcy in nature virtually always resulted in wells with *lower* percentage of non-darcy dP^2 after treatment.
3. Wells in which the non-darcy dP^2 was between 25 and 50% showed *mixed results* resulted after treatment.

The results of our ranking of the technical success of treatments showed the following:

1. On average, all treatment categories resulted in some reduction in the non-darcy component of the total dP^2 (i.e., a reduction in the f-factor)
    a. In carbonates, the average reduction in the non-darcy component of the total dP^2 was 17%, and the average rate gain associated with this reduction in non-darcy dP^2 was about 8 MMScf/D
    b. In sandstones, the average reduction in the non-darcy component of the total dP^2 was 29%, and the average rate gain associated with this reduction in non-darcy dP^2 was 2 MMScf/D
2. Although acid treatments in carbonates were shown to be technically successful, most of the treatment types in sandstones were more successful, with several being considerably more successful.
3. The three most technically successful treatments categories all involved hydraulically fracturing the well (fracturing; cleanout, perforating, and fracturing; and cleanout and fracturing).

In addition to evaluating the technical success of treatments, the economic success was also evaluated using an economic indicator (Mscf/D of additional rate per $1,000 of treatment cost). Using this economic indicator, we ranked the economic success of historical treatment categories, which showed the following:

1. Acid jobs are the most cost-effective treatments studied in both carbonates and sandstones.
2. Acid jobs in carbonates are 2-3 times more cost-effective than the best treatment types in sandstones.
3. For sandstones, although acid jobs are slightly more cost effective, no single treatment type stands out as clearly more cost-effective than the others.

Three models were developed in EXCEL™ for use by storage engineers in evaluating which treatment options are most effective at reducing non-darcy damage in UGS wells. The three models include an open hole completion model, a cased-hole model, and a fractured well model

Using these models, we evaluated the potential for reduction in non-darcy damage. The results of this evaluation are as follows:

1. Consistent with the field study results, the modeling work showed that hydraulic fracturing provided the greatest improvement in deliverability for both the open-hole and cased-hole scenarios. In these scenarios, the predicted performance for a well of a given completion type, with average reservoir and completion

properties from the AGA database, and in an undamaged condition, was compared to the predicted performance for a typical stimulation and a maximum stimulation for several different scenarios.

2. The open-hole model predicted only a small pressure drop attributable to non-darcy flow for any reasonable combination of reservoir and completion properties. Underreaming reduced the non-darcy component of the pressure drop by a small amount, while acidizing and fracturing both increased it slightly.

3. The cased-hole model showed the highest degree of non-darcy flow of the three models because of the high velocity as the gas converges on the perforations. Increasing the number of perforations or the depth of the perforation tunnels reduced the non-darcy component of the pressure drop, while the greatest benefit was obtained from fracturing.

4. The fracture model shows some improvement in deliverabilty could be obtained with a longer fracture, a wider fracture, or a higher fracture permeability.

Conclusions

The database developed for this study was useful for the identification of trends and evaluation of treatment effectiveness. The updating of this database and expansion to include more detailed test and treatment data could prove beneficial to the UGS industry.

When comparing the non-darcy component of total dP^2 in UGS wells, it is imperative that the comparison be done at a consistent flowrate, since non-darcy dP^2 is a rate-dependent phenomenon.

Non-Darcy damage is ubiquitous in UGS wells and results in a very significant amount of non-productive energy loss (i.e., pressure drop) that could be used to achieve additional deliverability if reduced or eliminated. Based on the trends identified in this study, if non-darcy pressure drop could be eliminated *just* in the wells wherein it represents the majority of the total pressure loss, The deliverability of the U.S. UGS industry could be raised by about 30 BCF per day.

Given the prevalence and magnitude of non-darcy damage in UGS wells, the ability to reduce or eliminate non-darcy pressure drop in these wells represents a huge potential for increased deliverability from UGS wells.

It is important to evaluate both the technical and economic success of treatments, since there may be overlooked opportunities to reduce the costs associated with the less technically successful treatment types.

It was demonstrated during the study that the most technically successful treatments are not necessarily the most economically successful. Therefore, UGS operators must guard against the temptation to compare only well performance when managing deliverability maintenance programs.

Studies using the *open-hole* model developed in this study suggest the following:

1. Costs aside, modeling results suggest that hydraulic fracturing is the most effective means to reduce the non-darcy component of dP^2 in *open-hole* completions, and that rate increases of 40-100% can be expected after treatment.

2. Open-Hole modeling shows that acidizing is the most cost-effective treatment to reduce the non-darcy component of dP^2 in *open-hole* completions, and that rate increases of 50% can be expected after treatment.

Studies using the *cased-hole* model developed in this study suggest the following:

3. Costs aside, modeling results suggest that hydraulic fracturing is the most effective means to reduce the non-darcy component of dP^2 in *cased-hole* completions, and that rate increases of 150-300% can be expected after treatment.
4. Cased-Hole modeling shows that increasing the number, depth, or diameter of perforations is the most cost-effective treatment to reduce the non-darcy component of dP^2 in *cased-hole* completions, and that rate increases of 20-60% can be expected after treatment.

Studies using the *fractured* model developed in this study suggest the following:

5. Costs aside, modeling results suggest that increasing the length or width of the fracture, or increasing the permeability in the fracture, all reduce the non-darcy component of dP^2 in *fractured completions*, and that rate increases of 20-40% can be expected after treatment.
6. Fractured modeling shows that increasing the length or width of the fracture is the most cost-effective treatment to reduce the non-darcy component of dP^2 in *fractured completions*, and that rate increases of 25-30% can be expected after treatment.

Recommendations

This study has demonstrated that non-darcy damage is both ubiquitous and significant in the UGS industry, and result in a very significant amount of unaccessible deliverability. Clearly, additional work in the area of non-darcy damage reduction is warranted, and therefore recommended.

Given its usefulness, we believe the study database should be periodically updated and expanded it to include the following data:

1. Detailed multi-rate pressure transient test analysis results, including mechanical skin damage ($S_{mechanical}$) and non-darcy damage coefficient (D-factor, which represents the slope of the line on a rate versus total skin plot from a multi-rate pressure transient test).

2. Detailed stimulation data, including amounts and types of treatment fluids used, treatment methods, pressures and rates, and multiple post-stimulation tests.

Modeling results suggest that the key to reducing non-darcy component of total dP^2 is to eliminate choke points in the completion where high gas velocities exist. Approaches to reducing the non-darcy component of total dP2 should focus on the following types of treatments:

1. In open-hole completions, make every effort to maximize the amount of sandface open to flow. In view of the high degree of non-darcy damage observed in many open-hole completions, it is likely that these wells have some degree of sandface obstruction.
2. In cased-hole completions focus on increasing the number, length, and depth of penetration ion order to reduces the effects of non-darcy flow.

3. In fractured completions, focus on increasing the length or width of the fracture, or increasing the permeability of the proppant pack, to reduce the effects of non-darcy flow. Of these factors, increasing the fracture length appears to the most feasible with current technology.

Relevance to Future Technological Developments

Perhaps the most significant outcome of this study was the demonstration of how prevalent and significant non-darcy damage is in the UGS industry. While the precision of the study results may be debatable, the order-of-magnitude of the results are indisputable – clearly, a significant percentage of UGS wells evidence a large amount of non-darcy damage that results in a huge reduction in deliverability.

Modeling results suggest that approaches to reducing the non-darcy component of total dP^2 should focus on eliminating choke points in the completion where high gas velocities exist. For open-hole completions, research should focus on determining whether or not partial sandface obstruction is a common cause of non-darcy flow, as suggested by the modeling study, and if so, identifying the most effective ways to remove or reduce the obstruction. Unfractured cased-hole completions should be used only where necessary for wellbore stability and where fracturing is not feasible. Under these conditions, cased-hole completions may be optimized by using a large number of deeply penetrating perforations. For fractured completions, research should focus on technologies to creater wider, more conductive fractures and to reduce fracturing costs.

EXPERIMENTAL

Development of Non-Darcy Damage Database

As part of this study, numerous UGS operators in North America were solicited to provide multi-rate backpressure test data before and after treatments in order to assess the impact of various treatments on the non-darcy damage component. Operators responded by providing multi-rate pre- and post-treatment test data for 103 wells, of which 64 were in sandstones (62%), and 39 were in carbonates (36%). Data was available for 22 treatment types, which were grouped into 13 treatment categories.

Data Available

Data entered into the study database include the following specific items:

- General well information
- General reservoir information
- General treatment information
    - Treatment dates
    - Treatment types
    - Approximate treatment costs
- Backpressure test data, including
    - Test Dates
    - Shut-in Pressures
    - Flowing Pressures
    - Flow Rates
    - Backpressure equation coefficients (C, n) calculated by the operator (if available)

Quality Control of Data

Data was entered and quality controlled to ensure that only valid data was analyzed. Any wells/treatments having questionable treatment data, erratic test data (i.e., very low r^2 values), or calculated parameters outside theoretically valid limits (e.g., calculated backpressure equation exponents less than 0.5 or more than 1.0) were excluded from the analysis process.

Data Processing

The various types of treatments in the study were grouped into major categories, with similar types of treatments grouped together. The treatment groupings are summarized in **Table 1** below.

Table 4: Grouping of primary treatments into treatment catagories

Lith	Treatment Catagory	Primary Treatment
Carbonate	ACID	Acid
Sandstone	ACID	Acid
Sandstone	ACID	Acid & Water
Sandstone	ACID & CO	Acid & CO
Sandstone	ACID & CO	Acid & CTC
Sandstone	ACID & CO	Acid & HB
Sandstone	ACID & CO	CTC & Acid
Sandstone	ACID & CO	Xylene & Acid & CO
Sandstone	ACID & PERF	Acid & OHPerf
Sandstone	ACID & UR	Acid & UR
Sandstone	CO	CO & HB
Sandstone	CO	CTC
Sandstone	CO & FRAC	CTC & Frac
Sandstone	CO & PERF	CTC & Perf
Sandstone	CO & Perf & Acid	Acid & CO & CHPerf
Sandstone	CO & Perf & Acid	CTC & Perf & Acid
Sandstone	CO & Perf & Frac	CTC & Perf & Frac
Sandstone	FRAC	FRAC
Sandstone	PERF	OHPerf
Sandstone	PERF	Perf
Sandstone	PERF	Perf & Surge
Sandstone	PERF & FRAC	Perf & Frac

Abbreviations		
ACID	==========	Acid Job
CHPerf	==========	Cased Hole Perforate
CO	==========	Cleanout
CTC	==========	Coiled Tbg Cleanout
FRAC	==========	Hydraulic Fracture
HB	==========	Hydroblast
OHPerf	==========	Open Hole Perforate
PERF	==========	Perforate
Surge	==========	Surge Well
UR	==========	Underream
Xylene	==========	Xylene Wash

Using the database, several key parameters were calculated at pre-treatment and post-treatment conditions. These pre-treatment and post-treatment parameters were then used to assess the effectiveness of specific treatments at reducing the non-darcy component of the total dP^2.

The calculations performed on each backpressure test dataset are summarized as follows (see **Appendix III** for the equations used in this process):

- The array of test rate and corresponding dP^2 values was retrieved.
- The extended flow period was identified
- The geometric mean flow rate for the test was calculated.
- The coefficients of the Hoeupert deliverability equation (a, b) were calculated via a least squares fit of the test data.
- The correlation coefficient (r^2 value) describing the quality of the least squares fit was calculated.

- Backpressure equation coefficients (C, n) were calculated from raw test data
- Backpressure equation coefficients (C, n) were calculated from the coefficients of the Hoeupert deliverability equation (a, b)
- Three f-values were calculated (Note: as discussed in more detail below, f-values are calculated using the Hoeupert equation, and are defined as $bq^2/(aq+bq^2)$, where a and b are the coefficients in the Hoeupert equation and q is the geometric mean flow rate during the test):
    - A pre-treatment f-value
        - a and b values are from the *pre*-treatment test analysis
        - q value is geometric mean flow rate during *pre*-treatment test
    - A "normalized" pre-treatment f-value
        - a and b values are from the *pre*-treatment test analysis
        - q value is geometric mean flow rate during *post*-treatment test
    - A post-treatment f-value
        - a and b values are from the *post*-treatment test analysis
        - q value is geometric mean flow rate during *post*-treatment test
- All results are stored in a database table

As discussed in **Appendix III**, the calculated f-values represent the fraction of the total dP^2 resulting from non-darcy damage. If the f-factor decreases after a treatment, we infer that the fraction of the total dP^2 resulting from non-darcy damage declined as a result of the treatment. Conversely, if the f-factor increases after a treatment, we infer that the fraction of the total dP^2 resulting from non-darcy damage increased as a result of the treatment

A "normalized" pre-treatment f-value was used in order to evaluate the change in non-darcy flow effects before and after treatment at a common flow rate. This is necessary, since non-darcy flow is a velocity-dependent phenomenon. A more detailed discussion concerning the calculation and use of the "normalized" pre-treatment f-value appears in the Results and Discussion section of this report.

Development of Tools to Assess Non-Darcy Damage Treatments

Theoretical Background

Three 4-pt test simulators have been developed for 1) open-hole completions, 2) cased-hole completions, and 3) hydraulically fractured completions. All three simulators couple a pseudosteady-state reservoir model with a tubing model to generate a synthetic 4-pt test. The open-hole and cased-hole simulators use different forms of the Jones equation to model pressure drop in the reservoir, while the fracture simulator uses a rate-dependent fracture conductivity to estimate an equivalent wellbore radius.

All three simulators use essentially the same solution method. To simulate a 4-point test, the flow rate is calculated for a series of four different wellhead pressures, chosen so that the flow rates form an approximate arithmetic progression. To use wellhead

pressures as the input, the simulator couples a tubing model with a reservoir model to estimate bottom hole pressures.

The tubing model allows the bottomhole pressure to be calculated, assuming the wellhead pressure and flow rate are known. The reservoir model allows the flow rate to be calculated, assuming the average reservoir pressure and sandface pressure are known. To couple the tubing and reservoir models, an iterative solution method is required. The bisection method is used for its simplicity and robustness.

Mathematical derivations and other details related to development of these models and spreadsheets can be found in **Appendix IV**.

Open Hole Simulator

In the open-hole simulator, the well is assumed to be centered in a circular drainage area of radius r_e, in a reservoir having uniform net pay thickness h, permeability k, porosity ϕ, and water saturation S_w. Any damage or stimulation is assumed to be caused by an altered zone around the wellbore, of radius r_a, having permeability k_a, porosity ϕ_a, and water saturation S_{wa}. Damage will be represented by an altered zone permeability ka that is lower than the formation permeability k, while stimulation will be represented by an altered zone permeability that is higher than the formation permeability. The well penetrates a distance h_p into the formation, so the model handles partial penetration. **Figure 29** shows a schematic of the open-hole completion model.

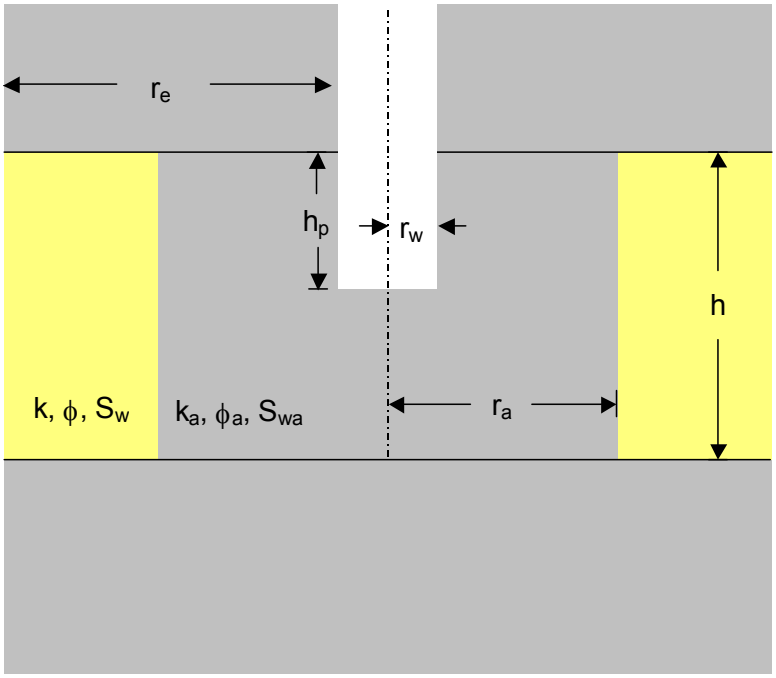

Figure 29: Schematic of the open hole completion model

Cased Hole Simulator

In the cased-hole simulator, as in the open-hole simulator, the well is assumed to be centered in a circular drainage area of radius r_e, in a reservoir having uniform net pay thickness h, permeability k, porosity ϕ, and water saturation S_w. Any damage or stimulation is assumed to be caused by an altered zone around the wellbore, of radius

r_a, having permeability k_a, porosity ϕ_a, and water saturation S_{wa}. Only the first h_p of the net pay is perforated.

Perforations are assumed to be uniformly spaced at n_s shots per foot. Each perforation has diameter d_p and length l_p. If there is an altered zone around the wellbore, the radius of the altered zone is assumed to be larger than the length of the perforations, so that the perforations do not extend into the unaltered reservoir. If there is an altered zone, the β-factor (as defined in the Forchheimer equation[2]) is estimated from the properties of the altered zone; otherwise, the β-factor is estimated from the bulk reservoir properties.

Figure 30 shows a schematic of the cased-hole completion model

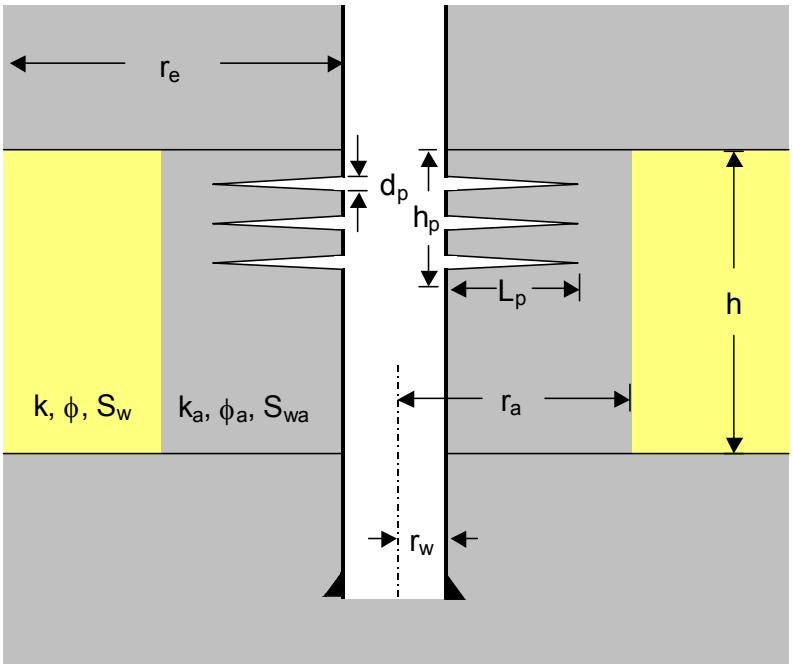

Figure 30: Schematic of the cased-hole completion model

The cased-hole simulator may also be used to predict the behavior of open-hole completions where the sandface is partially obstructed. In this scenario, the "perforations" correspond to that portion of the sandface that is in communication with the wellbore.

Fractured Simulator

In the fractured well simulator, as in the cased-hole and open-hole simulators, the well is assumed to be centered in a circular drainage area of radius r_e, in a reservoir having uniform net pay thickness h, permeability k, porosity ϕ, and water saturation S_w. The fracture is assumed to have equal length wings, each of length L_f, width w_f, and permeability k_f. All fluid is assumed to flow into the wellbore through the fracture. **Figure 31** shows a schematic of the fractured completion model.

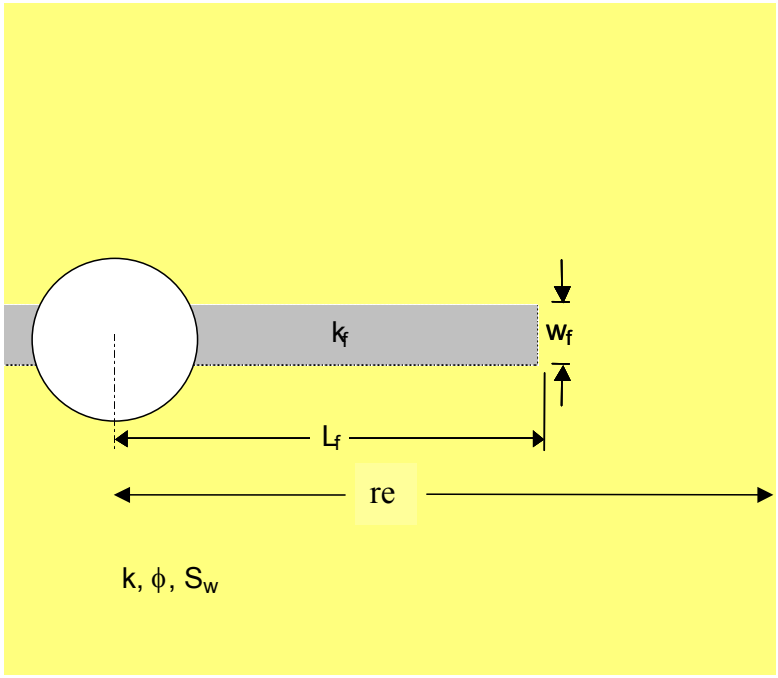

Figure 31: Schematic of the fractured completion model

A thorough discussion covering the theoretical development of these models, their use, and their limitations, is included in **Appendix IV**.

RESULTS AND DISCUSSION

Look-Back Study

Theoretical Background

It has been known for over a century that Darcy's law is inadequate to describe the high velocity flow of gases through porous media. In 1901, Forchheimer proposed adding a term proportional to the square of the velocity to the pressure drop predicted by Darcy's law in order to more realistically model the behavior of single phase flow[6]. Although other nonlinear relationships have been proposed to model high-velocity flow effects, the Forchheimer equation is the most widely accepted.

The Forchheimer equation describes pressure drop due to non-Darcy flow within the reservoir. A simplified approach to modeling non-Darcy flow is to treat the pressure drop due to non-Darcy flow as a rate-dependent skin factor, concentrated at the sand face or across the completion. This may occur, for example, in a well with a cased-hole completion, where high velocity flow occurs as flow converges toward the perforations[3], and, in a gravel-packed completion, through the sand in the perforation tunnels[4, 5]. For a cased-hole completion, velocities through the perforations may be 50 times higher than in an open-hole completion[6].

The Forcheimer Equation can be written as shown in **Eqn 1**, where P is pressure, x is the coordinate in the flow direction, u is viscosity, v is average velocity, k is permeability, β is the turbulence or beta factor, and ρ is fluid density.

$$\frac{\partial P}{\partial x} = \frac{uv}{k} + \beta \rho v^2 \qquad \textbf{Eqn 1}$$

The turbulence factor, β can be approximated as shown in **Eqn 2** below:

$$\beta = \frac{2.23x10^{10}}{k^{1.201}} \qquad \textbf{Eqn 2}$$

As is evident from **Eqn 1**, the non-darcy flow component of pressure drop for fluid flow in porous media, $\beta \rho v^2$, is a function of the turbulence factor (which is permeability-dependent), the velocity of the fluid, and the density of the fluid. The implication of these relationships suggests that there are at least four practical ways we can reduce the pressure drop due to non-darcy flow:

1. We could increase the effective permeability of the reservoir (thus reducing the beta-factor). Since most of the pressure drop occurs in the near-wellbore region, increasing the near-wellbore permeability may prove practical in carbonate formations, where "wormholes" from acidizing would increase the permeability.

2. Second, we could decrease the velocity of the fluids in the near-wellbore region by increasing the effective radius of the wellbore. This could be accomplished by underreaming in an open hole completion, by milling and underreaming in a cased hole completion, or by fracturing the well.

3. Third, we could decrease the velocity of the fluids in the near-wellbore region by increasing the shots per foot in a cased hole completion. This would reduce convergence of fluid flow into a limited flow area in the near-wellbore region, thus effectively reducing the velocity of the fluid through the porous media.

4. Fourth, in partially completed wells (i.e., wells that are not drilled completely through the reservoir), deepening the well through the entire reservoir would also reduce convergence of fluid flow in the near-wellbore region. As in the case of increasing the perforation shot density, the result would be to reduce the velocity of the fluid in the porous media.

Theoretical Considerations

As described in detail in **Appendix III**, the Rawlins-Schellhardt deliverability equation was combined with the Hoeupert deliverability equation to arrive at a method of determining the a and b coefficients in the Hoeupert equation from the C and n factors in the Rawlins-Schellhardt equation. This was done to enable operators with only the C and n-values to convert test results to a and b coefficients in the Hoeupert equation. Then, using the Hoeupert equation, the f-factor (which represents the fraction of total dP^2 attributable to non-Darcy flow) was defined as follows:

$$f = \frac{bq^2}{aq + bq^2} \quad \text{.....(3)}$$

where a and b are the coefficients of the Hoeupert equation as determined from analysis of test data, and q is the geometric mean flow rate during the test.

In this study, we assume that the change in f-factor resulting from a given treatment reflects how effective that treatment was at reducing the fraction of total dP^2 attributable to non-Darcy flow. For example, if the pre-treatment f-factor was 0.8 (i.e., 80% of the total dP^2 was attributable to non-darcy flow), and the post- treatment f-factor was 0.4 (i.e., 40% of the total dP^2 was attributable to non-darcy flow), we would conclude that the treatment resulted in a 50% reduction in the non-darcy component of the total dP^2. Stated more simply, albeit less precisely, the treatment resulted in a 50% reduction in the non-darcy pressure drop (i.e., dP^2) occurring during normal operating conditions.

It is clear from the above equation, however, that the fraction of total dP^2 attributable to non-Darcy flow is a function of the flow rate. Consequently, any comparison of f-factors *must* be made at a common flow rate. For example, suppose a treatment had no effect whatsoever on the wells deliverability. In such a case, the pre-treatment and post-treatment a and b coefficients in the Hoeupert equation would be identical. However, if pre-treatment rates (q_{pre}) used to calculate f_{pre} is different from the post-treatment rates (q_{post}) used to calculate f_{post}, the calculated change in the f-factor will *not* be zero. Obviously, this would result in the incorrect conclusion that the treatment affected the f-factor (the fraction of the total dP^2 attributable to non-Darcy flow).

Therefore in this study, we calculated a *normalized* pre-treatment f-factor, using the a and b Hoeupert coefficients calculated from pre-treatment test data, and the geometric mean flowrate from the post-treatment test, to ensure that the f-factor comparison was made at a common flowrate. The post-treatment flow rate was chosen because it is

generally considered to be more representative of normal operating conditions than the pre-treatment flow rate (which is likely too low, due to the presence of damage).

Figure 32 is a plot of the pre-treatment f-factor (calculated using the geometric mean flowrate from the *pre*-treatment test) versus the *normalized* pre-treatment f-factor (calculated using the geometric mean flowrate from the *post*-treatment test) for all study wells. If non-darcy pressure drop were *not* a function of rate, these two values would be the same, all points would fall on the unit slope line, and no normalization would be necessary. In reality, non-darcy pressure drop *is* a function of rate. After normalizing the pre-treatment f-factor to correspond to the post-treatment rate, we find that virtually all of the *normalized* pre-treatment f-factors fall above the unit slope line. This plot demonstrates how severely understated the non-darcy pressure drop can be without normalization. For example, pre-treatment f-factors around of 45% may actually represent *normalized* pre-treatment f-factors of up to 90%. Thus, in this example, without normalization we may underestimate the pre-treatment f-factor by 100%.

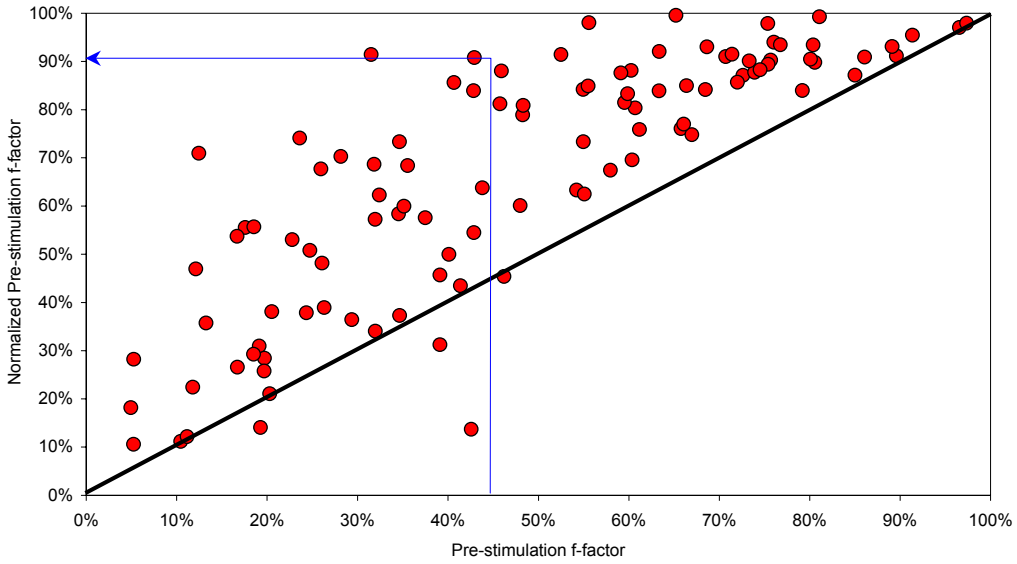

Figure 32: Pre-treatment f-factor versus *normalized* pre-treatment f-factor

Theoretically, f-factors approaching 1.0 suggest that virtually all of the dP^2 is due to non-darcy flow. Conversely, f-factor values approaching 0.0 suggest that virtually none of the dP^2 is due to non-darcy flow. It would be very tempting to conclude from this that high f-values always correspond to high non-darcy skin damage, and low f-factors always correspond to low non-darcy skin damage. However, lack of data (specifically, the non-darcy flow coefficient, or D-factor, as determined from multi-rate pressure transient test analysis) prevented us from confirming this hypothesis.

Moreover, there is a very complex relationship between the mechanical and non-darcy components of skin damage. For example, excessive scale covering the majority of pay in a wellbore (typically considered to be mechanical damage) may result in flow convergence into the small portion of pay that remains open, which causes non-darcy pressure drop. While a large portion of the total damage is non-darcy in nature, it is almost certainly caused by the presence of mechanical skin.

As shown in **Figure 33** and **Figure 34** comparisons of backpressure equation C- and n-values we calculated with those calculated by the operators generally showed very good agreement. We performed these calculations as a form of quality control.

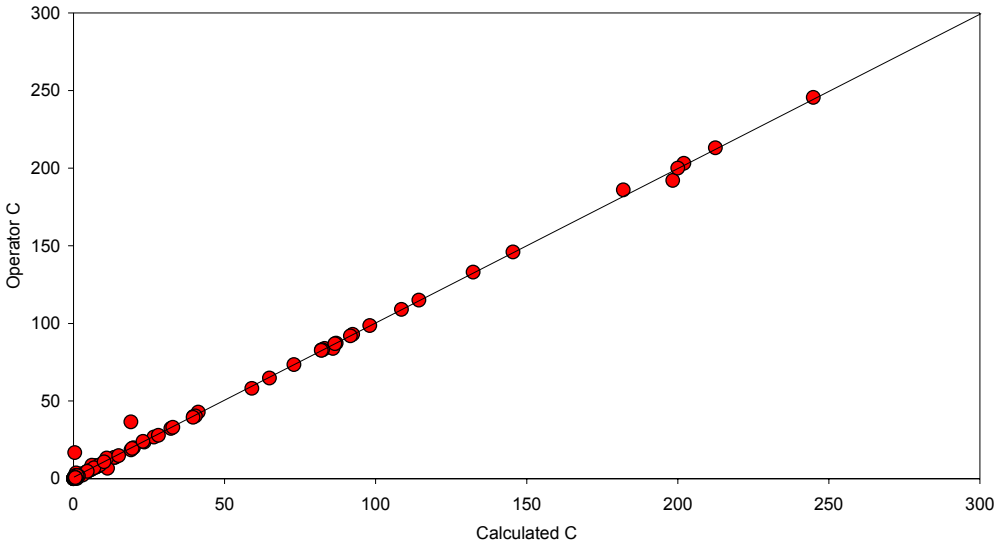

Figure 33: Comparison of calculated C-factors with C-factors reported by operators

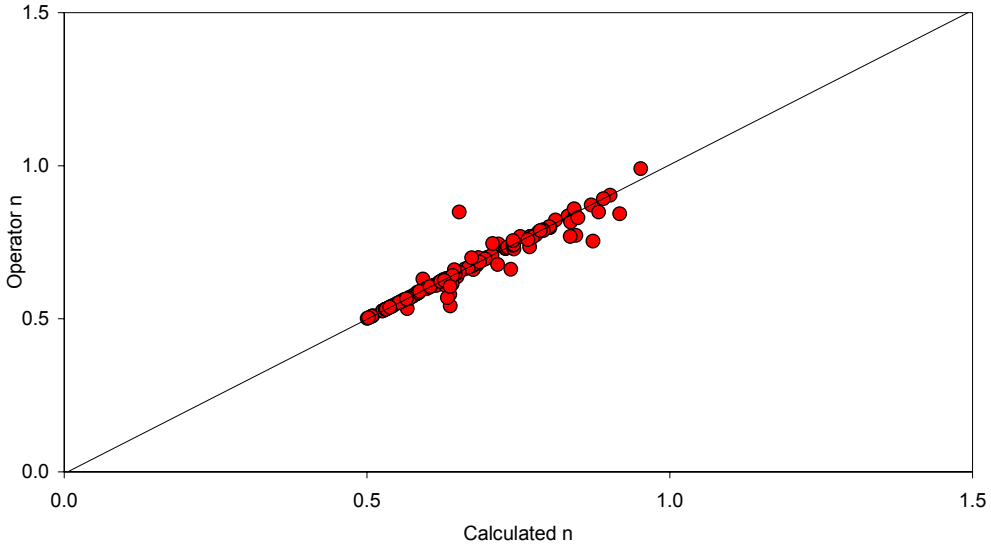

Figure 34: Comparison of calculated n-factors with n-factors reported by operators

Prevalence of Non-Darcy Damage

Our analysis suggests that the non-darcy damage component is both ubiquitous and significant in wells completed in both sandstone and carbonate reservoirs. Overall, in nearly half of the treated wells, the non-darcy component of the total dP^2 exceeded 50%. Stated differently, the *majority* of the dP^2 is due to non-darcy damage in nearly half of the study wells. This was true both before and after treatment, suggesting that even after treating wells the percentage of total dP^2 attributable to non-darcy flow is very significant.

It is wrong to conclude from this that treatments were not successful. Instead, the high post-treatment non-darcy dP^2 is the result of much higher post-treatment rates.

In carbonates, the non-darcy damage component was typically much larger than in sandstones. The non-darcy component of the total dP^2 exceed 50% in about 74% of treated wells completed in carbonate reservoirs, whereas in sandstones the non-darcy component of the total dP^2 exceed 50% in about 28% of treated wells. This difference is likely a function of the larger flow rates typically achieved from wells completed in carbonate reservoirs, and is reflected in the Q_{100} values (i.e., the flowrate achievable at a dP^2 of 100,000 psi^2). The average Q_{100} for study wells in carbonate reservoirs is about 15 MMscf/D in wells prior to treatment and about 33 MMScf/D after treatment. In contrast, the average Q_{100} values for study wells in sandstones is about 2 MMscf/D in wells prior to treatment and is about 4 MMScf/D after treatment.

Significance of Eliminating Non-Darcy Damage

Theoretically, if 50% of the total dP^2 in a well is due to non-darcy damage, elimination of the non-darcy damage will result in a doubling of the well's rate at the same dP^2. The implications of this are profound - the reduction or elimination of non-darcy damage in UGS wells represents a very significant opportunity to increase the deliverability available from existing UGS wells.

If the wells in the study database represent the industry as a whole (i.e., in half of the wells, the non-darcy component of the total dP^2 exceeded 50%) elimination of non-darcy damage just in the wells where the *majority* of the dP^2 is due to non-darcy damage could theoretically increase deliverability available from the UGS industry by 50%. This would represent a potential increase in deliverability from the U.S. UGS industry on the order of about 30 BCF/day. Additional deliverability may also be achievable in wells where the dP^2 due to non-darcy damage is less than 50%.

General Trends

Study data suggest that it is difficult to successfully reduce the non-darcy component of total dP^2 if that component is only a small percentage of the total dP^2. **Figure 35** shows a plot of the normalized pre-treatment f-factor versus the percent reduction in f-factor for all study wells.

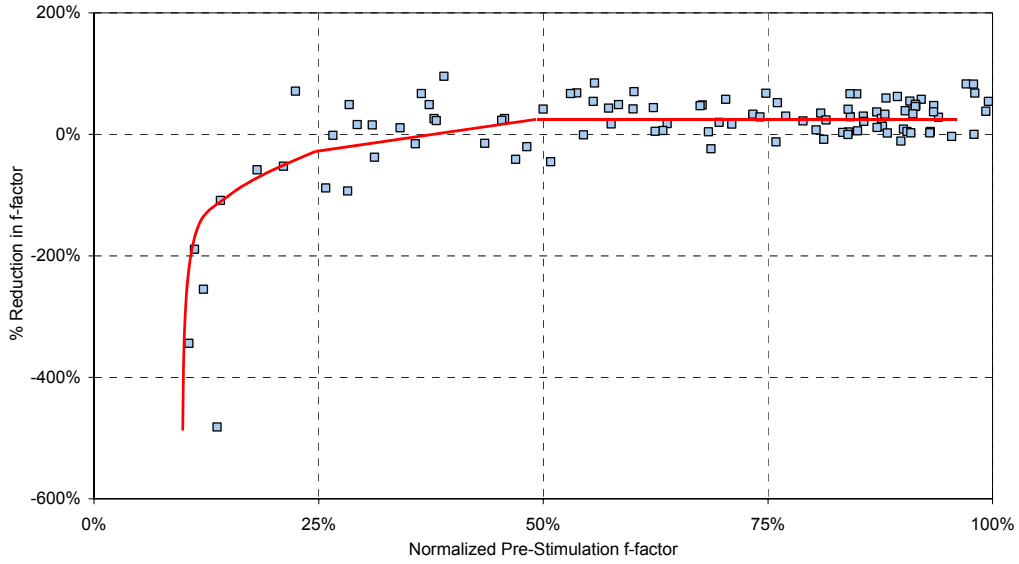

Figure 35: Normalized pre-treatment f-factor versus the percent reduction in f-factor

Three observations can be made. First, virtually all treatments *increase* the non-darcy component of total dP^2 in wells where the normalized pre-treatment f-factor is less than 25% (albeit a trend of only 7 points). Second when the normalized pre-treatment f-factor is greater than 50%, the vast majority of treatments reduce the non-darcy component of total dP^2. Third, in cases where the normalized pre-treatment f-factor is between 25% and 50%, treatments may or may not reduce the non-darcy component of total dP^2.

This trend is also evident from a review of charts comparing the average reduction of f-factors for the various treatment categories. **Figure 36** compares the average percent reduction in non-darcy dP^2 (i.e., the average change in f-factor) for all treatment categories and *all* ranges of the normalized pre-treatment f-factor, and suggests that, overall, treatments vary widely in their ability to reduce the non-darcy component of total dP^2. It is also interesting to note that three of the four best treatments shown in **Figure 36** involve hydraulic fracturing.

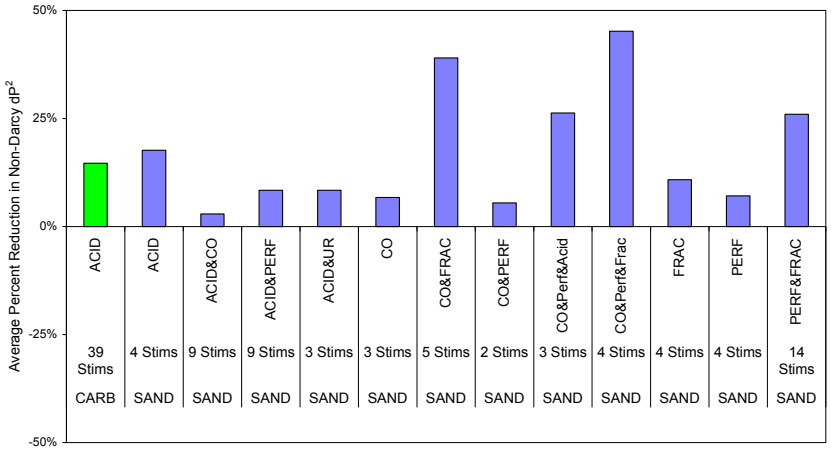

Figure 36: Average percent reduction in non-darcy dP^2 for all treatment categories and all ranges of the normalized pre-treatment f-factor

Figure 37 compares the average percent reduction in non-darcy dP^2 for all treatment categories and normalized pre-treatment f-factors *less than* 25%, and suggests that all treatments implemented under these conditions *increase* the non-darcy component of total dP^2.

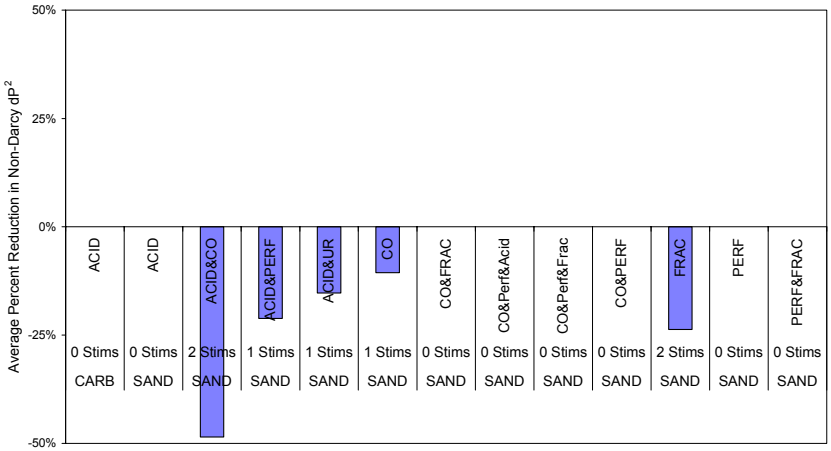

Figure 37: Average reduction in non-darcy dP^2 for all treatment categories and normalized pre-treatment f-factors < 25%

Figure 38 compares the average percent reduction in non-darcy dP^2 for all treatment categories and normalized pre-treatment f-factors *between 25% and 50%*, and suggests that treatments implemented under these conditions may *increase or decrease* the non-darcy component of total dP^2.

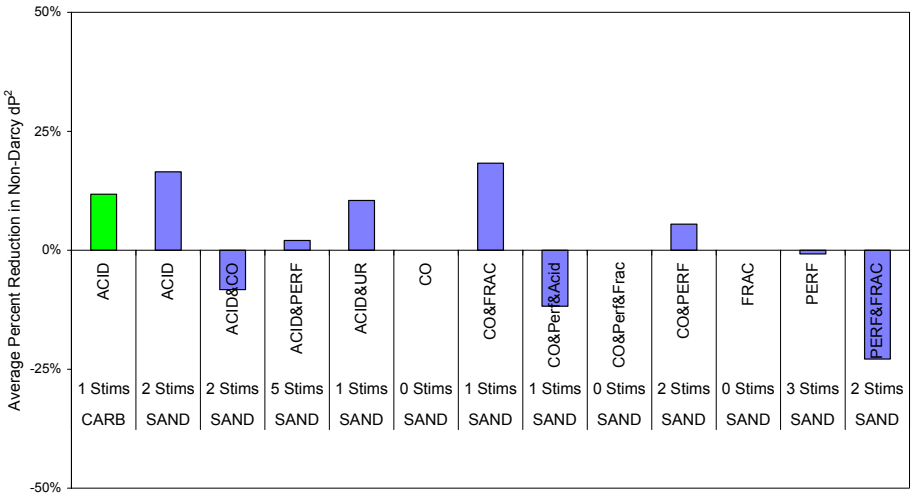

Figure 38: Average reduction in non-darcy dP^2 for all treatment categories and normalized pre-treatment f-factors between 25% and 50%

Figure 39 compares the average percent reduction in non-darcy dP^2 for all treatment categories and normalized pre-treatment f-factors *greater than 50%,* and suggests that, on average, all treatments implemented under these conditions *reduce* the non-darcy component of total dP^2.

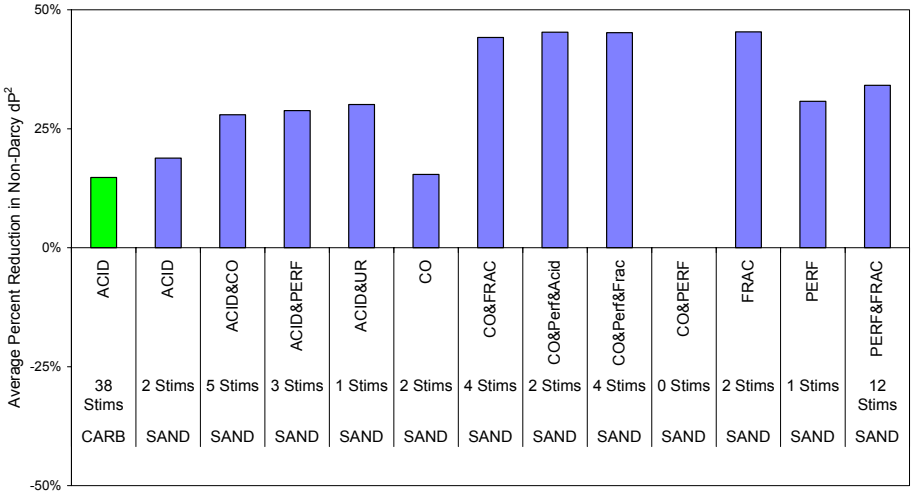

Figure 39: Average reduction in non-darcy dP^2 for all treatment categories and normalized pre-treatment f-factors > 50%,

These results suggest study treatments are very successful at reducing the non-darcy component of total dP^2 in cases where the majority of dP^2 is due to non-darcy effects.

However, study treatments are very unsuccessful at reducing the non-darcy component of total dP^2 in cases where the percentage of dP^2 is due to non-darcy effects is very small (i.e., less than 25%).

For the purpose of ranking treatment successes, we limited our analyses to wells that had normalized pre-treatment f-factors greater than 25%, since it would obviously be inappropriate to evaluate a treatment's effectiveness at eliminating non-existent damage.

Ranking Study Treatments

We ranked the success of various categories from two perspectives – technical and economical. Obviously, the bottom line in treatment selection is the economic indicator. However, there may be opportunities to reduce the costs associated with a treatment that is technically successful, but economically unsuccessful. Therefore, we ranked treatment success using two indicators. The rate gained per $1000 of treatment costs was used to rank the economic success of treatments, and the reduction in f-factor was the benchmark used to rank the technical success of the treatments.

Ranking Technical Success

As noted previously, assessment of the non-darcy component of the total dP^2 was done in a manner that ensured comparisons would be made at a consistent rate. Specifically, the pre-treatment f-factor was normalized by using the a and b coefficients in the Houepert equation (as determined from analysis of *pre*-treatment data) and the post-treatment geometric mean flowrate. We used the change in f-factor as the primary indicator of technical success, which is defined as the normalized pre-treatment f-factor minus the post-treatment f-factor. The results of our ranking are shown in **Figure 40.**

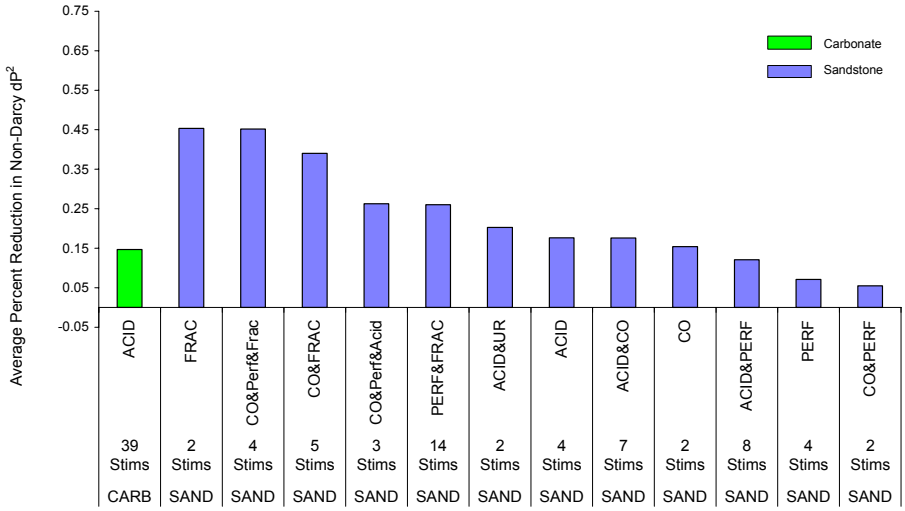

Figure 40: Treatment ranking in terms of technical success

A seen in **Figure 40**, four of the top five technically successful treatments in sandstones involve hydraulic fracturing, which tends to be a more expensive treatment than many of the alternatives. Accordingly, we might not necessarily expect the economic ranking of sandstone treatment to mimic the trend seen in **Figure 40**. It is also interesting to note that the three least successful treatments involve perforating (apart from hydraulic fracturing). If these perforating jobs were involved killing the well, there may be some cleanup issues resulting from altered relative permeability after treatment.

An alternate method of ranking technical success would be to rank by the potential increase in rate resulting from the decrease in non-darcy dP^2. **Figure 41** shows the average rate increases associated with each treatment category, and suggests the ranking using this criteria would be almost identical.

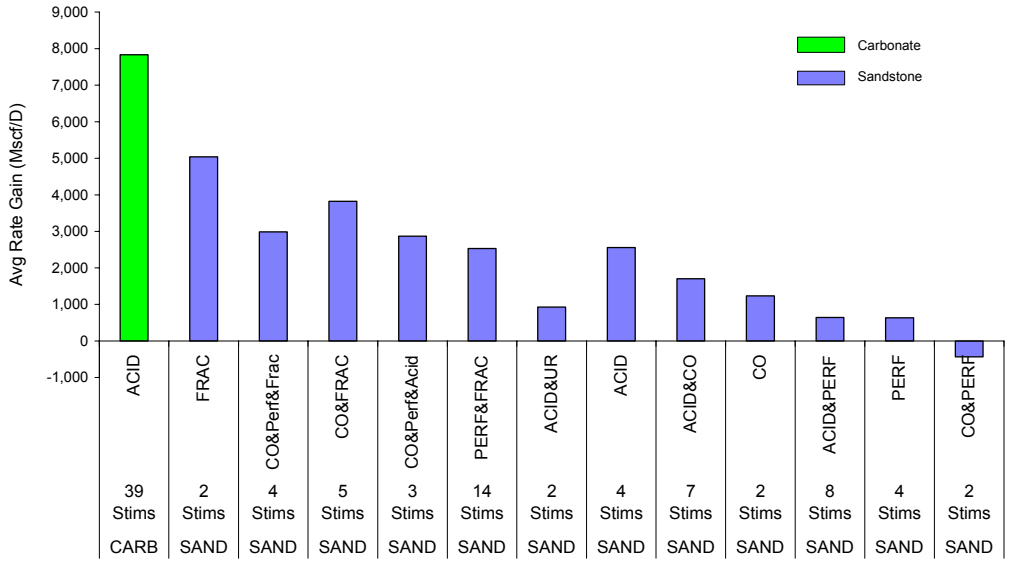

Figure 41: Average rate increases due to reduction in non-darcy dP^2 by treatment category

Cost Benefit Analysis

In order to perform a cost-benefit analysis, we needed to know two key items: 1) how much additional flow was achieved by a given treatment as a result of reducing the non-darcy component of the total dP^2, and 2) what did it cost to achieve that additional flow. It is important to keep in mind that our analysis was focused solely on the non-darcy components of the damage issue. Hence, our results should indicate which treatments best address the non-darcy component of total damage, but may not be indicative of which treatment has the best overall success at increasing deliverability.

It is important that the evaluation be done at conditions that approximate normal operating conditions. Accordingly, we assumed that the post-treatment dP^2 was fairly representative of normal operating conditions. For each study well, this dP^2 value was calculated using the Hoeupert equation, the a and b coefficients calculated from the post-treatment test data, and the geometric mean flow rate from the post-treatment test.

The additional dP^2 available in each well as a result of the change in f-factor was estimated by multiplying the reduction in f-factor (i.e., normalized pre-treatment f-factor – post treatment f-factor) by the post-treatment dP^2. For simplicity, the Rawlins-Schellhardt deliverability equation and the post-treatment C and n-values were used to estimate the additional flowrate achieved as a result of removing some of the non-darcy damage in the well. The average benefit per unit cost was then determined for each well, and averaged for all wells in a given treatment category. The average benefit per unit cost for all treatment categories was then plotted and compared to rank the various treatments.

The average benefit per unit cost for each treatment category is only intended for use as a ranking tool. It should not be used to calculate the actual “value” of the treatment, since the results represents an instantaneous improvement. In reality, successful treatments will result in some varying amount of deliverability improvement throughout

the withdrawal season. An accurate assessment of the actual value of a treatment can only be determined by considering *both* the increase in deliverability, and the longevity of the treatment. This calculation was beyond the scope of the project.

Figure 42 shows the ranking of treatment categories in terms of economic success, as measured by the average Mscf/D deliverability increase per $1,000 of treatment cost. Several observations are evident. First, acid treatments in carbonate reservoirs are very successful, relative to all treatments performed in sandstone reservoirs. The average Mscf/D gain per $1000 of treatment costs for acid treatments in carbonates is 2-3 times that of the best treatments in sandstone reservoirs. Also, no single treatment performed in sandstone reservoirs really stands out. Finally, the average Mscf/D gain per $1000 of treatment costs was negative for only one treatment category.

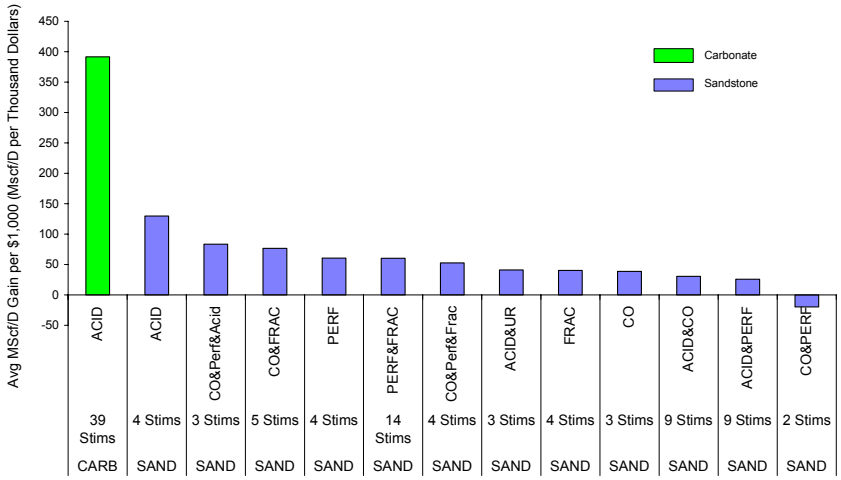

Figure 42: Ranking of treatment categories in terms of economic success

Operators provided treatment costs, and **Figure 43** shows the average costs for each treatment category. These costs represent the actual treatment costs, but do not include associated costs, such as well preparation and engineering time. For ease of comparison the data is ordered the same as in to **Figure 42.** As expected, simple operations such as perforating and cleaning out a well can be accomplished inexpensively, whereas treatments involving acid and fracturing and combination treatments and are generally much more expensive.

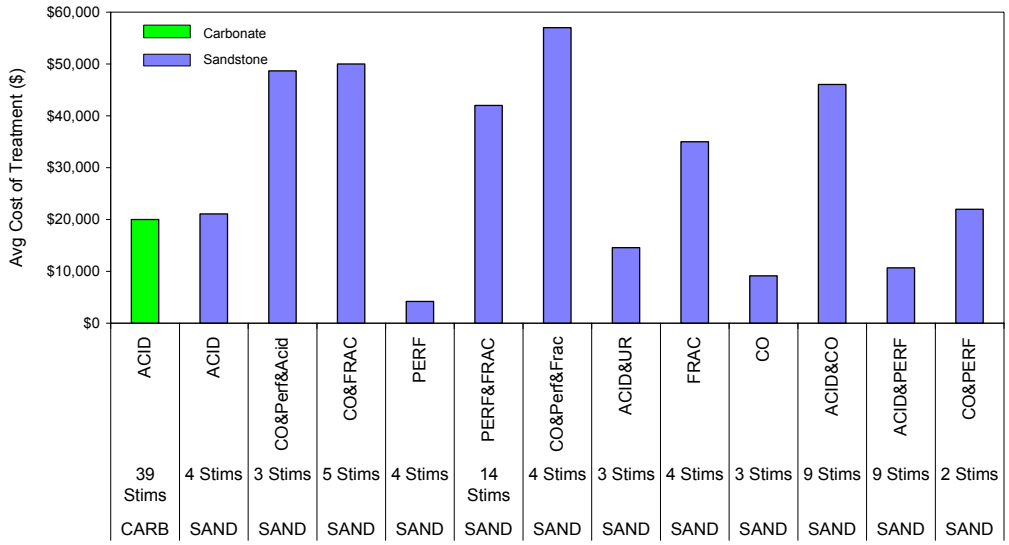

Figure 43: Average costs by treatment category

The average rate gain attributable to a reduction of the non-darcy component of total dP^2 for each treatment category is shown in **Figure 44**. In general, the more expensive treatments result in more increase in rate. Only one treatment resulted in a lower rate.

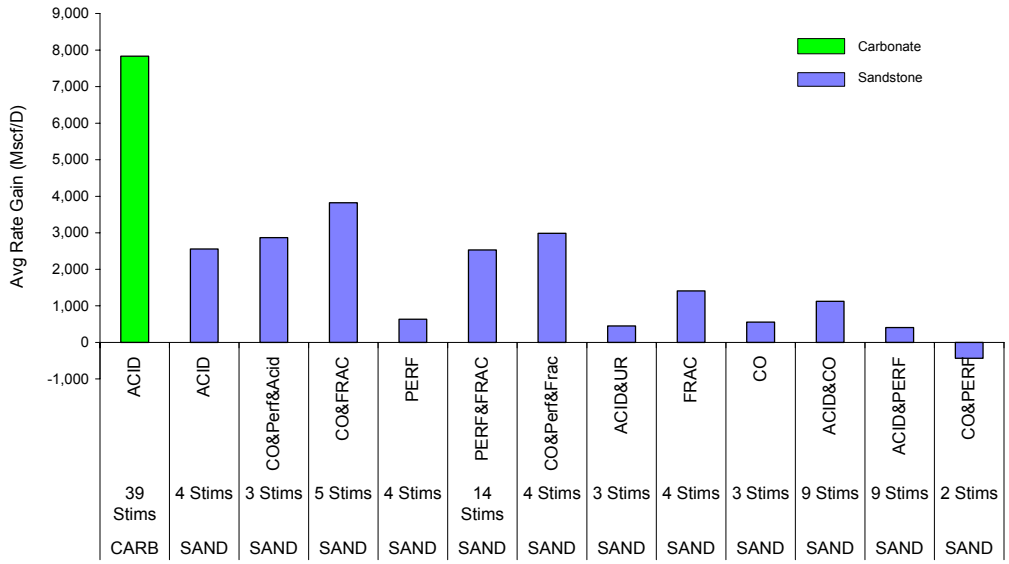

Figure 44: Average rate gain attributable to a reduction of the non-darcy component of total dP^2 by treatment category

Although this aspect of the study is limited to evaluating the impact of treatments on the *non-darcy* pressure drop in gas storage wells, the results are qualitatively similar to those published by Schlumberger Data and Consulting Services in a previous study[4]; UGS operators are much more successful at restoring deliverability in storage wells completed in carbonate reservoirs than in sandstone reservoirs.

Tool Predictions

The Non-Darcy Damage Assessment Tool was used to estimate the increase in deliverability, measured as a fractional increase in q_{100}, for several different pre- and post-treatment scenarios. The q_{100} value was chosen because it is widely used in the UGS industry as a deliverability benchmark. **Figure 45** compares the pre-stimulation flow rate with typical and maximum post stimulation flow rates for several different cases. **Figure 46** shows the predicted increase in deliverability (q_{100}) for the same set of cases and **Figure 47** shows the predicted *percent* increase in deliverability (q_{100}) for these cases. For the open-hole and cased-hole cases, hydraulic fracturing provided the greatest increase in deliverability.

Appendix V shows the deliverability graphs for each of these cases.

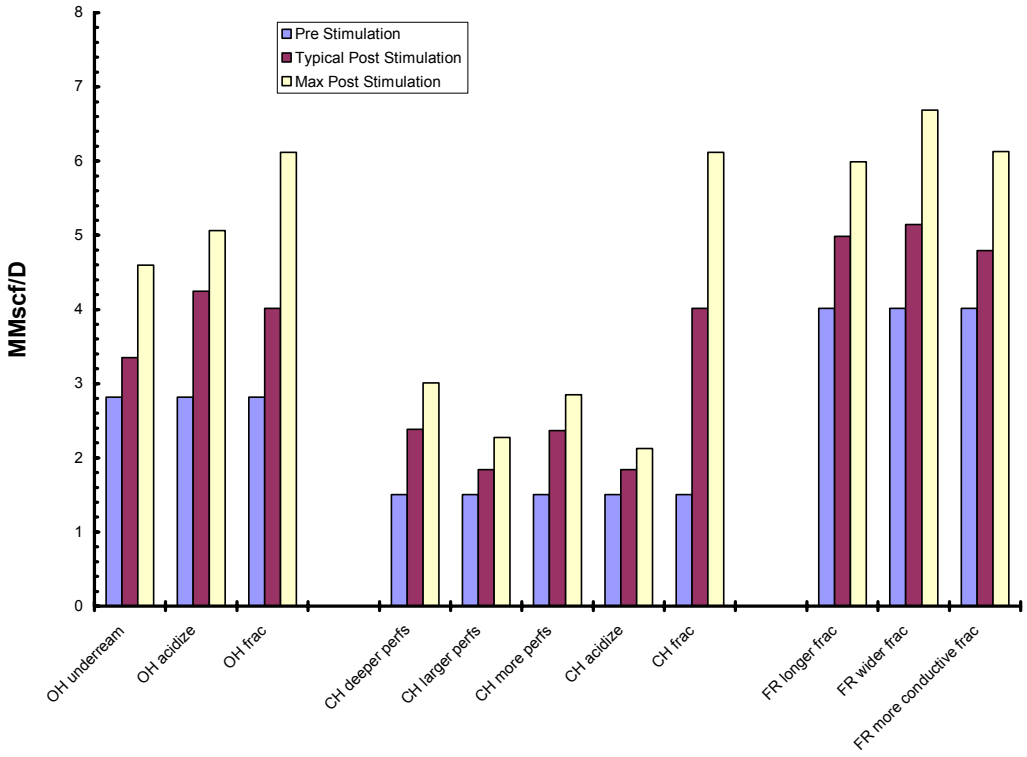

Figure 45: Comparison of predicted pre-stimulation rate with post stimulation rates for typical and maximum cases for different stimulation treatment types.

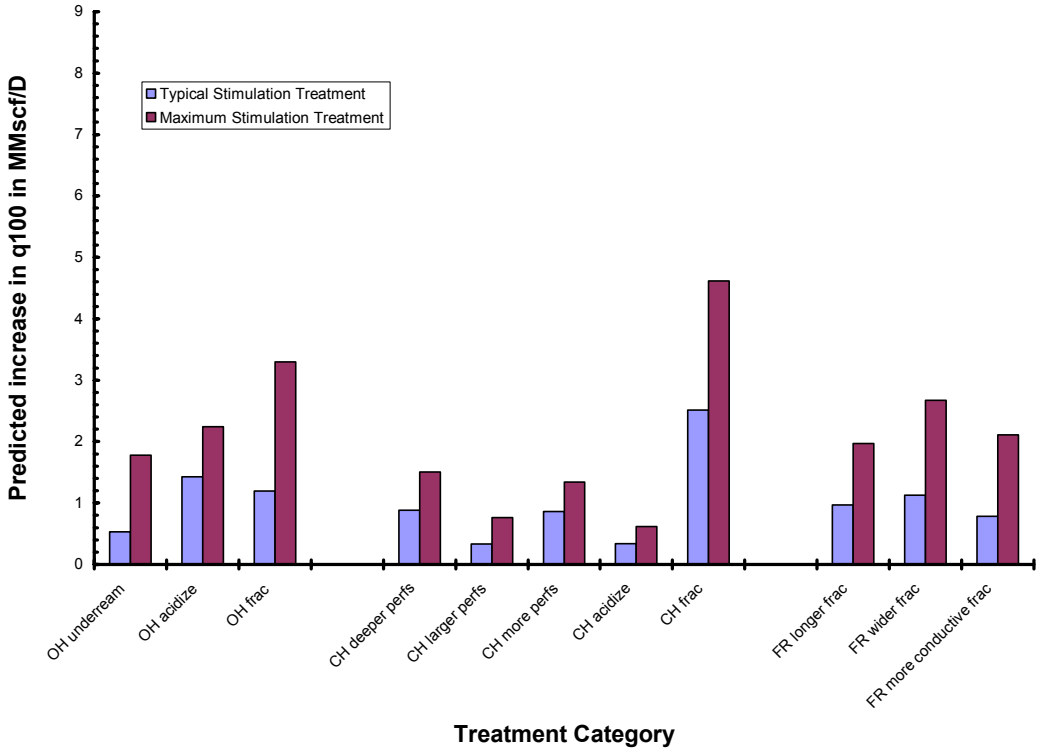

Figure 46: Predicted increase in q_{100} for typical and maximum cases for different stimulation treatment types.

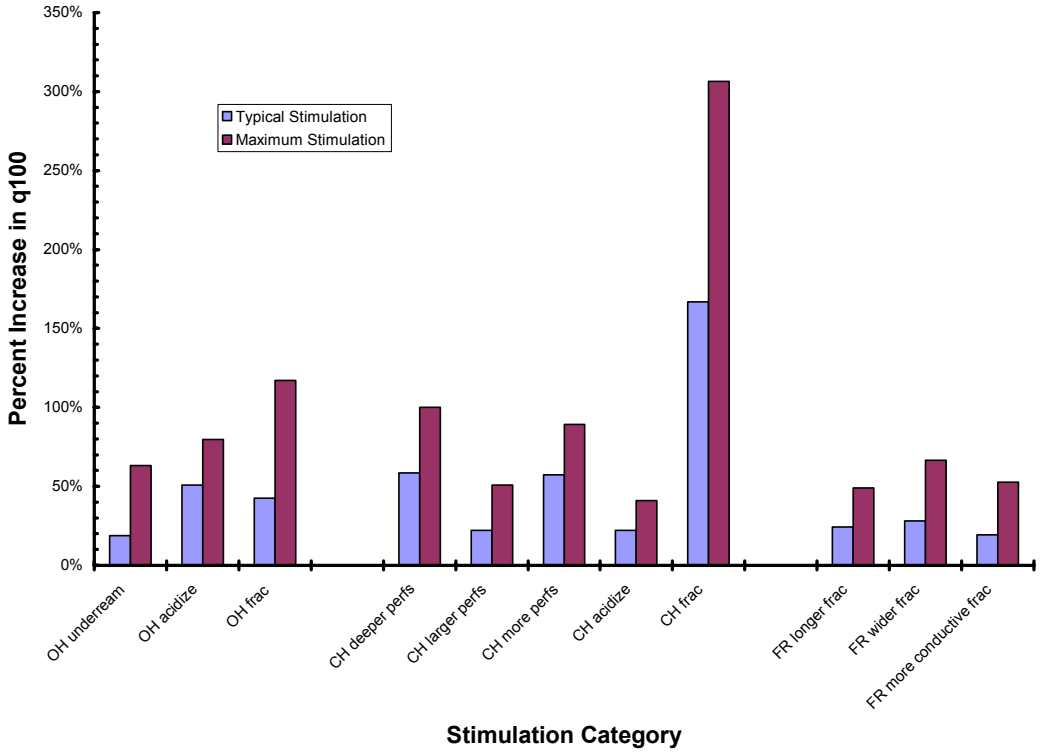

Figure 47: Predicted percent increase in q_{100} for typical and maximum cases for different stimulation treatment types.

In these scenarios, the predicted performance for a well of a given completion type, with average reservoir and completion properties from the AGA database, and in an undamaged condition, was compared to the predicted performance for a typical stimulation and a maximum stimulation for several different scenarios.

The open-hole model predicted only a small pressure drop attributable to non-darcy flow for any reasonable combination of reservoir and completion properties. Underreaming reduced the non-darcy component of the pressure drop by a small amount, while acidizing and fracturing both increased it slightly.

The cased-hole model showed the highest degree of non-darcy flow of the three models because of the high velocity as the gas converges on the perforations. Increasing the number of perforations or the depth of the perforation tunnels reduced the non-darcy component of the pressure drop, while the greatest benefit was obtained from fracturing.

The fracture model shows some improvement in deliverabilty could be obtained with a longer fracture, a wider fracture, or a higher fracture permeability.

Comparison of Non-Darcy Tool Prediction and Field Results

Of the predictive models, the cased-hole model predicted the highest degree of non-darcy flow, while the fracture model predicted the second highest. The open-hole model, in contrast, predicted very little non-darcy flow behavior for any reasonable combination of reservoir properties.

In general, models predicted increases in deliverability for the typical treatment case that compare fairly well with the field results.

Tool Limitations

In contrast to our expectations, the open-hole model does not predict a high degree of non-Darcy flow with values for reservoir parameters within the ranges typical of gas storage wells. This suggests that the mechanism responsible for non-Darcy flow in gas storage wells with open-hole completions is not accounted for in the open-hole model.

One possible explanation lies in the assumption of homogeneity or uniformity in reservoir properties in the near-wellbore region. While this assumption is quite successful in describing Darcy flow, it does not automatically follow that the same would hold true for non-Darcy flow as well. As discussed by S.C. Jones[7], the non-Darcy coefficient β may be a good indicator of heterogeneity at the core plug level, suggesting that heterogeneity in the near-wellbore region in a gas storage well may also cause much higher non-Darcy skin factors than would be observed in a homogeneous reservoir.

The correlations used to estimate the β-factor can provide only a rough estimate of the β. The β-factor is a function of the pore geometry, just as permeability and porosity are, but just as correlations of permeability as a function of porosity give only crude estimates of permeability, so β-factor correlations give only crude estimates of β-factor.

The Open-Hole Simulator assumes that the reservoir is homogeneous, and that damage or stimulation is uniformly distributed around the wellbore. This is an idealistic assumption that causes the Open-Hole Simulator to systematically underestimate the effects of non-Darcy flow for situations where there is significant heterogeneity, either in the reservoir permeability or in the distribution of damage or stimulation. As Jones shows, permeability heterogeneity can cause a dramatic increase in the magnitude of non-Darcy flow behavior.

The same considerations apply to the Cased-Hole and Fracture Simulators, but these models predict non-Darcy factors that are more in line with values obtained from deliverability tests.

The Cased-Hole Simulator assumes that the reservoir is homogeneous, that damage or stimulation is uniformly distributed around the wellbore, and that all perforations are identical. As with the Open-Hole Simulator, this is an idealistic assumption. Again, this assumption causes the Cased-Hole Simulator to tend to underestimate the effects of non-Darcy flow for situations where there is significant heterogeneity, either in the reservoir permeability or in the distribution of damage or stimulation.

As with the Open-Hole and Cased Hole Simulators, the Fracture Simulator assumes uniform reservoir properties. It also assumes that fracture properties (height, width, conductivity) are uniform over the entire length of the fracture.

CONCLUSIONS

Look Back Study

The database developed to specifically study non-darcy damage has provided many valuable insights into the prevalence and magnitude of non-darcy damage in UGS wells. It would be prudent to maintain this database by adding data from wells that are tested in the future.

There is also an opportunity to enhance the value of the database by expanding it to include additional stimulation details (e.g., treatment volumes, rates, pressures, etc.) and more detailed results derived from multi-rate pressure transient test analyses (e.g., mechanical skin S_m and the non-darcy damage coefficient, D). These additional data could allow for the optimization of treatment designs, more comprehensive analysis of non-darcy damage, and improvements in the simulators developed.

By their very nature, UGS wells are very prone to non-darcy pressure drops during normal operations, since they typically operate at very high flow rates, as compared to production wells. The study data bears this out.

Overall, the non-darcy component of the total dP^2 exceeds 50% in nearly half of the study wells. In carbonates, the non-darcy damage component was much larger (over 50% in about 74% of wells in carbonate reservoirs) than in sandstones (over 50% in about 18% of the wells).

The fact that these statistics are similar before and after treatment highlights the importance of assessing non-darcy damage at a common flowrate to ensure proper comparisons. To be sure, the percentage of the total dP^2 due to non-darcy damage is similar before and after treatment, but this is because the post-treatment rates are generally much higher than the pre-treatment rates. It is *not* because the treatments do no good. Clearly, any evaluation of non-darcy damage *must* be done at a common flowrate.

Another obvious implication of these statistics is that the reduction or elimination of the non-darcy damage component in UGS wells represents a *very* significant opportunity to increase the deliverability available from UGS industry as a whole. Although our study well group only comprised roughly 1% of U.S. gas storage wells, over 50% of the total dP^2 is due to non-darcy damage in about 50% of the wells, indicating a big potential to increase the overall UGS industry deliverability, assuming we can eliminate non-darcy damage in these wells. While it is likely that the complete removal of non-darcy pressure drop is an unrealistic goal, nonetheless, even a small advancement could result in a significant increase in deliverability. Consequently, we believe that this issue warrants additional scientific research.

The portion of the study that involved technical and economic ranking of study treatments has clearly shown that the treatments that are the most technically successful are *not necessarily* the most cost-effective, Therefore, gas storage engineers must continually guard against the temptation to evaluate deliverability enhancement programs solely on the increases in well performance. Cost benefit analyses are the appropriate means of managing deliverability enhancement efforts.

Non-Darcy Damage Assessment Tool

The three reservoir-completion models developed in EXCEL™ for the purpose of estimating performance increases in UGS wells provided many valuable insights into the types of treatments expected to significantly improve performance in wells with significant non-darcy damage. These models are easy to use and should be used as a screening tool by storage engineers to aid the selection of treatment types.

Analyses using these reservoir models suggest the following conclusions:

- In open-hole completions, fracturing, underreaming, and acidizing are recommended and can be expected to result in 20-100% improvement in deliverability.
- In cased-hole completions, fracturing, perforating with increased shot density, perforation diameter, or perforation depth, and acidizing are recommended and can be expected to result in 20-300% improvement in deliverability.
- In hydraulically fractured completions, using longer, wider or more conductive fractures is recommended and can be expected to result in 20-50% improvement in deliverability.

Recommendations for Future Work

As noted in other sections of this report, non-darcy damage is both ubiquitous and significant in UGS wells. This has profound implications for future R&D in the UGS industry. The potential deliverability increases realized from successful removal and/or reduction of non-darcy damage is enormous. As such, this damage mechanism demands additional study. Therefore, we recommend that future R&D devote funds to evaluate practical means of reducing the amount of non-darcy damage in UGS wells.

The database developed for this study is an important first step in the evaluation of treatments aimed at the reduction of non-darcy damage. As such, we believe its maintenance should be continued. New information should be added as it becomes available. In addition, expansion of the database to include multi-rate pressure transient test analysis results and stimulation details should be considered, as these features could allow for treatment optimization and additional study of the relationship between commonly available data (e.g., the C and n backpressure coefficients) and more descriptive damage parameters derived from multi-rate pressure transient testing (i.e., the mechanical damage and non-darcy damage coefficient).

A research area of particular importance would be evaluation of methods to reduce hydraulic fracturing costs, as this is clearly one of the most effective means of reducing non-darcy damage in UGS wells. Perhaps an alternative would be to make the drilling of numerous multilaterals in a UGS well affordable, as this could accomplish the same end result of a fracture – increased flow area.

The complex relationship between mechanical damage and non-darcy damage needs to be better understood. Multi rate pressure transient tests can be used to distinguish between mechanical damage and non-darcy damage, and even quantify the amount of each as a function of flowrate. However, we rarely know how much of the non-darcy damage is ultimately the result of severe mechanical damage totally preventing flow from sections of the wellbore. Running spinners, cameras, and perhaps logs concurrent with a multi-rate pressure transient test could allow for a more complete understanding how these phenomenon relate to one another, and should be encouraged.

Modeling results suggest that the key to reducing non-darcy component of total dP^2 is to eliminate choke points in the completion where high gas velocities exist. Approaches to reducing the non-darcy component of total dP2 should focus on the following types of treatments:

In open-hole completions, the effects of non-darcy flow are minimized when the entire sandface is open to flow. If portions of the sandface are plugged by mechanical damage, the velocity in the unblocked portions must increase if the same surface flow rate is to be maintained. In view of the high degree of non-darcy damage observed in many open-hole completions, it is likely that these wells have some degree of sandface obstruction.

In cased-hole completions, increasing the number of perforations and increasing the depth of penetration of those perforations reduces the effects of non-darcy flow more than any other treatment short of fracturing. Acidizing appears to give only a limited improvement, unless it can increase the effective number of perforations open to flow by removing damage from those perforations.

In fractured completions, increasing the length or width of the fracture, or increasing the permeability of the proppant pack, can all reduce the effects of non-darcy flow. Of these factors, increasing the fracture length appears to the most feasible with current technology.

The reservoir models developed during this study should be field tested by UGS personnel. If these tests demonstrate value to the operators, consideration should be given to making the models a more user friendly and more automated. It may be necessary to develop additional models to evaluate other alternatives, such as horizontal wells or multi-lateral completions.

REFERENCES

1. “Survey of Underground Gas Storage Facilities in the United States and Canada 1998” American Gas Association (1998).
2. “State-of-Technology Assessment and Evaluation of Gas Storage Well Productivity Enhancement Techniques”, Mauer Engineering Inc. and T. Joyce Associates, Inc., Gas Research Institute (1993).
3. “Investigation of Storage Well Damage Mechanisms, Final Report (April 1995-August 1997),” V.J. Yeager, M.E. Blauch, and F.R. Behenna, Gas Research Institute (1997)
4. “Monitoring of Damage in Gas Storage Wells, Final Report, Contract No. 7019,” GRI/Schlumberger Data and Consulting Services (2003)
5. Ramey, H.J. Jr.: “Non-Darcy Flow and Wellbore Storage Effects in Pressure Buildup and Drawdown of Gas Wells,” JPTi (February 1965) 223-233.
6. Forcheimer, P.: “Wasserbewegung durch Boden,” ZVDI (1901) Vol. 45, 1781.
7. Saleh, A.M., and Stewart, G.: “New Approach Towards Understanding of Near Well Bore Behaviour of Perforated Completions,” paper SPE 36866 presented at the 1996 SPE European Petroleum Conference, Milan, 22-24 October.
8. Nguyen, T.V.: “Experimental Study of Non-Darcy Flow Through Perforations,” paper SPE 15473 presented at the 61st Annual Technical Conference and Exhibition of the Society of Petroleum Engineers, New Orleans, 5-8 October, 1986.
9. Himmatramka, A.K.: “Analysis of Productivity Reduction Due to Non-Darcy Flow and True Skin in Gravel-Packed Wells,” paper SPE 10084 presented at the 56th Annual Fall Meeting, San Antonio, 5-7 October, 1981.
10. Burton, R.C.: “Use of Perforation-Tunnel Permeability To Assess Cased Hole Gravelpack Performance,” SPEDC (December 1999) 235-239.
11. Jones, S.C.: "Using the Inertial Coefficient, β, to Characterize Heterogeneity in Reservoir Rock," paper SPE 16949 presented at the 1987 SPE Annual Technical Conference and Exhibition, Dallas, 27-30 September.

BIBLIOGRAPHY

1. Brown, K.E., and Lea, J.F.: “Nodal Systems Analysis of Oil and Gas Wells,” *JPT* (October 1985) 1751-1763.
2. Ramey, H.J. Jr.: “Non-Darcy Flow and Wellbore Storage Effects in Pressure Build-Up and Drawdown of Gas Wells,” *JPT* (February 1965) 223-233.
3. Gringarten, A.C., Bourdet, D.P., Landel, P.A., and Kniazeff, V.J.: “A Comparison Between Different Skin and Wellbore Storage Type-Curves for Early-Time Transient Analysis,” paper SPE 8205 presented at the 54th Annual Fall Technical Conference and Exhibition of the Society of Petroleum Engineers, Las Vegas, 23-26 September, 1979.
4. Bourdet, D., Whittle, T.M., Douglas, A.A. and Pirard, Y.M.: “'A new set of type curves simplifies well test analysis,” *World Oil* (May 1983) 95-106.
5. Fair, W.B: “Pressure Buildup Analysis With Wellbore Phase Redistribution,” *SPEJ* (April 1981) 259-270.
6. Hegeman, P.S., Hallford, D.L., and Joseph, J.A.: “Well-Test Analysis With Changing Wellbore Storage,” *SPEFE* (September 1993) 201-207.
7. Jennings, A.R., Jr.: “Good Wells Make the Best Candidates for Well Stimulation,” *SPEPE* (November 1991) 371-376.
8. Chu, W.: “Application of Pressure Transient Testing for Stimulation Decisions,” paper SPE 36529 presented at the 1996 SPE Annual Technical Conference and Exhibition, Denver, 6-9 October.
9. Forcheimer, P.: “Wasserbewegung durch Boden,” *ZVDI* (1901) Vol. 45, 1781.
10. Saleh, A.M., and Stewart, G.: “New Approach Towards Understanding of Near Well Bore Behaviour of Perforated Completions,” paper SPE 36866 presented at the 1996 SPE European Petroleum Conference, Milan, 22-24 October.
11. Nguyen, T.V.: “Experimental Study of Non-Darcy Flow Through Perforations,” paper SPE 15473 presented at the 61st Annual Technical Conference and Exhibition of the Society of Petroleum Engineers, New Orleans, 5-8 October, 1986.
12. Himmatramka, A.K.: “Analysis of Productivity Reduction Due to Non-Darcy Flow and True Skin in Gravel-Packed Wells,” paper SPE 10084 presented at the 56th Annual Fall Meeting, San Antonio, 5-7 October, 1981.
13. Burton, R.C.: “Use of Perforation-Tunnel Permeability To Assess Cased Hole Gravelpack Performance,” *SPEDC* (December 1999) 235-239.
14. Swift, G.W., and Kiel, O.G., “The Prediction of Gas-Well Performance Including the Effect of Non-Darcy Flow,” *JPT* (July 1962) 791-798.
15. Muskat, M.: *The Flow of Homogeneous Fluids Through Porous Media*, J.W. Edwards, Inc., Ann Arbor, Michigan (1946).
16. Aronofsky, J.S. and Jenkins, R.: “A Simplified Analysis of Unsteady Radial Gas Flow,” *Trans. AIME* (1954) 201, 149.
17. Wattenbarger, R.A., and Ramey, H.J.: “Gas Well Testing With Turbulence, Damage, and Wellbore Storage,” *JPT* (August 1968) 877-887.

18. Jones, L.G., Blount, E.M., and Glaze, O.H.: “Use of Short Term Multiple Rate Flow Tests To Predict Performance of Wells Having Turbulence,” paper SPE 6133 presented at the 51st Annual Fall Technical Conference and Exhibition of the Society of Petroleum Engineers, New Orleans, 3-6 October.

19. Lee, R.L., Logan, R.W., and Tek, M.R.: “Effect of Turbulence on Transient Flow of Real Gas Through Porous Media,” *SPEFE* (March 1987) 108-120.

20. Finjord, J.: “A Study of Pseudotime,” paper SPE 12577.

21. Spivey, J.P.: “An Investigation of the Use of Pseudotime in Transient Test Analysis of Gas Wells,” PhD Dissertation, Texas A&M University (May 1984).

22. Spivey, J.P., and Lee, W.J.: “The Use of Pseudotime: Wellbore Storage and the Middle Time Region,” paper SPE 15229 presented at the Unconventional Gas Technology Symposium of the Society of Petroleum Engineers, Louisville, Kentucky, 18-21 May, 1986.

23. Reynolds, A.C., Bratvold, R.B., and Ding, W.: “Semilog Analysis of Gas Well Drawdown and Buildup Data,” paper SPE 13664 presented at the SPE California Regional Meeting, Bakersfield, 27-29 March, 1985.

24. Horne, R.N., and Kuchuk, F.: “Use of Simultaneous Flow-Rate and Pressure Measurements To Replace Isochronal Gas Well Tests,” *SPEFE* (June 1988) 467-470.

25. Warren, G.M.: “Numerical Solutions for Pressure Transient Analysis,” paper SPE 26177 presented at the SPE Gas Technology Symposium, Calgary, 28-30 June 1993.

26. Kim, J., and Kang, J.M.: “A Semianalytical Approach in Determining Non-Darcy Flow Coefficient From a Single-Rate Gas-Well Pressure-Transient Test,” paper SPE 28663, unsolicited, 18 March, 1994.

27. Lingen, P.L.: “Rate-Dependent Skin From Afterflow,” paper SPE 28832 presented at the European Petroleum Conference, London, 25-27 October, 1994.

28. Samaniego, V., F., and Cinco-Ley, H.: “Transient Pressure Analysis for Variable Rate Testing of Gas Wells,” paper SPE 21831 presented at the 1991 Rocky Mountain Regional Meeting and Low-Permeability Reservoirs Symposium, Denver, 15-17 April.

29. Nashawi, I.S., and Al-Mehaideb, R.A.: “A New Technique to Analyze Simultaneous Sandface Flow Rate and Pressure Measurements of Gas Wells with Turbulence and Damage,” paper SPE 29895 presented at the SPE Middle East Oil Show, Bahrain, 11-14 March, 1995.

30. Camacho-V., R., Vásquez-C., M., Roldán-C., J., Samaniego-V., F., and Macías-C., L.: “New Results on Transient Well Tests Analysis Considering Nonlaminar Flow in the Reservoir,” *SPEFE* (December 1996).

31. Kelkar, M.G.: “Estimation of Turbulence Coefficient Based on Field Observations,” *SPEREE* (April 2000), 160-164.

32. Holditch, S.A., and Morse, R.A.: “The Effects of Non-Darcy Flow on the Behavior of Hydraulically Fractured Gas Wells,” *JPT* (October 1976) 1169-1179.

33. Guppy, K.H., Cinco-Ley, H., Ramey, H.J. Jr., and Samaniego-V., F.: “Non-Darcy Flow in Wells With Finite-Conductivity Fractures,” *SPEJ* (October 1982) 681-698.

34. Gidley, J.L.: “A Method for Correcting Dimensionless Fracture Conductivity for Non-Darcy Flow Effects,” *SPEPE* (November 1991) 391-394.

35. Umnuayponwiwat, S., and Ozkan, E.: “Effect of Non-Darcy Flow on the Interpretation of Transient Pressure Responses of Hydraulically Fractured Wells,” paper SPE 63176 presented at the 2000 SPE Annual Technical Conference and Exhibition, Dallas, 1-4 October.

36. Settari, A., Stark, A.J., and Jones, J.R.: “Analysis of Hydraulic Fracturing of High Permeability Gas Wells to Reduce Non-Darcy Skin Effects,” *JCPT* (May 2000) 56-63.

37. Geertsma, J., “Estimating the Coefficient of Inertial Resistance in Fluid Flow Through Porous Media,” *SPEJ* (October 1971) 445-450.

38. Firoozabadi, A., and Katz, D.L.: “An Analysis of High-Velocity Gas Flow Through Porous Media,” *JPT* (February 1979) 211-216.

39. Li, D., and Engler, T.W.: “Literature Review on Correlations of the Non-Darcy Coefficient,” paper SPE 70015 presented at the SPE Permian Basin Oil and Gas Recovery Conference, Midland, Texas, 15-16 May 2001.

40. Thauvin, F., and Mohanty, K.K.: “Modeling of Non-Darcy Flow Through Porous Media,” paper SPE 38017 presented at the 1997 SPE Reservoir Simulation Symposium, Dallas, 8-11 June.

41. Cooper, J.W., Wang, X., and Mohanty, K.K.: “Non-Darcy-Flow Studies in Anisotropic Porous Media,” *SPEJ* (December 1999) 334-341.

42. Jones, S.C.: “Using the Inertial Coefficient, b, To Characterize Heterogeneity in Reservoir Rock,” paper SPE 16949 presented at the 1987 SPE Annual Technical Conference and Exhibition, Dallas, 27-30 September.

43. Narayanaswamy, G., Sharma, M.M., and Pope, G.A.: “Effect of Heterogeneity on the Non-Darcy Flow Coefficient,” *SPEREE* (June 1999) 296-302.

44. Fair, W.S.: “Generalization of Wellbore Effects in Pressure Transient Analysis,” paper SPE 24715 presented at the 1992 SPE Annual Technical Conference and Exhibition, Washington, D.C., 4-7 October.

45. Lee, W.J. and Holditch, S.A.: "Application of Pseudotime to Buildup Test Analysis of Low-Permeability Gas Wells With Long-Duration Wellbore Storage Distortion," *JPT* (December 1982) 2877-2887.

46. Fetkovich, M.J.: “The Isochronal Testing of Oil Wells,” paper SPE 4529 presented at the 48th Annual Fall Meeting of SPE, Las Vegas, 30 September – 3 October, 1973.

47. Blacker, L.K.: “An Analysis of Rate-Sensitive Skin in Oil Wells,” paper SPE 11187 presented at the 57th Annual Fall Technical Conference and Exhibition of the Society of Petroleum Engineers, New Orleans, 26-29 September, 1982.

48. Robinson, J.C., Chu, W.-C., Woods, M.E., and Hutchison, H.W.: “Pressure Buildup Testing as an Aid in Well Stimulation: Case History,” paper SPE 22750 presented at the 66th Annual Technical Conference and Exhibition of the Society of Petroleum Engineers, Dallas, 6-9 October, 1991.

49. Maurer Engineering Inc. and T. Joyce Associates, Inc: *State-of-Technology Assessment and Evaluation of Gas Storage Well Productivity Enhancement Techniques*, Gas Research Institute, (December 1993)

50. McVay, D.A., Spivey, J.P.:"Optimizing Gas Storage Reservoir Performance," paper SPE 28693 presented at the 1994 Annual Technical Conference and Exhibition, New Orleans, LA, September 25-28, 1994.
51. Zuber, M. D., Deters Jr., J. C., and Lee, W. J.: "A Practical Approach for Analysis of a Pressure Transient Test From a Horizontal Well in a Gas Storage Reservoir," paper SPE 22675 presented at the 66th SPE Annual Technical Conference & Exhibition, Dallas, TX, Oct. 6-9, 1991.
52. Sawyer, W.K.: "The Practical Consequences of Non-Darcy Flow in Gas Storage Wells," presentation at the 1999 SPE Gas Storage/Treatment Group Meeting, Morgantown, WV, June 17, 1999.
53. Yeager, V. J., Behenna, F. R.: “Investigation of Storage Well Damage Mechanisms – Final Report”, Halliburton Energy Resources, report, Gas Research Institute Contract No. 5095-270-3254, (1999).
54. Brown, K.G.: “Using Electronic Flow Measurement in Gas Storage Field Applications”, presentation at the 1998 SPE Gas Storage Meeting, 1998.
55. Lee, W.J., Well Testing, Society of Petroleum Engineering of AIME, pp. 76-88, 1982, New York, NY.

LIST OF ACRONYMS AND ABBREVIATIONS

ACRONYM	DEFINITION
a	Coefficient in Jones and Hoeupert deliverability equations
AGA	American Gas Association
AOF	Absolute open-flow rate
b	Coefficient in Jones and Hoeupert deliverability equations
BCF	Billion standard cubic feet
BCF/day	Billion standard cubic feet per day
beta	Or B-factor, the non-Darcy coefficient
BP	Back-pressure
BPM	Barrels per minute
Bscf/D	Billion standard cubic feet per day
C	Performance coefficient. Describes the position of the stabilized deliverability curve
CHPerf	Cased hole perforate
CO	Cleanout
Csg	Casing
CT	Computed tomography
CT	Coiled tubing
CTC	Coiled tubing cleanout
D	Or D-factor, the non-darcy damage coefficient
D-Factor	Non-darcy damage coefficient
Dim'less	Dimensionless
DOE	Department of Energy
D_p	Perforation diameter
DP^2	Difference of pressures squared, Pr^2-Pwf^2
EDAX	Energy Dispersive X-Ray Analysis
EDX	Energy Dispersive X-Ray
EXCEL	Spreasheet software by Microsoft
F	Or f-factor, the fraction of total dP2 attributable to non-darcy flow
f_{post}	Post-treatment fraction of total dP2 attributable to non-Darcy flow
F_{pre}	Pre-treatment fraction of total dP2 attributable to non-Darcy flow
FRAC	Hydraulic fracture
Gal	Gallon
GC	Gas Chromatograph
GCMS	Gas Chromatograph Mass Spectrometer
GRI	Gas Research Institute
H	pay thickness
HB	HydraBlast, a trade name for power washing using coiled tubing
h_{net}	Net pay thickness of formation
H_p	Distance a well penetrates into the formation
Hrs	Hours
ICP	Inductively Coupled Plasma
In	inch
Incr	Increase
Inj	Injection

ACRONYM	DEFINITION
K	Permeability, md
K	1000
K_a	Altered zone permeability
K_f	Fracture permeability
K_h	Permeability-thickness product, md-ft
L_f	Length of each fracture wing
L_p	Perforation length
md	Milldarcies
mm	Millimeter
MMscf/D	Million standard cubic feet per day
MScf/D	Thousand standard cubic feet per day
N	Exponent. Describes the inverse of the slope of the stabilized deliverability curve
N/A	Not available
N_s	Number of perforation shots per foot
OD	Outside diameter
OHPerf	Open hole perforate
P	Pressure
ρ	Fluid density
PERF	Perforate
pH	Negative logarithm of effective hydrogen ion concentration
Φ	Porosity
Φa	Altered zone porosity
POOH	Pull out of hole
ppm	Parts per million
ppt	Parts per thousand
P_r	Reservoir pressure
psi	Pounds per square inch
psig	Pounds per square inch, guage
P_{wf}	Well flowing pressure
Py-GC/MS	Pyrolysis-gas chromatography/mass spectrometry
Q	Flow rate
Q	geometric mean flow rate
Q_{100}	Natural gas flow rate (mscfd) at pressure-squared difference of 100,000 psia^2
q_{post}	Post-treatment flow rate
q_{pre}	Pre-treatment flow rate
R&D	Research and development
R^2	Correlation coefficient. Describes the quality of a least squares fit.
R_a	Altered zone radius
r_e	Circular drainage radius
RIH	Run into hole
RSWC	Rotary sidewall core
R_w	Wellbore radius
scf/bbl	Standard cubic feet per barrel
SCFM	Standard cubic feet per minute
SEM	Scanning electron microscope
SG	Specific gravity of natural gas
S_m	Mechanical component of the total skin damage
$S_{mechanical}$	Mechanical component of the total skin damage
S_{Total}	Total skin damage
S_w	Water saturation
S_{wa}	Altered zone water saturation
TD	Total depth

ACRONYM	DEFINITION
TOC	Total organic carbon
Ц	Viscosity
UCM	Unresolved complex mixture
UGS	Underground gas storage
UR	Underream
v	Average velocity
wf	Width of each fracture wing
WH	Wellhead
WHP	Wellhead pressure
WHP_r	Shut-in wellhead pressure
WHP_{wf}	Flowing wellhead pressure
X	Coordinate in the flow direction
XRD	X-ray diffraction
y-intercept	Distance from origin to point where a graph crosses the vertical coordinate axis

APPENDIX I

Conventional Core Analysis Results

Well W3

CL File No : Hou-000327
Date : November 08, 2000
Analysis : Long/Koster

CMS-300 ROTARY CORE ANALYSIS

Sample Number	Depth ft	Reservoir Net Overburden psig	Pore Volume cm3	Porosity %	Permeability Klinkenberg md	Permeability Kair md	b(He) psi	Beta ft(-1)	Alpha microns	Grain Density g/cm3
Well No. 1527P										
1R	2285.5	800	1.35	16.2	968.4	984.8	0.74	5.34E+06	1.67E+01	2.64
2R	2287.0	800	1.59	15.2	1141.	1159.	0.66	4.19E+06	1.54E+01	2.64
3R	2288.0	800	1.64	15.7	952.1	968.1	0.73	4.30E+06	1.32E+01	2.64
4R	2289.0	800	1.21	15.3	921.9	940.9	0.90	7.99E+06	2.38E+01	2.64
5R	2290.0	800	1.02	11.2	437.9	446.8	0.91	1.82E+07	2.58E+01	2.63
6R	2291.0	800	1.06	10.7	309.0	316.2	1.06	3.16E+07	3.16E+01	2.64
7R	2292.0	800	1.64	14.3	764.1	777.7	0.78	7.20E+06	1.78E+01	2.64
8R	2294.0	800	1.46	11.2	364.3	372.4	1.00	2.43E+07	2.86E+01	2.64
9R	2295.0	800	1.75	12.7	435.2	444.7	0.97	1.55E+07	2.18E+01	2.64
10R	2296.0	800	1.83	11.9	445.6	454.9	0.93	1.50E+07	2.18E+01	2.64
11R	2297.0	800	1.92	12.2	0.018	0.033	71.21	5.62E+13	3.16E+03	2.71

Table 1
THIN SECTION PETROGRAPHIC POINT COUNT

Job Number: 000327G
Well:
Date: October, 2000
Location:
Analyst: Wu

Depth (feet)		2285.50	2290.00	2291.00
Average Grain Size (millimeters)		0.30	0.38	0.46
Quartz	Monocrystalline	72.4	69.2	73.6
	Polycrystalline	2.8	0.8	2.4
	Total Quartz	75.2	70.0	76.0
Feldspar	Potassium Feldspar	0.8	0.4	0.4
	Plagioclase			
	Total Feldspar	0.8	0.4	0.4
Rock Fragments	Igneous Rock Fragments			
	Metamorphic Rock Fragments			
	Limestone Rock Fragments			
	Dolomite Rock Fragments			
	Sandstone Rock Fragments			
	Argillaceous Rock Fragments			
	Chert			
	Total Rock Fragments	0.0	0.0	0.0
Accessory Grains	Mica			
	Heavy Minerals	trace	trace	trace
	Fossil Fragments		trace	0.4
	Glauconite			
	Total Accessory	0.0	0.0	0.4
Detrital Matrix	Micrite			
	Clay			
	Silty			
	Total Matrix	0.0	0.0	0.0
Authigenic Clay	Chlorite			
	Kaolinite			
	Illite			
	Mixed-layer Illite/Smectite			
	Indterminate			
	Total Authigenic Clay	0.0	0.0	0.0
Non-Clay Cements	Authigenic Quartz	8.8	11.2	11.6
	Barite			
	Authigenic Feldspar			
	Fe-Dolomite			
	Calcite			
	Fe-Calcite (pore-filling)		0.8	0.8
	Fe-Calcite (grain-replacing)			
	Fluorite	0.8	0.8	trace
	Siderite			
	Analcime			
	Pyrite			
	Titanium Oxide	0.4		
	Total Non-Clay Cements	10.0	12.8	12.4
Porosity Type	Intergranular	14.0	16.8	10.4
	Intrafossil			
	Intragranular			0.4
	Fracture			
	Moldic			
	Microporosity			
	Total Porosity	14.0	16.8	10.8
Physical Properties	Porosity (%)	N/A	N/A	N/A
	Permeability (md)	N/A	N/A	N/A
	Grain Density (g/cm3)	N/A	N/A	N/A

APPENDIX II

Summary of Field Activities

Well Treatments

Field Activity Summary
Well W2

07:30 a.m.	TIH with coil tubing, pumping foam, 70Q foam, ~500 scf/min 0.53 bbl/min, press ~900 psi, wellhead 247 psi flowing ~2 MMcf/D pay 2,376-87'
08:15 a.m.	TIH 770 scf/min plus 1.01 bbl/min, circ press 2,082 psi, wellhead ~ 350 psi, pumping pickle acid ~8:30 a.m., pump foam 750 scf/min, 1.5 bbl/min - ~ 3 bbls then shut down Continue to pump N_2 ~ 750 scf/min
	Eastern Reservoir using a sand separator (heavy wall- 3,000 psi) and two separators in series (NFG concerned with getting foam and/or water in pipeline) flowing gas on another location.
08:47 a.m.	Start pumping WF 120 chemical wash, ~ 400 scf/min, ~ 2 bbl/min, depth at 2,390.7'
08:55 a.m.	Start washing perfs, move coil up and down ~ 5 ft/min
08:59 a.m.	Increase rates to ~500 scf/min and 3 bbl/min
09:03 a.m.	Press increase (wash hit bottom of coil?)
09:09 a.m.	Increased rates ~ 600 scf/min and 3 bbl/min
09:10 a.m.	Dropped rate, 400 scf/min and 2 bbl/min
09:11 a.m.	Dropped rate, 220 scf/min and 1 bbl/min
09:12 a.m.	Shut down (plugged off), circulate press 5,154 psi, wellhead 453 psi, 1.8 MMscf/D flow
	Sand quality was extremely poor looked like river sand. Flow coil tubing back to pumper. TOOH set tool on top of SI motor valve.
10:30 a.m.	Shear off coil tubing above tool. Circulating water to clean coil (pump having prime problems)
12:00 a.m.	Clean out tool. Reattach tool to coil. Redo treatment w/o sand. TIH losing weight at ~21' (possible sand bridge?) Flowing well and wash coil. Worked thru sand bridges.
12:45 p.m.	TIH ~1,500' start injection N_2 – tool plugged.
01:50 p.m.	TOOH. Remove tool – plugged with sand. Clean out tool. Circulated viscous pill – displace with N_2. Put tool on coil tubing and TIH.
02:30 p.m.	Pump ~ 18 bbl acid wash. Displacing with N_2 ~ 1,400 scf/min. Circulate pressure ~ 1,386 psi, wellhead ~ 254 psi. Moving tool up and down across perfs.

Field Activity Summary
Well W2
(Continued)

Time	N_2 Rate (scf/min)	Circ Press	Wellhead Press
2:42	1,400 scf/min	1,388	439
Coil @ 2,391'	-	-	-
2:44	1,400	1,347	486
2:45	1,400	1,314	529
2:46	1,400	1,301	549
2:47	1,400	1,290	569
2:48	1,400	1,280	586
2:49	1,400	1,270	596
2:50	~1,400	1,264	604
2:51	~1,400	1,257	608
2:52	~1,400	1,251	613
2:53	~1,400	1,246	614
2:54	Pumping 2 bbl/min	400 scf/min	
2:55	406 scf/min 2.15 bbl/min	1,740	605
2:56	400 scf/min 2.13 bbl/min	2,089	584
2:57	400 scf/min 2:14 bbl/min	2,400	569
2:58	400 scf/min 2.13 bbl/min	2,645	534
2:59	400 scf/min 2.12 bbl/min	2,883	553
3:00	Shut-in wellhead to displace acid with foam		
Moving coil up and down net pay	400 scf/min 2.12 bbl/min	3,015	591
3:01	400 scf/min 2.12 bbl/min	3,005	650
3:02	400 scf/min 2.12 bbl/min	2,951	684
3:03	410 scf/min 2.12 bbl/min	3,391	710
3:04	400 scf/min 2:11 bbl/min	3,750	732
3:05	Shut down water – continue to displace with N_2		
3:05	800 scf/min 0 bbl/min	1,830	644
3:06	800 scf/min -	1,420	586
3:07	800 scf/min -	1,188	506

Field Activity Summary
Well W2
(Continued)

Time	N_2 Rate (scf/min)	Circ Press	Wellhead Press
3:08	800	1,159	484
3:09	800	1,112	449
3:10	1,200	1,125	413
3:11 stop coil @ 2,392	1,200	1,198	381
3:12	1,200	1,230	353
3:13	1,200	1,246	327
3:14	1,200	1,259	302
3:15	1,200	1,271	279
3:16	1,200	1,284	266
3:17	1,200	1,298	289
3:18	1,200	1,314	331
3:19	1,200	1,310	379
3:20	1,200	1,297	424
3:21	1,200	1,273	471
3:22	1,200	1,250	500
3:23	1,200	1,227	523
3:24	1,230	1,208	545
3:25	1,230	1,193	565
3:26	1,200	1,180	587
3:27	1,200	1,166	606
3:28	1,200	1,153	627
Start TOOH 3:37 p.m.			

Field Activity Summary
Well W9

09:00 a.m.	Circulate sand off BP
09:45 a.m.	Unload fluid using N_2
09:45-10:15 a.m.	TOOH with plug, plug covered with black grease looking material
10:45 a.m.	RD plug and RU jetting tool Running in hole pumping foam, flowing gas at flow stack 390 scf/min, 1 bbl/min
11:45 a.m.	To 2,199'
11:50 a.m.	To 2,282 shut down N_2 pumping pickle acid, 1 bbl/min
11:55 a.m.	To 2,345.9'
11:56 a.m.	Up rate to 1.5 bbl/min
12:02 p.m.	Rate down to 1.36 bbl/min
12:04 p.m.	Shut down
12:05 a.m.	Increase pump rate to 4 BPM, total fluid 52.2 bbl, (mixing chemical wash)
12:07 p.m.	Up to 5.4 BPM recirculating not pumping in well
12:15 p.m.	Done mixing (fluid total 106.7 bbl)
12:18 p.m.	Start pumping chemical wash (no sand!) 200 scf/min, 1 bbl/min
12:28 p.m.	Increase rate to 1.5 BPM and 300 scf/min
12:30 p.m.	Start pulling coil up hole at 11 ft/min
12:32 p.m.	Pulled up to 2,319, start back down at 8-10 ft/min
12:35 p.m.	Stop at 2,346', start back up ~7'/min
12:38 p.m.	Up to 2,328', start down
12:41 p.m.	Stop pumping fluid, 31.1 bbls pumped, increase N_2 to ~800 scf/min, still moving coil
12:43 p.m.	N_2 up to 1,000 scf/min
1:07 p.m.	Reduce N_2 to 200 scf/min
1:08 p.m.	Start fluid at 1 BPM (treatment acid)
1:20 p.m.	SI flow line, start moving coil up hole
1:22 p.m.	Shut down fluid and increase N_2 to 1,000 scf/min, continue to move coil
1:24 p.m.	Start fluid at 2.5 BPM
1:26 p.m.	Shut down fluid, total 50.8 bbls
1:28 p.m.	Start pumping fluid at 2.68 BPM
1:29 p.m.	Shut down fluid, 54.5 bbls total, unload well
1:55 p.m.	Start pulling out of hole with coil, N_2: 1,000 scf/min rate
2:03 p.m.	Shut down N_2 at 1,324'
2:13 p.m.	To surface with jet blaster
2:48 p.m.	Shut in
	GT 3.1 MMscf/D

Field Activity Summary
Well W10

07:30 a.m.	RU to TIH with coil
08:00 a.m.	TIH to 100', open well, start pumping foam 1 BPM and 480 scf/min
08:10 a.m.	1093' increase rate, 750 scf/min
08:28 a.m.	2,350', shut down N_2, switch to pickle acid, (~12 bbls) 1 BPM continue TIH to 2,395', increase rate to 1.5 BPM
08:32 a.m.	Increase rate to 1.75 BPM, pulling up to 100' and back down
08:38 a.m.	Pump 3 bbls water flush, shut down to mix chemical wash
08:50 a.m.	Start wash, 1.5 BPM, ~300 scf/min
08:58 a.m.	13 bbls pumped, start moving coil up and down, total pumped 23 bbls, increase rate to 1.75 BPM
09:04 a.m.	Change to foam (5 bbls), increase N_2 to 750 scf/min
09:07 a.m.	Stop foam – continue N_2
09:17 a.m.	Shut down N_2, continue to flow to tank, shut-in well
09:35 a.m.	ERS defoamer in pump not working RD & RU pump line from SLB pumper to well to inject diluted defoamer
09:41 a.m.	Restart N_2 displacement 1,000 scf/min, pumping @ 0.20 BPM defoamer into return line (not in well)
10:15 a.m.	Shut down N_2 and defoamer
10:16 a.m.	Start acid 1.6 BPM, 300 scf/min, 8.4 bbls
10:21 a.m.	On flush (5 bbls)
10:24 a.m.	Start moving coil
10:25 a.m.	Shut down water injection, increase N_2 to 1,000 scf/min for displacement
10:48 a.m.	Start TOOH
11:01 a.m.	Shut down N_2 and defoamer coil at ~1,380'
11:14 a.m.	Coil at surface
11:41 a.m.	Flowing well GT-2.8 MMscf/D, shut-in well to RD

APPENDIX III

Derivation of Equations
For Non-Darcy Flow Effect Calculations

Deliverability Equations

The Rawlins-Schellhardt deliverability equation is:

$$q = C\left(\bar{p}^2 - p_{wf}^2\right)^n \quad \text{.....(1)}$$

The Hoeupert deliverability equation is

$$\bar{p}^2 - p_{wf}^2 = aq + bq^2 \quad \text{.....(2)}$$

Calculating *C* and *n* from *a* and *b*

The constants *a* and *b* in the Hoeupert equation can be used to calculate the constants *C* and *n* in the Rawlins-Schellhardt equation and vice-versa by forcing the curves for the two equations to be tangent to one another at a specific flow rate *q*. Rewriting Eq. 1 with *q* as the independent variable, and defining

$$\Delta p^2 \equiv \bar{p}^2 - p_{wf}^2 \text{,} \quad \text{.....(3)}$$

we have

$$\Delta p^2 = \left(\frac{q}{C}\right)^{1/n} \quad \text{.....(4)}$$

At the point of tangency, the expressions for Δp^2 given by Eqs. 2 and 4 and their derivatives must be equal.

The derivative of Eq. 2 with respect to q is:

$$\frac{d\Delta p^2}{dq} = a + 2bq \quad \text{.....(5)}$$

while the derivative of Eq. 4 is

$$\frac{d\Delta p^2}{dq} = \frac{1}{Cn}\left(\frac{C}{q}\right)^{1/n=1} \quad \text{.....(6)}$$

We can now form a set of two equations in two unknowns.

$$\left(\frac{q}{C}\right)^{1/n} = aq + bq^2 \quad \text{.....(7)}$$

$$\frac{1}{Cn}\left(\frac{q}{C}\right)^{1/n-1} = a + 2bq \quad \text{.....(8)}$$

$$\frac{1}{Cn}\left(aq + bq^2\right)\left(\frac{C}{q}\right) = a + 2bq \quad \text{.....(9)}$$

$$\frac{1}{nq} = \frac{a + 2bq}{aq + bq^2} \quad \text{.....(10)}$$

$$\frac{1}{n} = \frac{a + 2bq}{a + bq} \quad \text{.....(11)}$$

$$n = \frac{a + bq}{a + 2bq} \quad \text{.....(12)}$$

$$C = \frac{q}{\left(aq + bq^2\right)^n} \quad \text{.....(13)}$$

Eqs. 12 and 13 allow the engineer to calculate *C* and *n* for use in the Rawlins-Schellhardt equation when the Hoeupert coefficients *a* and *b* are known.

Note that a specific value of *q* is required. This is the value of q for which the Rawlins-Schellhardt and Hoeupert equations are forced to be tangent. For a deliverability test, we recommend using the geometric mean of the rates observed during the test.

Calculating *a* and *b* from *C* and *n*

We may also calculate *a* and *b* if *C* and *n* are known. Define

$$r = \frac{a}{b} \quad \text{.....(14)}$$

Then,

$$n = \frac{\frac{a}{b} + q}{\frac{a}{b} + 2q} = \frac{r + q}{r + 2q} \quad \text{.....(15)}$$

$$r + q = nr + 2nq \quad \text{.....(16)}$$

$$r - nr = 2nq - q \quad \text{.....(17)}$$

$$r = q\frac{2n - 1}{1 - n} \quad \text{.....(18)}$$

From the Hoeupert equation, define the fraction of total pressure drop that is attributable to non-Darcy flow as *f*, which may be calculated from

$$f = \frac{bq^2}{aq + bq^2}$$
$$= \frac{1}{\frac{r}{q} + 1} \quad \text{.....(19)}$$
$$= \frac{1-n}{n}$$

Setting Eqs. 2 and 4 equal, we have

$$aq + bq^2 = \left(\frac{q}{C}\right)^{1/n} \text{.....(20)}$$

$$a + bq = \frac{1}{q}\left(\frac{q}{C}\right)^{1/n} \text{.....(21)}$$

$$\frac{a}{b}b + bq = b(r+q) = b\left(q\left(\frac{2n-1}{1-n}\right) + q\right) \text{.....(22)}$$

We can now calculate *b* from

$$b = \frac{1}{q^2}\frac{\left(\frac{q}{C}\right)^{1/n}}{\left(\frac{2n-1}{1-n} + 1\right)} \text{.....(23)}$$
$$= \frac{1}{q^2}\left(\frac{q}{C}\right)^{1/n}\frac{(1-n)}{n}$$

Finally, we obtain *a* from

$$a = rb \text{ .....(24)}$$

However, as *n* approaches 1, *r* approaches ∞, and Eq. 24 becomes undefined. We may obtain a second pair of expressions for *a* and *b* as follows. Define *u*:

$$u = \frac{b}{a} = \frac{1}{r} = \frac{1-n}{q(2n-1)} \text{.....(25)}$$

$$a + \frac{b}{a}aq = a + uaq = \frac{1}{q}\left(\frac{q}{C}\right)^{1/n} \text{.....(26)}$$

$$a = \frac{1}{q}\left(\frac{1}{1+uq}\right)\left(\frac{q}{C}\right)^{1/n} = \frac{1}{q}\left(\frac{2n-1}{n}\right)\left(\frac{q}{C}\right)^{1/n} \quad \text{.....(27)}$$

and finally

$$b = ua \quad \text{.....(28)}$$

As n approaches 0.5, u approaches ∞ and Eq. 28 becomes undefined. The best approach, which works for all values of n, is to use Eq. 27 to calculate a, and Eq. 23 to calculate b:

$$a = \frac{1}{q}\left(\frac{2n-1}{n}\right)\left(\frac{q}{C}\right)^{1/n} \quad \text{.....(27)}$$

$$b = \frac{1}{q^2}\left(\frac{1-n}{n}\right)\left(\frac{q}{C}\right)^{1/n} \quad \text{.....(23)}$$

APPENDIX IV

Technical Reference for
4-Pt Test Simulator Spreadsheets

Completion Models

Three 4-pt test simulators have been developed for 1) open-hole completions, 2) cased-hole completions, and 3) hydraulically fractured completions. All three simulators couple a pseudosteady-state reservoir model with a tubing model to generate a synthetic 4-pt test. The open-hole and cased-hole simulators use different forms of Jones' equation to model pressure drop in the reservoir, while the fracture simulator uses a rate-dependent fracture conductivity proposed by Gidley to estimate an equivalent wellbore radius.

In contrast to our expectations, none of these models predicts a high degree of non-Darcy flow with values for reservoir parameters within the ranges typical of gas storage wells. While disappointing, this suggests that the mechanism responsible for non-Darcy flow in gas storage wells is distinct from any of the mechanisms we have considered in constructing these three models.

One possible explanation lies in the assumption of homogeneity or uniformity in reservoir properties in the near-wellbore region. While this assumption is quite successful in describing Darcy flow, it does not automatically flow that the same would hold true for non-Darcy flow as well. As discussed by S.C. Jones[8], the non-Darcy coefficient β may be a good indicator of heterogeneity at the core plug level. This suggests that heterogeneity in the near-wellbore region in a gas storage well may also cause much higher non-Darcy skin factors than would be observed in a homogeneous reservoir.

Parameters common to all models

Each spreadsheet model has an Input worksheet for the user to enter the data for his reservoir. **Table 1** shows the data that is common to all three models, while **Table 2**, **Table 3**, and **Table 4**, and show the data specific to the Open-Hole, Cased-Hole, and Fracture completion models, respectively.

Table 1 – Input Data Common to All Completion Models

Variable	Units	Description
Fluids		
γ_g	(air=1)	Gas specific gravity
y_{H2S}	mole fraction	H_2S content
y_{CO2}	mole fraction	CO_2 content
y_{N2}	mole fraction	N_2 content
T_{sc}	deg F	Standard temperature (usually 60 deg F)
p_{sc}	psia	Standard pressure
Reservoir		
h	ft	Net pay thickness
ϕ	fraction	Porosity
S_w	fraction	Water saturation (water is assumed to be immobile)
k	md	Permeability to gas at reservoir conditions
k_v/k_h	dimensionless	Ratio of permeability in vertical direction to the geometric mean permeability in the horizontal direction
β correlation	integer (1-5)	Index to indicate which β correlation 1=Firoozabadi & Katz, JPT (Feb. 1979) 2=Jones, SPE 16949 (k only) (1987) 3=Jones, SPE 16949 (k & f) (1987) 4=Tek, JPT (July 1962) 5=Noman et al., SPE 14207 (1985)
β multiplier	dimensionless	User-input factor for increasing or decreasing beta from the correlation estimate
T_f	deg F	Reservoir temperature
A	acre	Drainage radius or well spacing.
Well		
r_w	ft	Wellbore radius. One half the diameter of the drill bit used to drill through the pay section.
TbgID	in	ID of flow string, either tubing or casing
Rough	in	Absolute roughness of flow string surface, usually taken to be 0.00060 to 0.00065.
TVD	ft	True vertical depth
MD	ft	Measured depth
Operating Conditions		
FWHT	deg F	Flowing wellhead temperature
P_{avg}	psia	Average reservoir pressure
$FWHP_{min}$	psia	Wellhead pressure corresponding to the maximum flow rate for the four-point test. For the lower rates in the four-point test, wellhead pressures are selected to give roughly equal steps in rate for the four test points.

Open-Hole Simulator

In the open-hole simulator, the well is assumed to be centered in a circular drainage area of radius r_e, in a reservoir having uniform net pay thickness h, permeability k, porosity ϕ, and water saturation S_w. Any damage or stimulation is assumed to be caused by an altered zone around the wellbore, of radius r_a, having permeability k_a, porosity ϕ_a, and water saturation S_{wa}. Damage will be represented by an altered zone permeability k_a that is lower than the formation permeability k, while stimulation will be represented by an altered zone permeability that is higher than the formation permeability. The well penetrates a distance h_p into the formation. **Figure 1** shows a schematic of the open-hole completion model, while **Table 2** shows the input data required for this model.

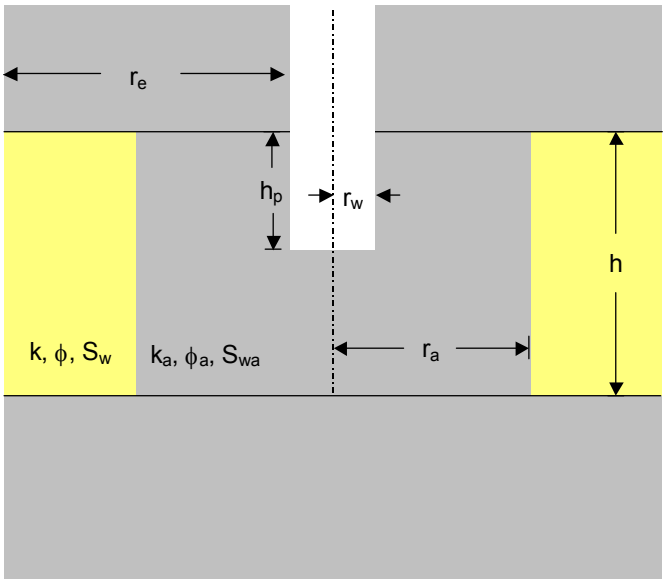

Fig. 1 – Schematic of open-hole completion model (not to scale).

Table 2 – Input data specific to open-hole completion.

Variable	Units	Description
Completion		
h_p	Ft	Portion of net pay open to the wellbore.
r_a	Ft	Radius of altered zone (zone affected by either damage or acid stimulation).
ϕ_a	fraction	Porosity of altered zone.
S_{wa}	fraction	Water saturation in altered zone.
k_a	md	Permeability of altered zone.

The Open-Hole Simulator assumes that the reservoir is homogeneous, and that damage or stimulation is uniformly distributed around the wellbore. This is an idealistic assumption that causes the Open-Hole Simulator to systematically underestimate the effects of non-Darcy flow for situations where there is significant heterogeneity, either in the reservoir permeability or in the distribution of damage or stimulation. As Jones[7] shows, permeability heterogeneity can cause a dramatic increase in the magnitude of non-Darcy flow behavior.

Cased-Hole Simulator

In the cased-hole simulator, as in the open-hole simulator, the well is assumed to be centered in a circular drainage area of radius r_e, in a reservoir having uniform net pay thickness h, permeability k, porosity ϕ, and water saturation S_w. Any damage or stimulation is assumed to be caused by an altered zone around the wellbore, of radius r_a, having permeability k_a, porosity ϕ_a, and water saturation S_{wa}. Only the first h_p of the net pay is perforated. Perforations are assumed to be uniformly spaced at n_s shots per foot. Each perforation has diameter d_p and length l_p. If there is an altered zone around the wellbore, the radius of the altered zone is assumed to be larger than the length of the perforations, so that the perforations do not extend into the unaltered reservoir. If there is an altered zone, the β-factor is estimated from the properties of the altered zone; otherwise, the β-factor is estimated from the bulk reservoir properties. **Figure 2** shows a schematic of the cased-hole completion model, while **Table 2** shows the input data required for this model.

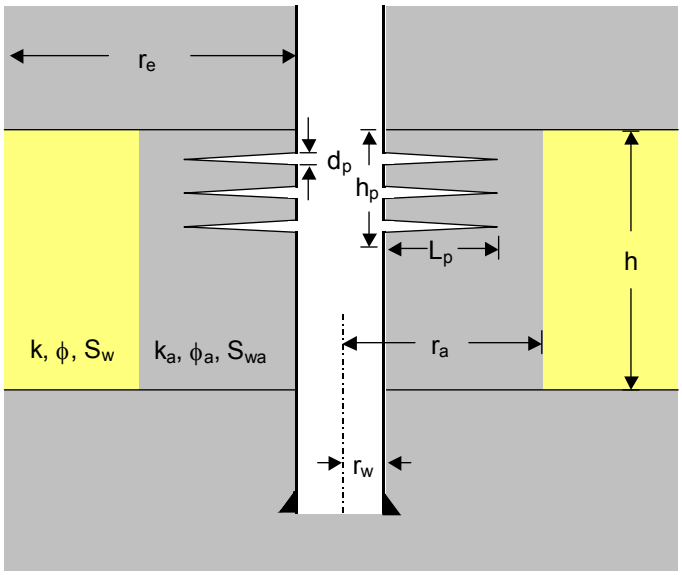

Fig. 2 – Schematic of cased-hole completion model (not to scale)

Table 2 – Input data specific to cased-hole completion.

Variable	Units	Description
Completion		
h_p	Ft	Portion of net pay open to the wellbore.
r_a	Ft	Radius of altered zone (zone affected by either damage or acid stimulation).
ϕ_a	Fraction	Porosity of altered zone.
S_{wa}	Fraction	Water saturation in altered zone.
k_a	Md	Permeability of altered zone.
n_s	ft^{-1}	Number of perforations (shots) per foot.
d_p	In	Diameter of perforation tunnel.
l_p	In	Length of perforation tunnel.

The Cased-Hole Simulator assumes that the reservoir is homogeneous, that damage or stimulation is uniformly distributed around the wellbore, and that all perforations are identical. As with the Open-Hole Simulator, this is an idealistic assumption. Again, this assumption causes the Cased-Hole Simulator to systematically underestimate the effects of non-Darcy flow for situations where there is significant heterogeneity, either in the reservoir permeability or in the distribution of damage or stimulation.

Fracture Simulator

In the fractured well simulator, as in the cased-hole and open-hole simulators, the well is assumed to be centered in a circular drainage area of radius r_e, in a reservoir having uniform net pay thickness h, permeability k, porosity ϕ, and water saturation S_w. The fracture is assumed to have equal length wings, each of length L_f, width w_f, and permeability k_f. All fluid is assumed to flow into the wellbore through the fracture. **Figure 3** shows a plan-view schematic of one wing of the fracture completion model, while **Table 3** shows the input data required for this model.

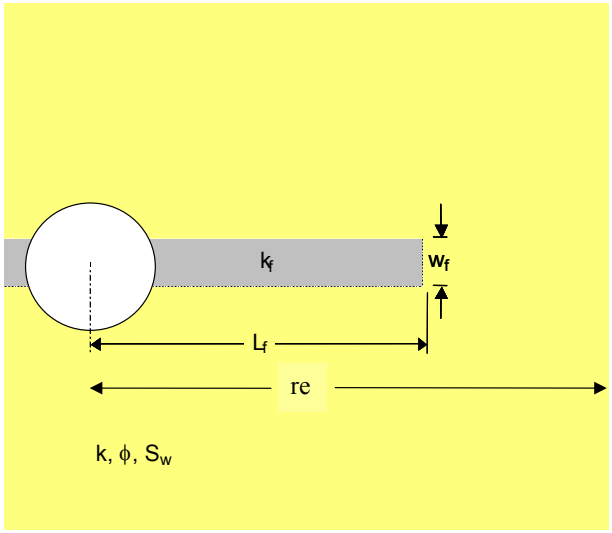

Fig. 3 – Schematic of hydraulically fractured well completion (not to scale)

Table 3 – Input data specific to hydraulic fracture completion.

Variable	Units	Description
Completion		
h_p	ft	Portion of net pay open to the wellbore.
r_a	ft	Radius of altered zone (zone affected by either damage or acid stimulation).
ϕ_a	fraction	Porosity of altered zone.
S_{wa}	fraction	Water saturation in altered zone.
k_a	md	Permeability of altered zone.
Fracture		
L_f	ft	Fracture half-length
w_f	in	Fracture width
k_f	md	Fracture permeability
Sand size	integer (0-4)	Index to indicate proppant size (used in calculating the β-factor) 0=No ND flow 1=8-12 mesh 2=10-20 mesh 3=20-40 mesh 4=40-60 mesh

The Fracture Simulator implicitly assumes that the flow rate in the fracture is the same at any point in the fracture. This tends to overestimate the impact of non-Darcy flow in the fracture, as compared to finite-difference simulation. As with the Open-Hole and Cased Hole Simulators, the Fracture Simulator assumes uniform reservoir properties. It also assumes that fracture properties (height, width, conductivity) are uniform over the entire length of the fracture.

Technical Reference

Solution Method

All three simulators use essentially the same solution method. To simulate a 4-point test, the flow rate is calculated for a series of four different wellhead pressures, chosen so that the flow rates form an approximate arithmetic progression. To use wellhead pressures, the simulator couples a tubing model with a reservoir model.

The tubing model allows the bottomhole pressure to be calculated, assuming the wellhead pressure and flow rate are known. The reservoir model allows the flow rate to be calculated, assuming the average reservoir pressure and sandface pressure are known. To couple the tubing and reservoir models, an iterative solution method is required. The bisection method is used for its simplicity and robustness.

Open-Hole Simulator

The Open-Hole and Cased-Hole Simulators use Jones' equation, given as

$$\bar{p}^2 - p_{wf}{}^2 = aq^2 + bq \quad \text{.....(1)}$$

For a fully penetrating open-hole completion, the coefficients *a* and *b* are calculated from

$$a = 1422 \frac{\mu_{g,wf} z_{g,wf} TD}{kh} \quad \text{.....(2)}$$

$$b = 1422 \frac{\mu_g z_g T}{kh} \left(\ln\left(\frac{r_e}{r_w}\right) - \frac{3}{4} + s \right) \quad \text{.....(3)}$$

The rate-dependent skin coefficient *D* is given by[9]

$$D = \frac{2.715 \times 10^{-15} \beta k_g M p_{sc}}{h r_w T_{sc} \mu_{g,wf}} \quad \text{.....(4)}$$

The non-Darcy flow coefficient β is estimated from one of the following five correlations.

Firoozabadi and Katz[10]:

$$\beta = \exp\left(-1.201 \ln(k) + 23.83\right) \quad \text{.....(5)}$$

Jones[7], permeability only:

$$\beta = \frac{6.15 \times 10^{10}}{k^{1.55}} \quad \text{.....(6)}$$

Jones[7], permeability and porosity:

$$\beta = \frac{1.88 \times 10^{10}}{k^{1.47} \phi^{0.53}} \quad \text{.....(7)}$$

Tek[11]:

$$\beta = \frac{5.5 \times 10^{9}}{k^{1.25} \phi^{0.75}} \quad \text{.....(8)}$$

Noman *et al.*[12]:

$$\beta = \frac{5.5 \times 10^{9}}{k^{1.25} \left(\phi(1 - S_w)\right)^{0.75}} \quad \text{.....(9)}$$

Unfortunately, these correlations can provide only a rough estimate of the β-factor. The β-factor is a function of the pore geometry, just as permeability and porosity are, but just as correlations of permeability

as a function of porosity give only crude estimates of permeability, so β-factor correlations give only crude estimates of β-factor.

To account for partial penetration effects, Eqs. 2 and 3 are modified as follows:

$$a = 1422 \frac{\mu_{g,wf} z_{g,wf} TD}{kh} \left(\frac{h}{h_p} \right)^2 \quad \text{.....(2a)}$$

$$b = 1422 \frac{\mu_g z_g T}{kh} \left(\ln\left(\frac{r_e}{r_w} \right) - \frac{3}{4} + s_t \right) \quad \text{.....(3a)}$$

where s_t is defined as

$$s_t = \begin{cases} \dfrac{h}{h_p} s + s_p, \; s \geq 0 \\ s + s_p, \; s < 0 \end{cases}$$

The geometric skin due to partial penetration, s_p, is calculated from[13]

$$s_p = \left(\frac{1}{h_{pD}} - 1 \right) \ln \frac{\pi}{2 r_{wD}} + \frac{1}{h_{pD}} \ln \left[\frac{h_{pD}}{2 + h_{pD}} \left(\frac{A-1}{B-1} \right)^{1/2} \right]$$

where

$$r_{wD} = \frac{r_w}{h} \left(\frac{k_v}{k_h} \right)^{1/2}$$

$$h_{pD} = \frac{h_p}{h}$$

$$h_{1D} = \frac{h_1}{h}$$

$$A = \frac{1}{h_{1D} + \dfrac{h_{pD}}{4}}$$

$$B = \frac{1}{h_{1D} + \frac{3h_{pD}}{4}}$$

In this model, h_1 is the distance from the top of the formation to the top of the perforations, and is taken to be zero for the open-hole simulation case.

The skin factor s is calculated from

$$s = \left(\frac{k}{k_a} - 1\right)\ln\left(\frac{r_a}{r_w}\right).$$

Cased-Hole Simulator

In the Cased-Hole Simulator, the coefficient a in Jones' equation is calculated from Eq. 2a, with D calculated from[14]

$$D = 2.262 \times 10^{-16} \frac{f_{ND}^{s} \beta k}{\mu r_s^{\,3} n_s^{\,2} h} M \frac{p_{sc}}{T_{sc}} \quad \text{.....(10)}$$

where q is the flow rate in Mscf/day, M is the molecular weight of the gas, n_s is the number of shots per foot, and r_s is the equivalent spherical radius of a perforation tunnel, defined as

$$r_s = \sqrt{r_p l_p}\ , \quad \text{.....(11)}$$

where r_p and l_p are, respectively, the radius and length of the perforation tunnel in ft. The quantity f_{ND}^{s} in Eq. 10 is a geometric constant of order unity, which we will set to 1.0. Eq. 10 is adapted from Eq. 29b of Ref. 14, as discussed in the Appendix.

The coefficient b in Jones' equation is calculated from Eq. 3a, with s_t defined as

$$s_t = \begin{cases} \frac{h}{h_p} s_c + s_p, s_c \geq 0 \\ s_c + s_p, s < 0 \end{cases}$$

where s_c is defined as

$$s_c = \begin{cases} \ln\left(\frac{r_w}{r_a}\right) + \frac{k}{k_a}\ln\left(\frac{r_a}{r_w + l_p}\right) + \frac{k}{2\left(\frac{k_v}{k_h}\right)^{\frac{1}{3}} n_s r_s k_a}, r_a > r_w \\ \ln\left(\frac{r_w}{r_w + l_p}\right) + \frac{1}{2\left(\frac{k_v}{k_h}\right)^{\frac{1}{3}} n_s r_s}, r_a \leq r_w \end{cases}$$

Fractured Well Simulator

In the Fractured Well Simulator, the dimensionless fracture conductivity is calculated from[15]

$$C_{r,eff} = \frac{C_r}{1 + N_{\mathrm{Re}}} \quad \text{.....(12)}$$

where N_{Re} is the Reynolds number, calculated as

$$N_{Re} = 8.399 \times 10^{-11} \frac{\beta k_f q_g}{\mu_g w_f h} \quad \text{.....(13)}$$

where β is in ft^{-1}, k_f is in md, and q_g is in MMscf/D, and where C_r is defined as

$$C_r = \frac{w k_f}{\pi k L_f} \quad \text{.....(14)}$$

The apparent wellbore radius is calculated from

$$r_{wa} = \frac{r_{wa}}{Lf} L_f$$

where $\frac{r_{wa}}{L_f}$ is calculated from

$$\frac{r_{wa}}{L_f} = \frac{C_{r,eff}}{2C_{r,eff} + 1} + \frac{r_w}{L_f} \quad \text{.....(15)}$$

Eq. 15 reproduces Fig. 14 from Cinco and Samaniego[16] within a few percent while obeying the limiting condition

$$\lim_{C_r \to 0} \frac{r_{wa}}{L_f} = \frac{r_w}{L_f}, \quad \text{.....(16)}$$

i.e. as the fracture conductivity goes to zero, the well acts as if it were unfractured.

Since the Reynolds number defined in Eq. 13 depends on the flow rate which in turn depends on the effective dimensionless fracture conductivity, we have to solve for the flow rate using an iterative method.

Unfortunately, this procedure tends to over-estimate the impact of non-Darcy flow in the fracture, as discussed in Ref. 15. However, we are not aware of a more accurate way of calculating the production rate from a hydraulically fractured well without using a finite-difference fracture simulator.

Appendix

Fluid properties

State-of-the-art correlations are used to estimate fluid properties used in these simulators.

Pseudocritical Temperature and Pressure

Pseudocritical temperature and pressure are estimated from the following correlations[17]:

$$T_{pc} = \frac{K^2}{J} \quad \text{.....(17)}$$

$$p_{pc} = \frac{T_{pc}}{J} \quad \text{.....(18)}$$

where J and K are defined as

$$J = \alpha_0 + \sum_{i=1}^{3} \alpha_i y_i \left(\frac{T_c}{p_c} \right)_i + \alpha_4 \gamma_g + \alpha_5 {\gamma_g}^2 \quad \text{.....(19)}$$

$$K = \beta_0 + \sum_{i=1}^{3} \beta_i y_i \left(\frac{T_c}{\sqrt{p_c}} \right)_i + \beta_4 \gamma_g + \beta_5 {\gamma_g}^2 \quad \text{.....(20)}$$

The coefficients for Eqs. 19 and 20 are given in Table 5.

Table 5 – Coefficients used in pseudocritical temperature and pressure correlations.

i	α_i	β_i
0	1.1582E-01	3.8216E+00
1	-4.5820E-01	-6.5340E-02
2	-9.0348E-01	-4.2113E-01
3	-6.6026E-01	-9.1249E-01
4	7.0729E-01	1.7438E+01
5	-9.9397E-02	-3.2191E+00

Z-Factor

Z-factors are calculated from the Dranchuk and Abou-Kassem (DAK) equation of state[18], given as

$$\begin{aligned} z = 1 &+ \left(A_1 + \frac{A_2}{T_r} + \frac{A_3}{{T_r}^3} + \frac{A_4}{{T_r}^4} + \frac{A_5}{{T_r}^5} \right) \rho_r \\ &+ \left(A_6 + \frac{A_7}{T_r} + \frac{A_8}{{T_r}^2} \right) {\rho_r}^2 \\ &- A_9 \left(\frac{A_7}{T_r} + \frac{A_8}{{T_r}^2} \right) {\rho_r}^5 \\ &+ A_{10} \left(1 + A_{11} {\rho_r}^2 \right) \frac{{\rho_r}^2}{{T_r}^3} \exp\left(- A_{11} {\rho_r}^2 \right) \end{aligned} \quad \text{.....(21)}$$

where

$$\rho_r = 0.27 \frac{p_r}{z T_r} \quad \text{.....(22)}$$

Table 6 gives the coefficients used in Eq. 21.

Table 6 – Coefficients for DAK Equation of State.

A_1 =	0.3265	A_2 =	-1.0700	A_3 =	-0.5339
A_4 =	0.01569	A_5 =	-0.05165	A_6 =	0.5475
A_7 =	-0.7361	A_8 =	0.1844	A_9 =	0.1056
A_{10} =	0.6134	A_{11} =	0.7210		

Eqs. 21 and 22 are solved for z as a function of T_r and p_r using Newton's method. The derivative of z with respect to ρ_r is given by

$$\begin{aligned}\frac{\partial z}{\partial \rho_r} = &\left(A_1 + \frac{A_2}{T_r} + \frac{A_3}{T_r^3} + \frac{A_4}{T_r^4} + \frac{A_5}{T_r^5} \right) \\ &+2\left(A_6 + \frac{A_7}{T_r} + \frac{A_8}{T_r^2} \right)\rho_r \\ &-5A_9\left(\frac{A_7}{T_r} + \frac{A_8}{T_r^2} \right)\rho_r^4 \\ &+2A_{10}\frac{\left(1 + A_{11}\rho_r^2 - A_{11}^2\rho_r^4\right)}{T_r^3}\exp\left(-A_{11}\rho_r^2\right)\rho_r\end{aligned} \quad \text{.....(23)}$$

Formation Volume Factor

The formation volume factor is given in Mscf/bbl by

$$B_g = \frac{1000}{5.61458333}\frac{zTp_{sc}}{z_{sc}T_{sc}p} \quad \text{.....(24)}$$

Gas Compressibility

The coefficient of isothermal compressibility is given by[19]

$$c_g = \frac{1}{p_c}\left(\frac{1}{p_r} - \frac{0.27}{z^2T_r}\frac{\frac{\partial z}{\partial \rho_r}}{1 + \frac{\rho_r}{z}\frac{\partial z}{\partial \rho_r}} \right) \quad \text{.....(25)}$$

Viscosity

The viscosity is calculated using the correlation proposed by Lee, Gonzalez, and Eakin[20]:

$$K = \frac{(9.379 + 0.01607M)T_r^{3/2}}{209.2 + 19.26M + T_r} \quad \text{.....(26)}$$

$$X = 3.448 + \frac{986.4}{T_r} + 0.01009M \quad \text{.....(27)}$$

$$Y = 2.447 - 0.2224X \quad \text{.....(28)}$$

$$\mu_g = \frac{K}{1000}\exp\left(X\rho^Y\right) \quad (29)$$

Tubing Model

Fanning friction factor

The Fanning friction factor is calculated from[21]

$$f = \frac{1}{\left(2.28 - 4\log_{10}\left(\delta + \frac{21.25}{R_e^{0.9}}\right)\right)^2} \quad (30)$$

where δ is the relative roughness, and R_e is the Reynolds number, calculated as

$$R_e = 20{,}011\frac{\gamma_g|q|}{\mu D} \quad (31)$$

Pressure gradient

The pressure gradient is given by[22]

$$\frac{dp}{dx} = \frac{\frac{dh}{dx}\left(\frac{p}{Tz}\right)^2 + 2666.5\frac{fq^2}{D^5}}{53.34\frac{p}{Tz\gamma_g} - 111.1\frac{q^2}{D^4 p}} \quad (32)$$

Eq. 32 is integrated using the 4th order Runga-Kutta method.

Derivation of Expression for Non-Darcy Flow in Spherical Geometry

From Saleh & Stewart, Eq. 29, in Darcy units,

$$p_{DSS} = \frac{(p_e - p_w)2\pi kh}{q\mu} = \ln\left(\frac{r_e}{r_w}\right) + S_c + \frac{f_{ND}^s \beta\rho q k h}{24\pi\mu {r_s}^3 {N_p}^2} \quad (33)$$

We can identify the third term in this expression as

$$Dq = \frac{f_{ND}^s \beta\rho q k h}{24\pi\mu {r_s}^3 {N_p}^2} \quad (34)$$

so, in Darcy units,

$$D = \frac{f_{ND}^s \beta\rho k h}{24\pi\mu {r_s}^3 {N_p}^2} = \frac{f_{ND}^s \beta\rho k}{24\pi\mu {r_s}^3 {n_s}^2 h} \quad (35)$$

Variable	To convert Field Units	to Darcy Units	Multiply by
β	ft^{-1}	$atm\text{-}s^2/g$	1/30883860
ρ	lbm/ft^3	g/cm^3	1/62.4279606

k	md	Darcy	0.001
μ	cp	cp	1
r_s	ft	cm	30.48
n_s	ft^{-1}	cm^{-1}	1/30.48
h	ft	cm	30.48
D	D/bbl	s/cm^3	0.543439651

$$D\left(\frac{day}{bbl}\right)=\frac{f_{ND}^{s}\beta\left(ft^{-1}\right)\left(\frac{1\frac{atm\cdot s^2}{g}}{30883860\,ft^{-1}}\right)\rho\left(\frac{lbm}{ft^3}\right)\left(\frac{1\frac{g}{cm^3}}{62.4279606\frac{lbm}{ft^3}}\right)k(md)\left(\frac{1Darcy}{1000md}\right)}{24\pi\mu(cp)r_s(ft)^3\left(\frac{30.48cm}{1ft}\right)^3 n_s\left(\frac{1}{ft}\right)^2\left(\frac{1ft}{30.48cm}\right)^2 h(ft)\left(\frac{30.48cm}{1ft}\right)}\left(\frac{s}{cm^3}\right)\left(\frac{\frac{1day}{86400s}}{\frac{1bbl}{158987.295cm^3}}\right) \quad .....(36)$$

$$D\left(\frac{day}{bbl}\right)=\frac{1.027\times10^{-15}}{24\pi}\frac{f_{ND}^{s}\beta\rho k}{\mu r_s^{\,3}n_s^{\,2}h}=1.363\times10^{-17}\,\frac{f_{ND}^{s}\beta\rho k}{\mu r_s^{\,3}n_s^{\,2}h} \quad .....(37)$$

The coefficient in Eq. 37 differs from Saleh & Stewart Eq. 29b by a factor 62.43. Saleh & Stewart's Eq. 29b is correct if density is in g/cm^3 instead of lbm/ft^3 as they claim.

To express Eq. 37 in a form suitable for use with a pressure-squared formulation, we need *D* in units of days/Mscf. Noting that the term qB_g has units of bbls/day when *q* is in Mscf/D and B_g is in bbls/Mscf, we find that multiplying *D* from Eq. 37 by B_g will give *D* in units of D/Mscf.

$$\rho=\frac{m}{V}=\frac{Mnp}{znRT}=\frac{Mp}{zRT}$$

$$B_g=\frac{1000}{5.6146}\frac{zRT}{p}\frac{p_{sc}}{z_{sc}RT_{sc}}$$

Thus, we have

$$\begin{aligned}D\left(\frac{day}{Mscf}\right)&=1.363\times10^{-17}\,\frac{f_{ND}^{s}\beta k}{\mu r_s^{\,3}n_s^{\,2}h}\frac{Mp}{zRT}\frac{1000}{5.6146}\frac{zRT}{p}\frac{p_{sc}}{z_{sc}RT_{sc}}\\&=1.363\times10^{-17}\,\frac{1000}{5.6146}\frac{f_{ND}^{s}\beta k}{\mu r_s^{\,3}n_s^{\,2}h}M\frac{p_{sc}}{z_{sc}RT_{sc}}\\&=2.4276\times10^{-15}\,\frac{f_{ND}^{s}\beta k}{\mu r_s^{\,3}n_s^{\,2}h}M\frac{p_{sc}}{RT_{sc}}\end{aligned}$$

where we have assumed z_{sc} = 1.0 in the final step. Taking R=10.732 we have

$$D\left(\frac{day}{Mscf}\right) = 2.262\times10^{-16}\,\frac{f_{ND}^{s}\beta k}{\mu r_s^{\,3} n_s^{\,2} h}\,M\,\frac{p_{sc}}{T_{sc}}$$

$$= 1.851\times10^{-16}\,\frac{f_{ND}^{s}\beta k}{\mu r_s^{\,3} n_s^{\,2} h}\,\gamma_g$$

where we have taken M_{air} = 28.96 g/g-mole, p_{sc} = 14.696 psia and T_{sc} = 520 deg R in the final step.

APPENDIX V

Non-Darcy Damage Prediction Tool

Deliverability Plots for Sensitivity Runs

Open-Hole Completion - Underream

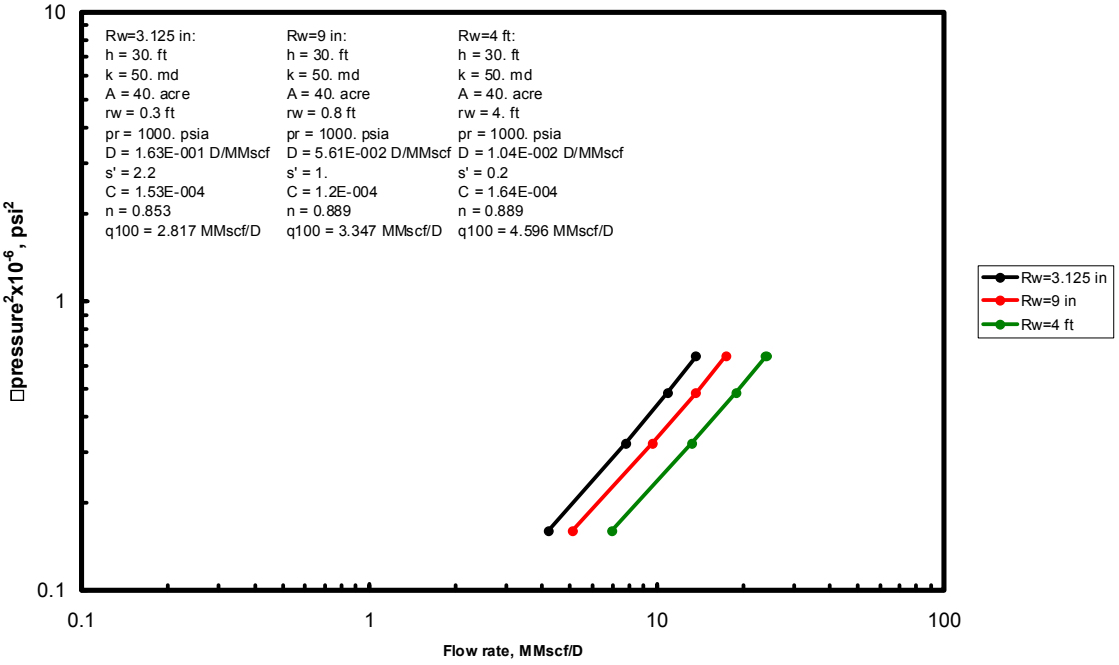

Open-Hole Completion - Acidize

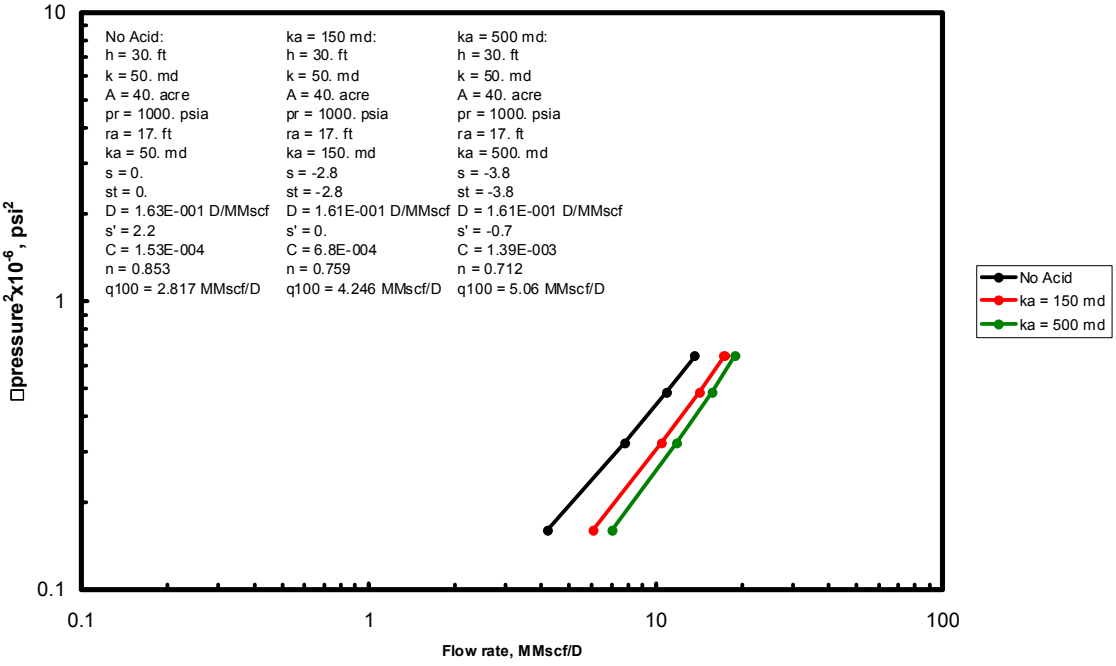

Open-Hole Completion - Fracture

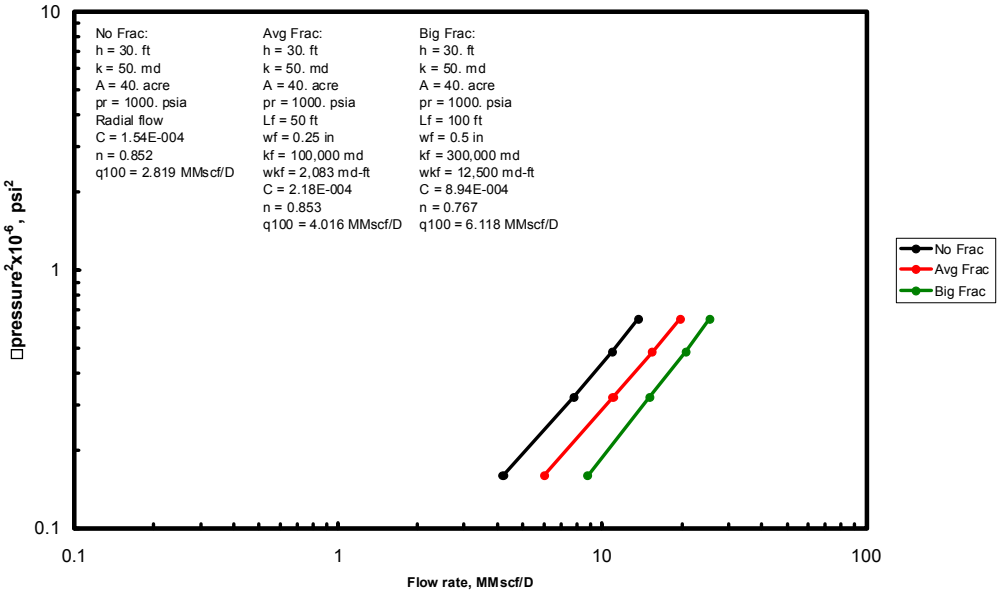

Cased-Hole Completion - Deeper Perforations

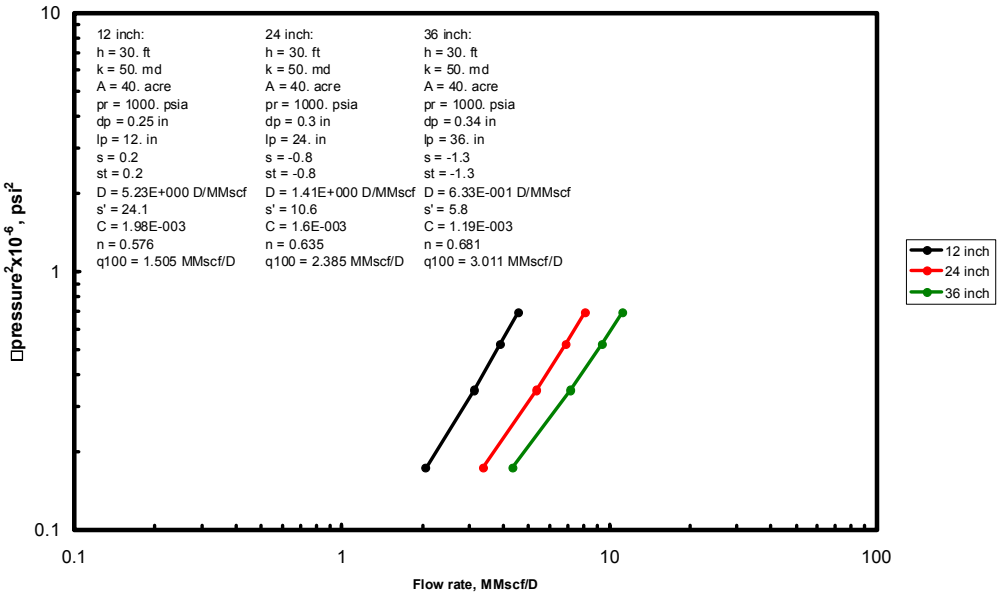

Cased-Hole Completion - Bigger Perforations

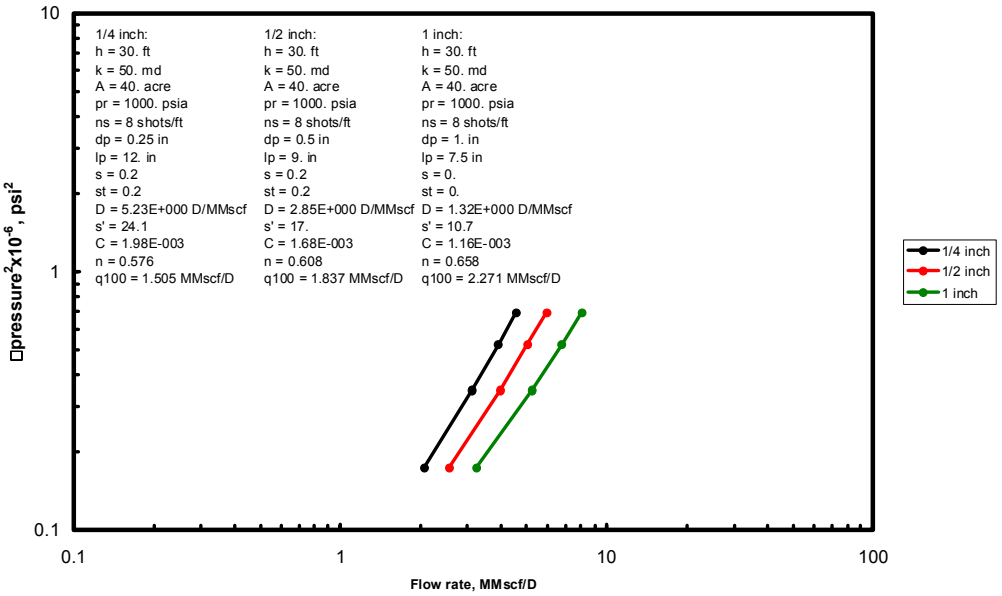

Cased-Hole Completion - More Perforations

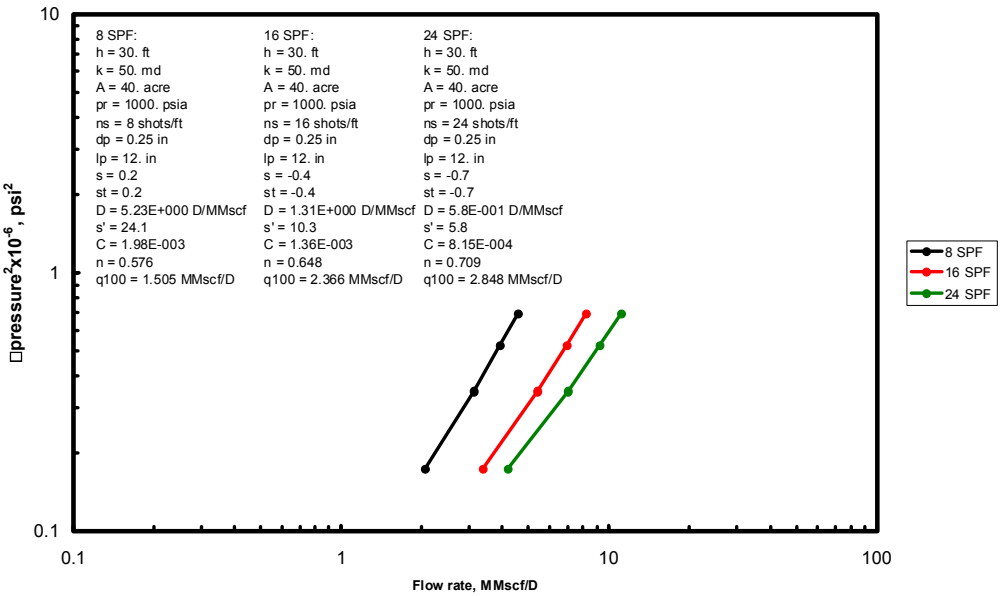

Cased-Hole Completion - Acidize

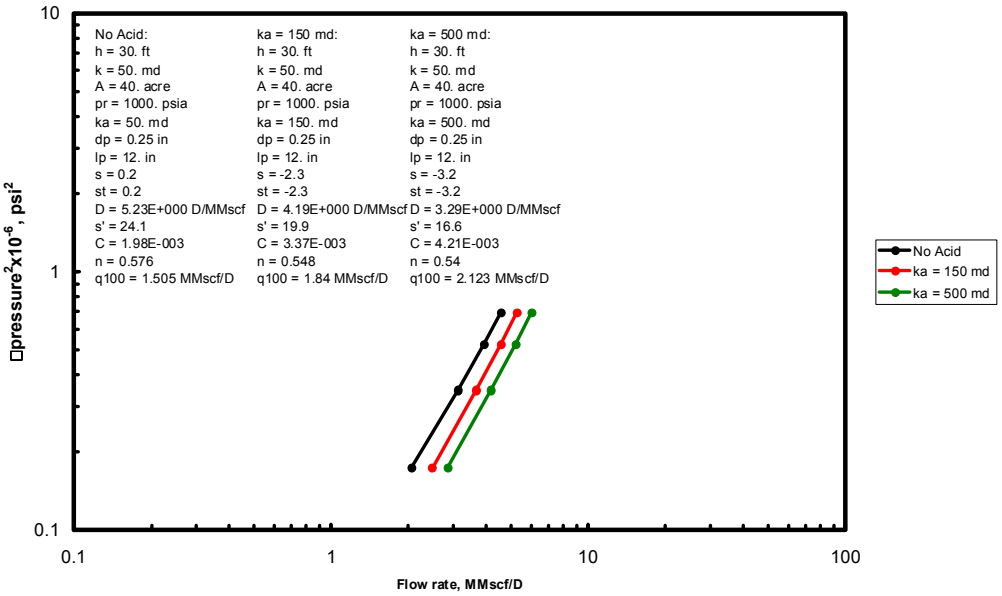

Cased-Hole Completion - Fracture

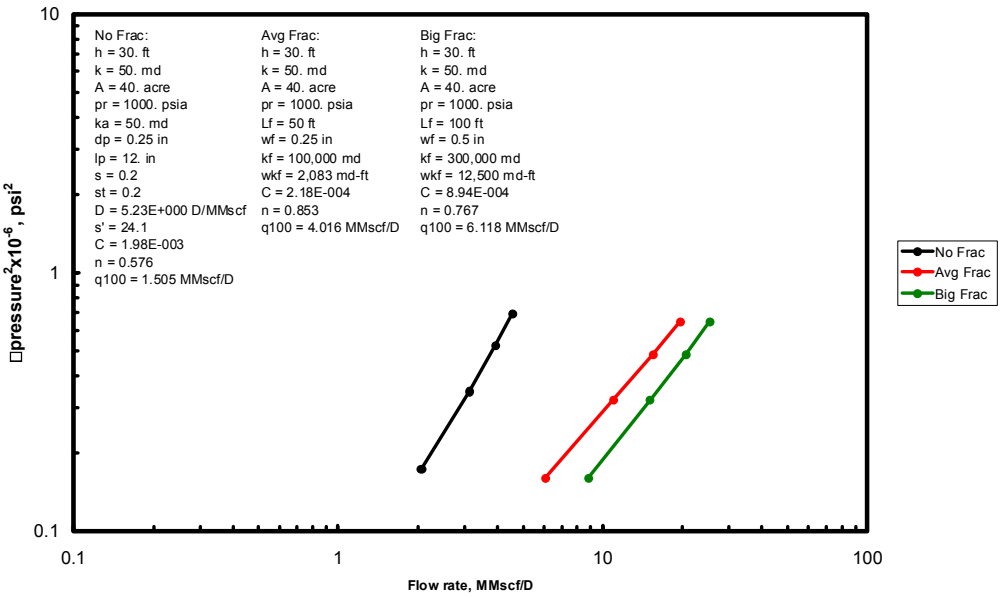

Hydraulic Fracture Completion - Long Fracture

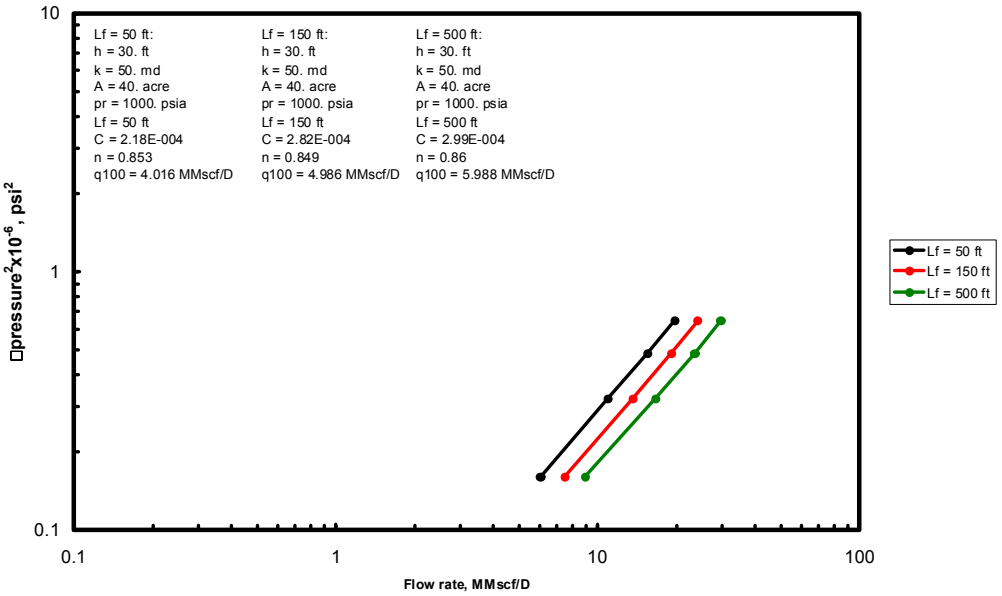

Hydraulic Fracture Completion - Wide Fracture

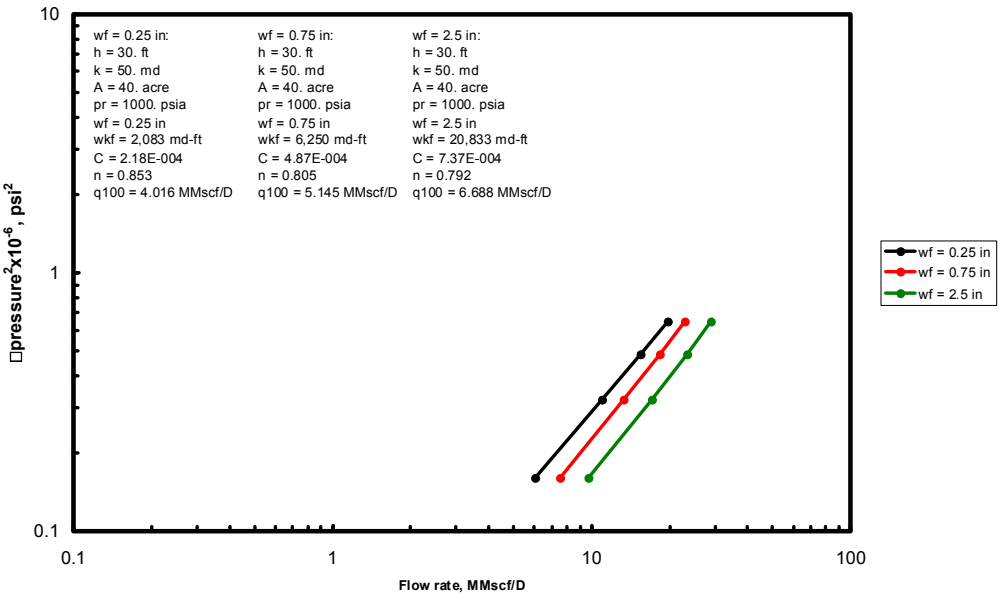

Hydraulic Fracture Completion - High Permeability Fracture